NASA Technical Paper 1084

Entry Dynamics of Space Shuttle Orbiter With Longitudinal Stability and Control Uncertainties at Supersonic and Hypersonic Speeds

Howard W. Stone and Richard W. Powell

OCTOBER 1977

NASA

NASA Technical Paper 1084

Entry Dynamics of Space Shuttle Orbiter With Longitudinal Stability and Control Uncertainties at Supersonic and Hypersonic Speeds

Howard W. Stone and Richard W. Powell
Langley Research Center
Hampton, Virginia

National Aeronautics
and Space Administration

**Scientific and Technical
Information Office**

1977

SUMMARY

A six-degree-of-freedom simulation analysis was conducted to examine the effects of longitudinal static aerodynamic stability and control uncertainties on the performance of the space shuttle orbiter automatic (no manual inputs) entry guidance and control systems. To establish the acceptable boundaries, the static aerodynamic characteristics were varied either by applying a multiplier to the aerodynamic parameter or by adding an increment. The vehicle stability and control was found to be most critical from Mach 4 to 5 for the range of the entry trajectory studied. The boundaries were established as those which provided satisfactory flight in this Mach range and satisfactory trajectory targeting with either of two previously identified control system modifications included in the system.

INTRODUCTION

A reusable Earth-to-orbit transportation system known as the space shuttle is being developed by the National Aeronautics and Space Administration. The space shuttle will be capable of inserting payloads of up to 29 500 kg (65 000 lb) into a near-Earth orbit, retrieving payloads already in orbit, and landing with a payload of up to 14 500 kg (32 000 lb). The space shuttle consists of an orbiter, an external fuel tank, and two solid rocket boosters (SRB). The SRB's will be recovered after each launch for reuse. The external tank is designed for one use and is not recovered.

The orbiter will have the capability to enter the Earth's atmosphere, fly up to 2040 km (1100 n. mi.) cross range, and land horizontally. A closed-loop guidance system is being developed to provide the necessary roll-angle and angle-of-attack commands for either the automatic flight control system (primary mode) or a pilot-operated, augmented flight control system. A general description of the configuration and mission is given in reference 1.

The orbiter aerodynamic configuration has evolved through several design iterations, and wind-tunnel test data have been obtained at various conditions throughout the design evolution. There are data uncertainties due to variations in wind-tunnel conditions, instrumentation uncertainties, extrapolation of previous configuration data to the latest configuration, extrapolation of wind-tunnel data to flight, and evolutionary configuration changes from the present design to the flight hardware. Thus, to establish confidence in the overall system design, it is necessary to determine the range of uncertainties in the aerodynamic parameters with which the guidance and control systems can cope.

With the aid of a six-degree-of-freedom simulation, an analysis was undertaken to establish the ability of the system to cope with uncertainties in the aerodynamic characteristics during entry. This report presents results of the longitudinal stability and control portion of this analysis. The results of the

lateral-directional stability and control portion of the analysis are presented in reference 2.

The shuttle orbiter longitudinal stability and control characteristics have been varied during a 600-sec period of the entry during which the Mach number decreases from 13 to 1.5 and the altitude decreases from 56.4 km (185 000 ft) to 21.3 km (70 000 ft). These 600 seconds represent the period during which the orbiter performs its most extreme maneuvers and where the aerodynamic parameters are undergoing significant changes as the vehicle decelerates from hypersonic to low supersonic velocities and the angle of attack is lowered from its deorbit value of 34.25° to 10°. These results have been obtained without considering external disturbance sources such as winds. This simulation study considered the orbiter center of gravity to be located at the most forward entry operational center of gravity (65 percent of the fuselage reference length) and offset laterally by 0.0381 m (1.5 in.), the maximum expected lateral offset.

SYMBOLS

Values are given in SI Units and U.S. Customary Units. Calculations were made in U.S. Customary Units. All coefficients and vehicle rates are in the body axis system. A G before any aerodynamic coefficient indicates a multiplication gain.

$\bar{c}$ mean aerodynamic chord, m (ft)

C_m pitching-moment coefficient, $\frac{\text{Pitching moment}}{q_\infty S\bar{c}}$

C_{m_α} $= \frac{\partial C_m}{\partial \alpha}$, deg^{-1}

ΔC_m pitching-moment increment

$\Delta C_{m,\delta BF}$ pitching-moment increment due to body flap deflection

$\Delta C_{m,\delta e}$ pitching-moment increment due to elevon deflection

$\Delta C_{m,\delta SB}$ pitching-moment increment due to speed brake deflection

I_{sp} specific impulse, sec

I_X moment of inertia about body roll axis, $kg\text{-}m^2$ ($slug\text{-}ft^2$)

I_Y moment of inertia about body pitch axis, $kg\text{-}m^2$ ($slug\text{-}ft^2$)

I_Z moment of inertia about body yaw axis, $kg\text{-}m^2$ ($slug\text{-}ft^2$)

I_{XZ} cross product of inertia about body roll and yaw axes, $kg\text{-}m^2$ ($slug\text{-}ft^2$)

L/D lift-drag ratio

M	Mach number
p	body roll rate, deg/sec
q	body pitch rate, deg/sec
q_∞	free-stream dynamic pressure, Pa (lb/ft^2)
S	reference area, m^2 (ft^2)
V_R	Earth relative velocity, m/sec (ft/sec)
α	angle of attack, deg
$\Delta\alpha$	change in angle of attack, deg
$\Delta\alpha_c$	change in commanded angle of attack, deg
β	sideslip angle, deg
δ_a	aileron deflection angle, $(\delta_{e,left} - \delta_{e,right})/2$, deg
δ_{BF}	body flap deflection angle (positive down), deg
δ_e	elevon deflection angle, $(\delta_{e,left} + \delta_{e,right})/2$, deg
δ_r	rudder deflection angle (positive trailing edge, left), deg
δ_{SB}	speed brake deflection angle (positive open), deg
ϕ	body roll angle, deg

Subscripts:

i	initial condition
c	command

SPACE SHUTTLE ORBITER DESCRIPTION

The physical characteristics of the space shuttle orbiter used in this study are summarized in table I. A sketch of the orbiter is shown in figure 1. The mission used was a once-around return from a 104° inclined orbit launched from the Western Test Range. Figure 2 depicts this entry on a world map and figure 3 shows some of the trajectory parameters.

Guidance System

A guidance system has been designed to provide the necessary roll-angle and angle-of-attack commands for either the automatic flight control system or for

pilot displays for an augmented manual flight control system. The entry guidance is designed to direct the orbiter from 121.9 km (400 000 ft), the atmospheric interface, down to 21.3 km (70 000 ft), the beginning of the landing phase. The entry down range and cross range are controlled through roll-angle modulation, whereas the angle of attack follows a preselected schedule. The guidance system is described in more detail in appendix A of reference 3.

Automatic Flight Control System

This control system compares the vehicle attitude with the guidance commands and directs aerodynamic control-surface deflections and the reaction control system (RCS) jet firings. The aerodynamic control surfaces depicted in figure 1 include elevons (which are used as ailerons and elevators), a rudder with speed brake capability, and a body flap for longitudinal trim. RCS jets are used to supplement control about the roll, pitch, and yaw axes. The roll and pitch jets are used only during the early part of the entry at low dynamic pressures. The jets have a nominal vacuum thrust of 3870 N (870 lb). To approximate the effects of thrust buildup with time and thrust loss due to back pressure increases with decreasing altitude, an average thrust level of 3336 N (750 lb) and an I_{sp} of 242 seconds for each jet were used in this study.

The longitudinal part of the control system uses the elevons to achieve the commanded angle of attack and provide pitch rate damping. The body flap deflection is based on the longitudinal center-of-gravity location and in the study was at the upward deflection limit of -11.7°. The speed brake follows the deflection schedule shown in figure 4 which provides a nose-up increment in pitch and allows the elevons to have a more downward deflection.

The lateral-directional part of the control system operates in two basic modes. In the spacecraft mode ($\alpha > 18^{\circ}$ or $M > 5$), the roll-angle command from the guidance system is directed to the yaw RCS channel, which produces a yawing rate and a small β, and allows the effective dihedral of the orbiter to generate a rolling moment. The ailerons are used for turn coordination. In the spacecraft mode the rudder is not engaged. The control system switches to the aircraft mode when $\alpha \leq 18^{\circ}$ and $M \leq 5$. In this mode the ailerons are used for roll control and the rudder, now activated, with yaw jet augmentation is used for turn coordination. The control system is described in more detail in appendix B of reference 3.

SIMULATION DESCRIPTION

The automatic reentry flight dynamics simulator (ARFDS) used for this study is an automatic (unmanned), nonlinear, six-degree-of-freedom, interactive, digital computer program developed at the Langley Research Center that utilizes hardware developed for real-time simulations (ref. 3). ARFDS is controlled from a console where changes can be made between and during runs; such changes include multiplying aerodynamic parameters by constants or adding increments, modifying initial conditions, and altering system gains. This capability has been used to start at different points in the trajectory when flying with the guidance system or to bypass the guidance system and put in step commands to the control system

at various conditions. The vehicle response is observed on time-history strip charts.

The nominal entry trajectory used in this study was for a once-around southerly launch from the Western Test Range requiring approximately 1852 km (1000 n. mi.) cross range.

The nominal aerodynamic characteristics used in this study are from the data base available as of June 1974. These data include longitudinal and lateral-directional static aerodynamic characteristics and damping derivatives. The nominal values of the longitudinal stability and control derivatives are shown in figures 5 to 8. Interference and cross-coupling effects from reaction control system (RCS) jets were also accounted for throughout the speed range as described in reference 3. The actuators for the elevons and rudder were approximated by first-order lag filters with rate and position limiting.

AERODYNAMIC PARAMETER VARIATION

Four longitudinal stability and control parameters were varied both independently and in combination to determine how uncertainties in these parameters would affect vehicle controllability and the vehicle capability to meet the guidance performance requirements. The longitudinal parameters were: the pitching moment for undeflected controls (C_m), the pitching-moment increment for elevon control effectiveness ($\Delta C_{m,\delta e}$), the pitching-moment increment for body flap control effectiveness ($\Delta C_{m,\delta BF}$), and the pitching-moment increment for speed brake control effectiveness ($\Delta C_{m,\delta SB}$). The nominal data at Mach numbers 1.5, 3.0, 4.0, and 5.0 are shown in figures 5 to 8. The pitching moment for undeflected controls was varied both by an increment and/or a multiplier. The increment of C_m (ΔC_m) varied the level of the pitching moment only, whereas the multiplier also varied the stability $\left(C_{m_\alpha}\right)$.

CRITERIA FOR SATISFACTORY FLIGHT

There are several criteria by which the simulation results can be judged and those used in this study are shown in table II. The normal acceleration limit was never exceeded in this study unless control was lost completely. Varying the longitudinal characteristics generally resulted in changing the elevon angle at a given Mach number and angle-of-attack combination. Since the elevons were also used for roll control and the yaw due to aileron changed with elevon angle (see ref. 2), the lateral-directional dynamics were directly affected by varying the longitudinal characteristics. Thus, the ϕ oscillation and the RCS fuel consumption were appropriate criteria in this study.

CRITICAL COMBINATIONS

Vehicle response to step commands and guidance system directed entry simulations were performed with the multipliers or increments on the aerodynamic parameters held constant during a simulation. The simulation results were compared with these criteria to determine when the system exhibited satisfactory perform-

ance. The aerodynamic parameters in these simulations were varied first independently, since the four longitudinal parameters were considered to be independent of one another, and then in combination to establish critical combinations. A critical combination is a set of off-nominal parameters in which a criteria violation will occur if the variation from the nominal of any one of the parameters is increased. In some instances the variation of a parameter was reduced to allow larger variation in other parameters to obtain more reasonable parameter variation bounds. These critical combinations determined the boundary values for each parameter.

DISCUSSION OF RESULTS

During the entry phase under study (see fig. 3), the nominal pitching moment of the orbiter with undeflected controls was negative (nose down). Some nose-up moment (positive C_m) is provided by deflecting the speed brake through the deflection schedule shown in figure 4. The resulting nominal elevon deflection angle and the angle-of-attack trends with Mach number are shown in figure 9. The elevon history results from changing pitching-moment characteristics with Mach number and angle of attack, the pitch down motion, cross coupling from roll reversal maneuvers, and the speed brake schedule. From Mach 4.5 to Mach 4, the speed brake closes down from 85° to 55°. Thus, the elevon deflection goes from its least negative value to about Mach 4.6 to nearly its most negative value just below Mach 4 as is seen in figure 9.

Entry simulations, in which guidance commands are fed to the control system, revealed that the major impact of varying the longitudinal stability and control parameters was to change the elevon deflection required to follow the commanded angle-of-attack schedule. Thus, the elevon angles and vehicle response at Mach 5 and Mach 4 are used hereafter as key indicators of the effects of uncertainties in the presentation of the simulation results.

Variation of C_m

The pitching moment for undeflected controls was varied both by applying increments (which result in a shift of the pitching-moment curves) and by multipliers (which also change the stability level). The results are presented in figures 10 to 12.

Increments from -0.014 to 0.014 were applied to the pitching-moment coefficient and the resulting elevon angles that occurred at Mach 4 and 5 in the entry simulations are shown in figure 10. There was substantial change in the elevon angle at both Mach numbers but no significant effect was noted in the entry simulations. A further test of the effect of this change on the system is shown in figure 11. The vehicle response to a step roll-angle command and a constant angle-of-attack command is presented for nominal aerodynamics and with a pitching-moment increment of 0.014. These results are for $M_i = 4$ which is just after the switchover to the aircraft mode. At this point in the trajectory, the lateral-directional control system is weak (see ref. 2) and is therefore very sensitive to the elevon angle. In these simulations the vehicle is untrimmed directionally (the center of gravity is offset laterally 0.0381 m (1.5 in.)) so

the control activity during the first 10 seconds is to establish the trim. At 10 seconds the control system receives a 60° roll-angle step command. Figure 11(a) shows that the vehicle responds by producing a maximum roll rate of about 5°/sec with little sideslip (β). The roll angle reaches the command value at about 25 seconds and experiences a slight overshoot which is quickly nulled. There is a very small pitch rate and α is constant. With a pitch increment of 0.014, figure 11(b) shows that the vehicle has some difficulty accomplishing the maneuver. The maximum roll rate (p) is about 4°/sec and there is about 5° overshoot in roll angle followed by a convergent oscillation. This type of response will be discussed in more detail later in this paper. The vehicle response was also examined for a pitching-moment increment of -0.014 at both Mach 4 and 5 and both of these cases had less overshoot than the one shown in figure 11. In these simulations there was no longitudinal stability or control problem and the vehicle was able to target properly in closed loop simulations.

The elevon deflection angles that occurred at Mach 4 and 5 in entry simulations with a multiplier on C_m are shown in figure 12. Decreasing the multiplier results in a more downward deflection of the elevons to provide a nose-down increment to counter the loss of the nose-down increment in C_m. Increasing the multiplier or the nose-down increment drives the elevon in the negative direction to provide a nose-up increment. Between GC_m values of 0.2 to 1.6, the vehicle remains controlled and achieves the guidance targeting requirements. For a value of 1.8, the vehicle followed the control commands well but was unable to meet the targeting requirements at 457 m/sec (1500 ft/sec). The degraded L/D due to negative elevon was apparently insufficient for the guidance algorithm.

A GC_m value of zero drove the elevon sufficiently positive so that the adverse yaw due to aileron resulted in a buildup in β when the aileron tried to control the roll angle and control was lost. In these simulations there still was no indication of a longitudinal stability or control problem due to these variations in GC_m.

Variation of Control Effectiveness

The effect of multiplier variation $G\Delta C_{m,\delta e}$ on elevon deflection at $M = 4$ and 5 during entry simulation is shown in figure 13. As the control authority of the elevon is increased, the elevon angle (δ_e) is driven toward zero. As the effectiveness is decreased, a more negative deflection is required to produce the positive (nose-up) increment. For a $G\Delta C_{m,\delta e}$ value of 0.3, δ_e reached the limit of -35° (data point not shown). With $G\Delta C_{m,\delta e} = 0.4$, the vehicle was unable to meet the guidance targeting requirements because of the degraded L/D.

The effects of applying multipliers to the nose-up increments due to the fixed body flap and scheduled speed brake in entry simulations are shown in figure 14. Multipliers from 0.2 to 1.6 on each of these parameters separately did not significantly affect the elevon deflection angle or the ability of the vehicle to remain controlled.

Although the elevon angle at Mach 5 is one of the more positive elevon angles in the trajectory, it does not seem to be a significant point in the trajectory in this study. The control problems have been shown to develop after

switchover to the rudder-aileron system. The ranges of the multipliers used in this study have not been found to affect the system prior to switchover except when δ_e in the entry simulations went to -35°. Therefore, in the ensuing discussion, only the δ_e that occurs in the entry simulations at Mach 4 is presented in the results.

Combined Variation of C_m and $\Delta C_{m,\delta e}$

The effects of multiplier variation on C_m for degraded elevon effectiveness on the entry simulation elevon deflection at Mach 4 are shown in figure 15. The decreased control effectiveness had a marked effect upon the variation of δ_e with GC_m as the figure shows. At Mach 4, the combination of increased stability and decreased control effectiveness required elevon deflections near the upper limit. For $G\Delta C_{m,\delta e} = 0.6$ and $GC_m = 1.4$, vehicle response simulation results after switchover showed that control was lost because of insufficient aileron remaining for roll control. For $GC_m = 1.3$, the vehicle failed to meet the guidance algorithm targeting requirements as roll control after switchover was loose and L/D was degraded. For $G\Delta C_{m,\delta e} = 0.7$ and $GC_m = 1.4$ the vehicle also failed to achieve the targeting requirements for the aforementioned reasons. A series of plots depicting the vehicle response to a step roll-angle command at $M_i = 4$ is presented in figure 16 for $G\Delta C_{m,\delta e} = 0.7$ and $GC_m = 1.4$. Since δ_e was less than -30° and the elevon position limit is -35°, there was insufficient aileron control to arrest the reversal and control was lost. For $G\Delta C_{m,\delta e} = 0.7$ with $GC_m = 1.3$ and $G\Delta C_{m,\delta e} = 0.6$ with $GC_m = 1.2$, the vehicle achieved the targeting requirements even though the roll angle was difficult to maintain.

For $GC_m = 0.2$ and $G\Delta C_{m,\delta e} = 0.6$, control was lost when the vehicle was unable to control β and the roll angle after switchover. For $GC_m = 0.3$ and $G\Delta C_{m,\delta e} = 0.6$, the vehicle recovered from a β of 1.7° and a roll-angle error oscillation of 33° after switchover to fly the guidance system roll-angle limits and achieve the targeting requirements. Also 86 kg (190 lb) of yaw RCS fuel was expended to augment the rudder after switchover. For $GC_m = 0.4$ and $G\Delta C_{m,\delta e} = 0.6$ and 0.7, the vehicle recovered from roll-angle errors of 11° and 10°, respectively, and achieved the targeting requirements.

Figure 17 presents the vehicle response to a step roll-angle command at $M_i = 4$ for both $GC_m = 0.3$ and 0.4 and $G\Delta C_{m,\delta e} = 0.6$. For $GC_m = 0.3$ (fig. 17(a)) the roll oscillation following the roll-angle change was rather severe with large sideslip angles. The rudder along with significant yaw jet firing (the steps in the δ_r curve indicate when the yaw jets fire) was eventually able to control the sideslip angle satisfactorily. For $GC_m = 0.4$, the rudder was able to control the sideslip angle without yaw jet augmentation, and roll-angle control was improved.

Increased elevon effectiveness ($G\Delta C_{m,\delta e} > 1$) reduced the effect of GC_m variation as is shown in figure 18 where the δ_e occurring at Mach 4 in entry simulations is plotted. The vehicle handled properly and achieved the guidance targeting requirements for all the data points shown.

The elevon effectiveness was varied for several values of GC_m and the δ_e values occurring at Mach 4 in entry simulations are shown in figure 19. As $G\Delta C_{m,\delta e}$ was decreased, δ_e goes toward the extremes depending upon the value of GC_m. For $GC_m = 0.4$ and $G\Delta C_{m,\delta e} = 0.4$, the vehicle was barely able to achieve the targeting requirements after recovering from a roll-angle control problem after switchover. The guidance targeting requirements were achieved for $GC_m = 0.6$ for the values of $G\Delta C_{m,\delta e}$ shown ($G\Delta C_{m,\delta e} > 0.6$). Also the targeting requirements were met for $GC_m = 1.2$ and the values of $G\Delta C_{m,\delta e}$ shown. For $GC_m = 1.3$, $G\Delta C_{m,\delta e}$ must be equal to or greater than 0.7 to generate sufficient L/D to achieve the targeting requirements. Thus, some critical values of GC_m and $G\Delta C_{m,\delta e}$ are identifiable, namely $G\Delta C_{m,\delta e} = 0.7$, $GC_m = 0.4$, and $GC_m = 1.3$. A $G\Delta C_{m,\delta e}$ value of 1.8 is a boundary value because simulation tests were not conducted at larger values.

Combined Variation of C_m, $\Delta C_{m,\delta e}$, $\Delta C_{m,\delta BF}$, and $\Delta C_{m,\delta SB}$

Both the body flap and speed brake provide positive (nose-up) pitching-moment increments (figs. 7 and 8) and variations in these coefficients have been shown to have little effect on the vehicle with otherwise nominal aerodynamics. The positive pitch increment of these devices will result in more positive elevon deflections for multipliers greater than one. (See fig. 14.) Thus, whenever GC_m and $G\Delta C_{m,\delta e}$ are near boundary values for positive elevon deflections, multipliers on body flap and/or speed brake pitching moment will affect controllability and targeting capability.

For $G\Delta C_{m,\delta e} = 1.8$ and GC_m between 0.4 and 1.3, body-flap multiplier variations from 0.6 and 1.4 have little effect on the elevon deflection (fig. 20(a)) and the controllability. For $GC_m = 0.4$, $G\Delta C_{m,\delta e} = 0.7$, and $G\Delta C_{m,\delta BF} = 1.4$ (fig. 20(b)), δ_e was increased to the point where the adverse yaw due to aileron made roll-angle control poor after switchover and the vehicle barely missed achieving the targeting requirements. For $GC_m = 0.6$ and the values of $G\Delta C_{m,\delta BF}$ shown, targeting requirements were met. The vehicle response to a step roll-angle command at $M_i = 4$ for $GC_m = 0.4$ and 0.6 with $G\Delta C_{m,\delta e} = 0.7$ and $G\Delta C_{m,\delta BF} = 1.4$ is shown in figure 21. The difficulty with roll angle (ϕ) and sideslip (β) for $GC_m = 0.4$ is apparent and the improvement in going to $GC_m = 0.6$ is evident as δ_e was decreased from about 3° to -1° which decreases the adverse yaw due to aileron. Reducing $G\Delta C_{m,\delta BF}$ to 1.3 for $GC_m = 0.4$ and $G\Delta C_{m,\delta e} = 0.7$ had negligible effect on the system performance.

For $G\Delta C_{m,\delta e} = 0.7$ and $GC_m = 1.3$ (fig. 20(b)), the vehicle tended to roll off after switchover but it was able to meet the targeting requirements for the values of $G\Delta C_{m,\delta BF}$ shown. For $GC_m = 1.2$, the vehicle did not experience the roll-off tendency.

The effects of variations of the speed brake effectiveness in the presence of increased and/or decreased C_m and elevon effectiveness are presented in figure 22. For $G\Delta C_{m,\delta e} = 1.8$, there is little effect for both increased and decreased C_m. (See fig. 22(a).) For decreased elevon effectiveness, $G\Delta C_{m,\delta e} = 0.7$, and for decreased C_m, $GC_m = 0.4$ (fig. 22(b)), the vehicle barely met the targeting requirements for $G\Delta C_{m,\delta SB} = 1.4$. The sideslip angle β reached 1.35° after switchover and roll-angle control was very poor. For

increased stability, $GC_m = 1.2$, roll angle tended to be poor but the vehicle was able to meet the targeting requirements for the values of $G\Delta C_{m,\delta SB}$. For $GC_m = 1.3$ and $G\Delta C_{m,\delta SB} < 0.7$ the vehicle was unable to meet the targeting requirements because of the degraded L/D.

The preceding discussion has shown that degraded elevon effectiveness, when combined with variations in C_m and either body-flap or speed-brake effectiveness variations, resulted in marginal performance for several combinations. This performance was poorest when all four parameters were varied. For example, although $GC_m = 0.4$, $G\Delta C_{m,\delta e} = 0.7$, and $G\Delta C_{m,\delta SB} = 1.4$ barely met the targeting requirements, adding in $G\Delta C_{m,\delta BF} = 1.4$ resulted in control loss. For $G\Delta C_{m,\delta SB} = G\Delta C_{m,\delta BF} = 1.3$, $GC_m = 0.4$, and $G\Delta C_{m,\delta e} = 0.7$, roll-angle control was very poor and the targeting requirements were not met. A further decrease in the multipliers for speed brake and body flap effectiveness provided satisfactory performance; however, it was decided to retain some tolerance in both the speed brake and body flap effectiveness and decrease the tolerance in C_m, that is, make $GC_m = 0.6$ a boundary value instead of $GC_m = 0.4$. Similarly, it was decided to change the upper GC_m boundary from 1.3 to 1.2, since when $GC_m = 1.3$, $G\Delta C_{m,\delta e} = 0.7$, and $G\Delta C_{m,\delta SB} = 0.7$, the vehicle failed to meet targeting requirements. The multiplier $G\Delta C_{m,\delta e}$ could have been changed to 0.8 from 0.7 and achieved the same result; however, to obtain a more symmetrical tolerance band for GC_m, it was decided to change the boundary value for GC_m in lieu of $G\Delta C_{m,\delta e}$. With these boundary values for GC_m established, the effects of varying $G\Delta C_{m,\delta SB}$ and $G\Delta C_{m,\delta BF}$ together are shown in figures 23 to 25.

For $G\Delta C_{m,\delta e} = 1.8$ (fig. 23), there was little effect on δ_e at Mach 4 in the entry simulations over the range of variations shown. With $GC_m = 0.6$ and $G\Delta C_{m,\delta BF} = G\Delta C_{m,\delta SB} = 1.4$, the vehicle met the targeting requirements and controlled satisfactorily. The vehicle response to a step roll-angle command at $M_i = 4$ for these multiplier values is shown in figure 24. There was some roll-angle overshoot and an oscillation which damps out.

The elevon deflection angles occurring at Mach 4 in entry simulations for $G\Delta C_{m,\delta e} = 0.7$ are shown in figure 25. For $GC_m = 0.6$ and the values of $G\Delta C_{m,\delta BF} < 1.0$ (shown in fig. 25(a)), the vehicle roll-angle errors were minimal and targeting requirements were met. For $G\Delta C_{m,\delta BF} = 1.4$ and the values of $G\Delta C_{m,\delta BF}$ shown, the vehicle also performed satisfactorily. For $G\Delta C_{m,\delta BF} = 1.6$ and $G\Delta C_{m,\delta SB} = 1.6$, however, the vehicle was unable to meet targeting requirements, and roll-angle excursions were greater than 20° after switchover. $G\Delta C_{m,\delta SB} = 1.4$ resulted in some improvement over $G\Delta C_{m,\delta SB} = 1.6$. The vehicle response at $M_i = 4$ for $G\Delta C_{m,\delta BF} = 1.6$ and $G\Delta C_{m,\delta SB} = 1.4$ is shown in figure 26. The oscillation following the reversal does not appear to be damping out readily; thus, this combination was not considered to be satisfactory.

The results for $GC_m = 1.2$ are shown in figure 25(b). For $G\Delta C_{m,\delta BF} = 1.4$, the vehicle performed satisfactorily for all values of $G\Delta C_{m,\delta SB}$ shown. For $G\Delta C_{m,\delta BF} = 0.8$, the vehicle also performed satisfactorily for the points shown. For $G\Delta C_{m,\delta BF} = 0.7$ and $G\Delta C_{m,\delta SB} = 1.0$, the vehicle was required to fly the guidance minimum roll-angle limits to meet the targeting requirements. Nevertheless, the targeting capability was adequate for $G\Delta C_{m,\delta SB} = 0.8$ and 0.7 whereas the vehicle was unable to meet targeting requirements for $G\Delta C_{m,\delta SB} = 0.6$.

Parameter Boundary Values

At this point some apparent boundary values for each of the four parameters have emerged, based on controllability and the targeting ability. The boundary values of the multipliers are as follows: the pitching moment GC_m can be varied between 0.6 and 1.2; the elevon effectiveness in pitch $G\Delta C_{m,\delta e}$ can be varied from 0.7 to 1.8; the body flap effectiveness in pitch $G\Delta C_{m,\delta BF}$ can be varied from 0.7 to 1.4; and the speed brake effectiveness in pitch $G\Delta C_{m,\delta SB}$ can be varied from 0.7 to 1.4. The ranges for each of these coefficients assume that each of the other coefficients is within its respective boundaries and the lateral-directional aerodynamics are nominal. Also, it was shown initially that an increment in pitching moment from -0.014 to 0.014 can be tolerated by the system.

Discussion of Roll-Off Tendency

In the previous discussion, it was shown that when the elevon deflection was positive at switchover, there tended to be a build-up of the sideslip angle β accompanied by poor roll-angle control which sometimes resulted in loss of control. A detailed analysis of this tendency discussed in reference 2 showed that the rolling moment due to sideslip angle can be sufficient to overpower the aileron. This was particularly true when the yaw due to aileron deflection was adverse which means that as the aileron was deflected to counter the induced rolling moment, a yawing moment was generated which increased the sideslip angle and induced more adverse rolling moment. The rudder is designed to control this yawing tendency but at switchover at $\alpha = 18^\circ$, the rudder is weak. Increasing the yaw jet augmentation of the rudder after switchover, as proposed in reference 2, has been found to improve the sideslip control and reduce the tendency to roll off. For $GC_m = 0.6$, $G\Delta C_{m,\delta e} = 0.7$, $G\Delta C_{m,\delta BF} = 1.4$, and $G\Delta C_{m,\delta SB} = 1.4$, increased yaw jet augmentation of the rudder reduced β from 0.64° to 0.28° and reduced roll-angle error from about 11° to less than 3° in the entry simulations. The system consumed 23 kg (51 lb) more RCS fuel with increased augmentation and the targeting capability was improved slightly. Other combinations of boundary values of the multipliers also showed improved roll-angle control and required less than the increment of 23 kg (51 lb) of RCS fuel. Figure 27 shows the vehicle response to a roll-angle reversal at $M_i = 4$ with and without increased rudder augmentation by the yaw jets for $GC_m = 0.6$, $G\Delta C_{m,\delta e} = 0.7$, and $G\Delta C_{m,\delta BF} = G\Delta C_{m,\delta SB} = 1.4$. With the increased augmentation the oscillation following the roll reversal is virtually eliminated. Notice the sawtooth appearance of the rudder curve with increased augmentation that indicated the firing of the yaw jet. Delaying the switchover to an angle of attack of 15°, as discussed in reference 2, for the condition $GC_m = 0.6$, $G\Delta C_{m,\delta e} = 0.7$, $G\Delta C_{m,\delta BF} = 1.4$, and $G\Delta C_{m,\delta SB} = 1.4$ also resulted in smaller sideslip angles and bank angle errors after the switchover since the rudder is more effective at the lower angle of attack and lower Mach number. Again the targeting was slightly improved and about 18 kg (39 lb) more RCS fuel was consumed as the entry controller, using the yaw RCS jets for roll-angle control, was used for a longer period of time.

System Response Analysis

The control system was commanded to respond to both 2° angle-of-attack step commands and 30° roll-angle step commands (as defined in the procurement specification) separately at 3048 m/sec (10 000 ft/sec), 1524 m/sec (5000 ft/sec), 1067 m/sec (3500 ft/sec), and 610 m/sec (2000 ft/sec). Generally, the system performed well even with the boundary values for the coefficients. The procurement specification response envelope was not met in all cases as is shown in figure 28. For $GC_m = 1.2$, $G\Delta C_{m,\delta e} = 0.7$, $G\Delta C_{m,\delta BF} = 0.7$, and $G\Delta C_{m,\delta SB} = 0.7$, the elevon was deflected up and when the system was commanded to pitch up 2°, the elevon moved to very near the up deflection limit at 1067 m/sec (3500 ft/sec) and 610 m/sec (2000 ft/sec). This was the worst response of the combinations and conditions tested. Thus, the boundary values herein established do not necessarily meet the procurement specification but they are not far from the response of the nominal system. With nominal lateral-directional aerodynamics and these boundary values, the system did respond satisfactorily to 30° roll-angle step commands with increased rudder augmentation.

CONCLUSIONS

A six-degree-of-freedom simulation analysis was conducted to examine the effects of longitudinal static aerodynamic stability and control uncertainties on the performance of the space shuttle orbiter automatic (no manual inputs) entry guidance and control systems. To establish the acceptable boundaries, the static aerodynamic characteristics were varied either by applying a multiplier to the aerodynamic parameter or by adding an increment. The vehicle stability and control was found to be most critical from Mach 4 to 5 for the range of the entry trajectory studied and the vehicle was found to fly satisfactorily in this Mach range on or within the following boundaries:

1. The pitching-moment coefficient can be decreased to 0.6 or increased to 1.2 times its nominal value.

2. The elevon effectiveness in pitch can be from 0.7 to 1.8 times its nominal value.

3. The body flap effectiveness in pitch can be from 0.7 to 1.4 times the nominal value.

4. The speed brake effectiveness in pitch can be from 0.7 to 1.4 times the nominal value.

5. If an increment in the pitching moment is allowed to cover all these off-nominal values, the increment can be from -0.014 to 0.014.

Basically, the system appeared sound in longitudinal stability and controllability. However, lateral-directional stability and control weaknesses were affected

by pitching-moment variations and two system modifications were found to help establish satisfactory performance in the boundaries listed.

Langley Research Center
National Aeronautics and Space Administration
Hampton, VA 23665
August 17, 1977

REFERENCES

1. Malkin, M. S.: Space Shuttle/The New Baseline. Astronaut. & Aeronaut., vol. 12, no. 1, Jan. 1974, pp. 62-78.

2. Stone, Howard W.; and Powell, Richard W.: Entry Dynamics of Space Shuttle Orbiter With Lateral-Directional Stability and Control Uncertainties at Supersonic and Hypersonic Speeds. NASA TP-1011, 1977.

3. Kaylor, Jack T.; Rowell, Lawrence F.; and Powell, Richard W.: A Real-Time Digital Computer Program for the Simulation of Automatic Spacecraft Reentries. NASA TM X-3496, 1977.

TABLE I.- PHYSICAL CHARACTERISTICS OF SPACE SHUTTLE ORBITER

Mass properties:	
Mass, kg (lb)	83 001 (182 986)
I_X, kg-m^2 (slug-ft^2)	1 029 052 (759 000)
I_Y, kg-m^2 (slug-ft^2)	7 816 187 (5 765 000)
I_Z, kg-m^2 (slug-ft^2)	8 015 489 (5 912 000)
I_{XZ}, kg-m^2 (slug-ft^2)	177 609 (131 000)
Wing:	
Reference area, m^2 (ft^2)	249.91 (2690.0)
$\bar{c}$, m (ft)	12.06 (39.57)
Span, m (ft)	23.79 (78.06)
Elevon:	
Reference area, m^2 (ft^2)	19.51 (210.0)
Chord, m (ft)	2.30 (7.56)
Rudder:	
Reference area, m^2 (ft^2)	9.30 (100.15)
Chord, m (ft)	1.86 (6.1)
Body flap:	
Reference area, m^2 (ft^2)	12.54 (135.0)
Chord, m (ft)	2.06 (6.75)

TABLE II.- SYSTEM PERFORMANCE CRITERIA

Entry guidance target requirements at a velocity of 457 m/sec (1500 ft/sec)	Altitude error $\leq$+0.3 km (+1000 ft); range error $\leq$+9.3 km (+5 n. mi.); flight-path angle error $\leq\pm1^\circ$
Normal acceleration	$\leq$2.5g
Amplitude of ϕ oscillation	$\leq\pm10^\circ$
Increase in RCS fuel consumption due to off-nominal aerodynamics	$\leq$135 kg (300 lb)

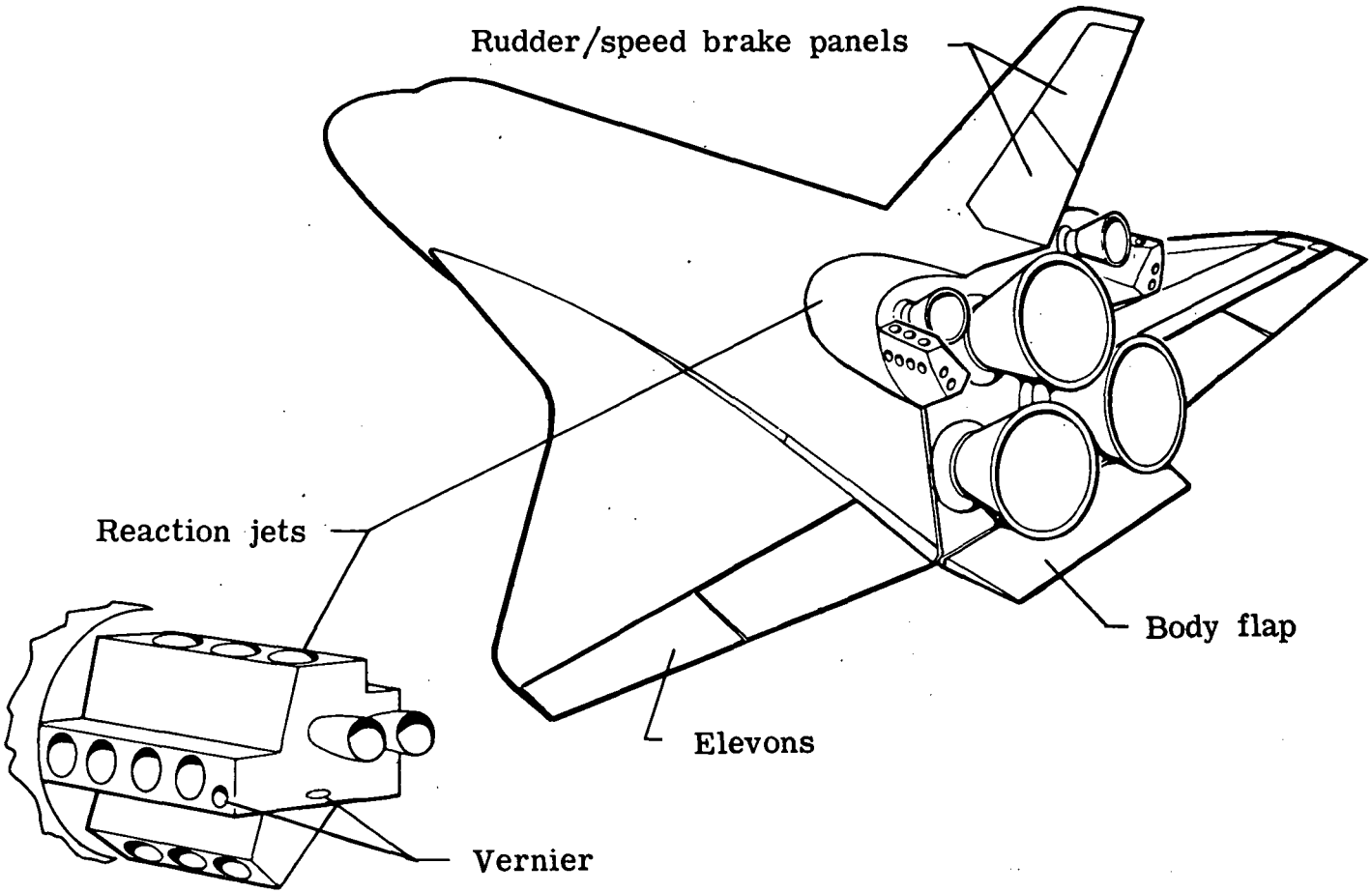

Figure 1.- Space shuttle orbiter.

Figure 2.- Space shuttle orbiter entry.

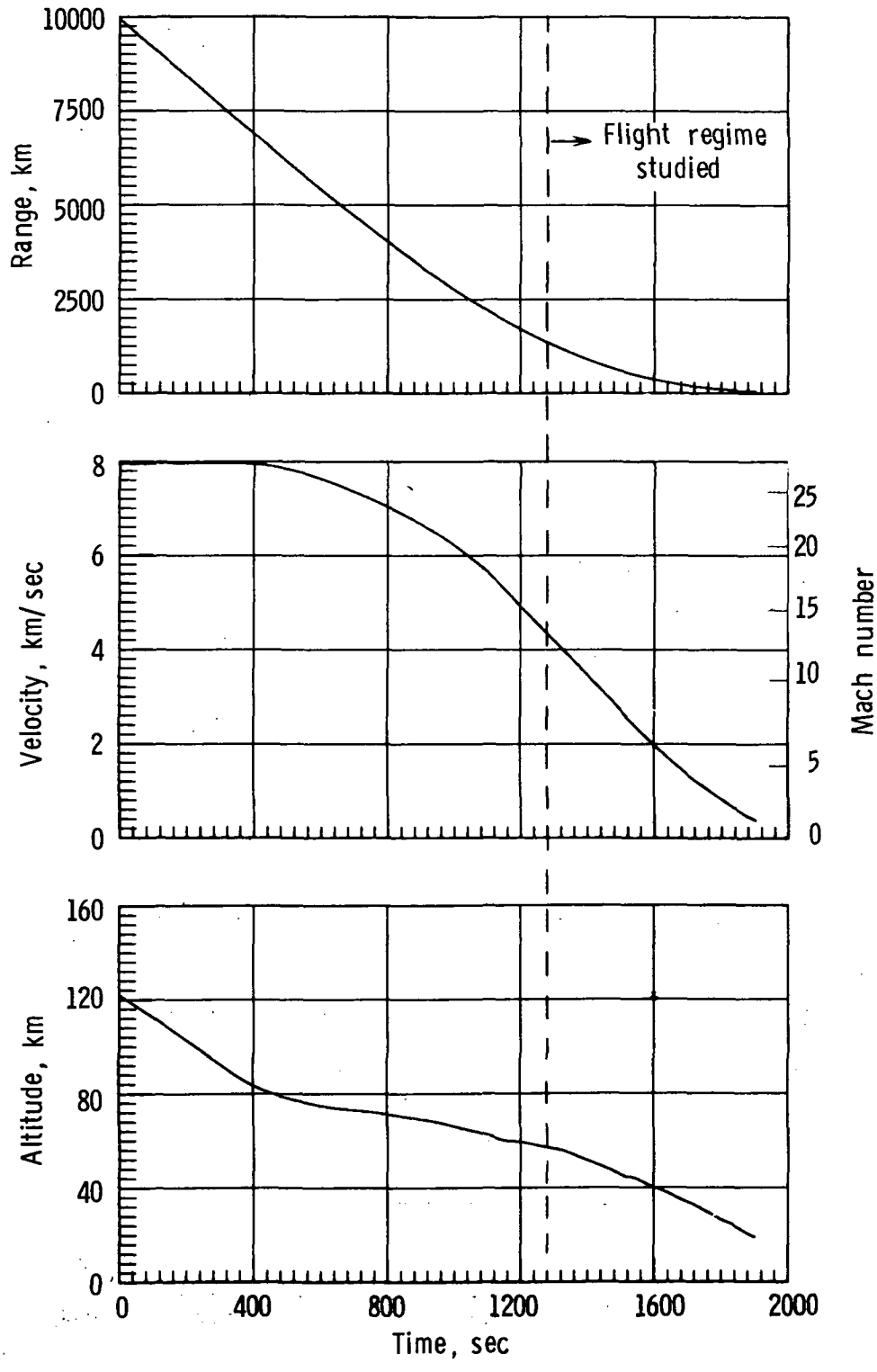

Figure 3.- Space shuttle orbiter entry trajectory parameters.

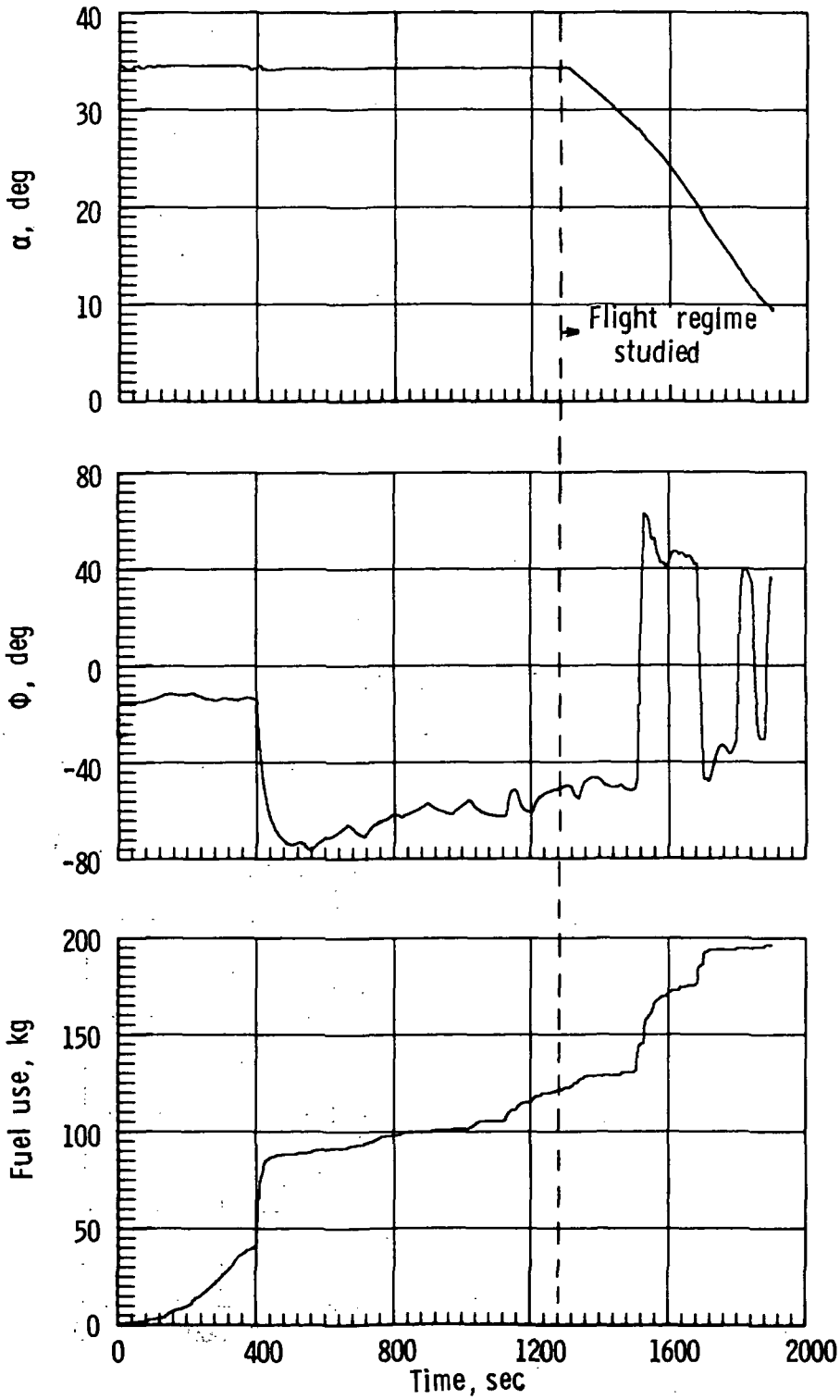

Figure 3.- Concluded.

Body flap schedule

Forward center of gravity, $\delta_{BF} = -11.7^{\circ}$

Aft center of gravity, $\delta_{BF} = 16.3^{\circ}$

Speed brake schedule

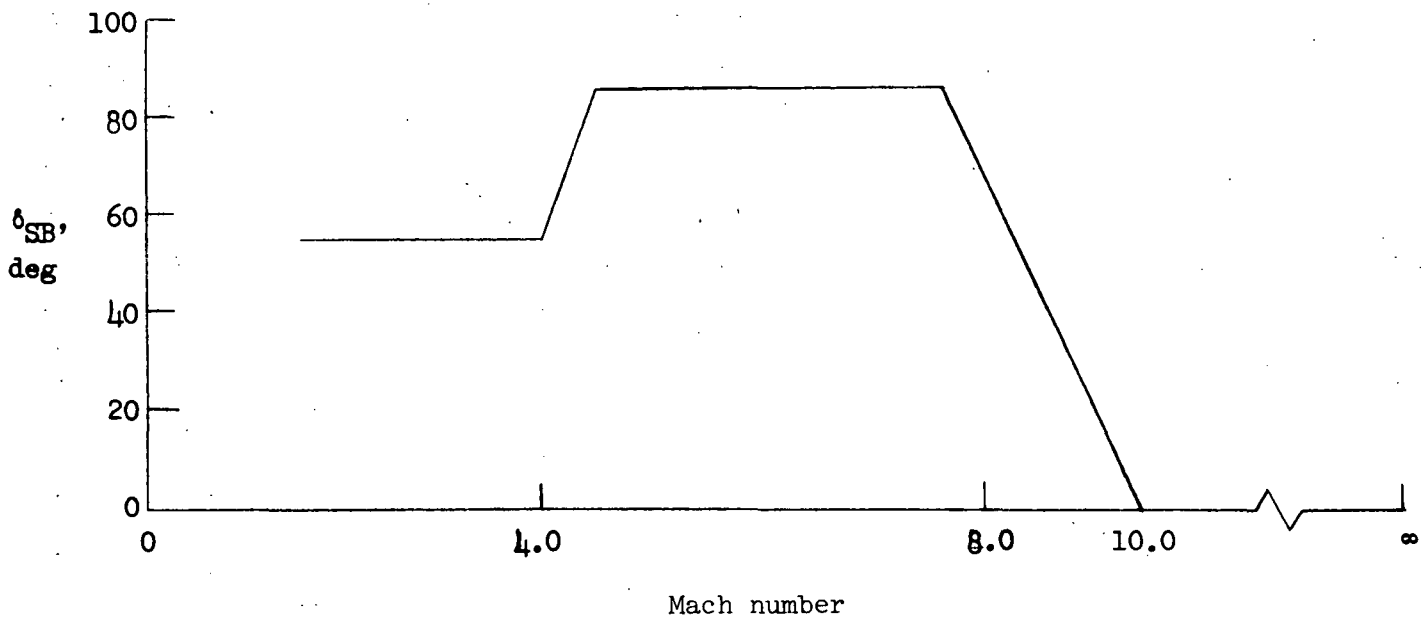

Figure 4.- Body flap and speed brake schedules.

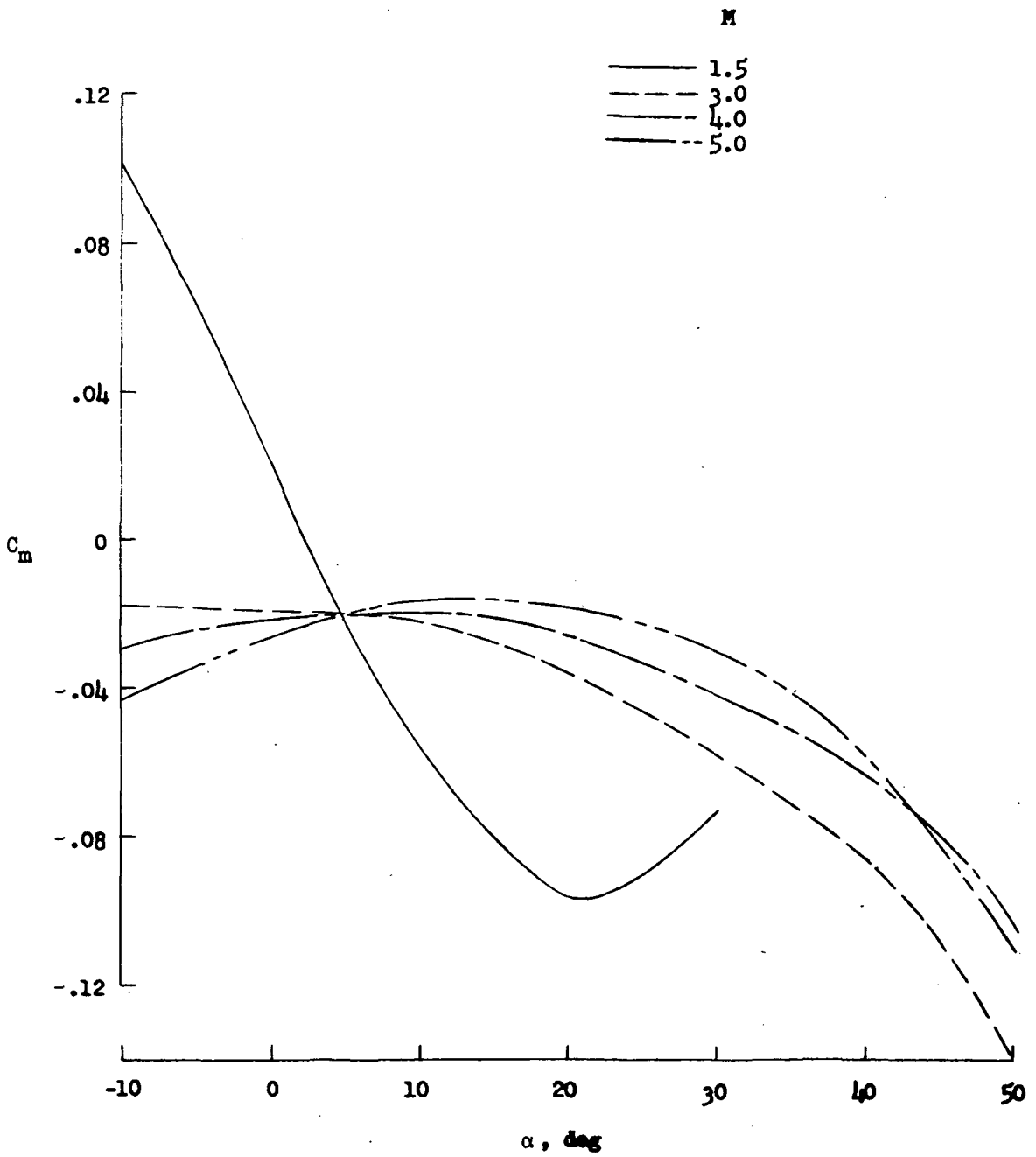

Figure 5.- Pitching moment for undeflected controls.

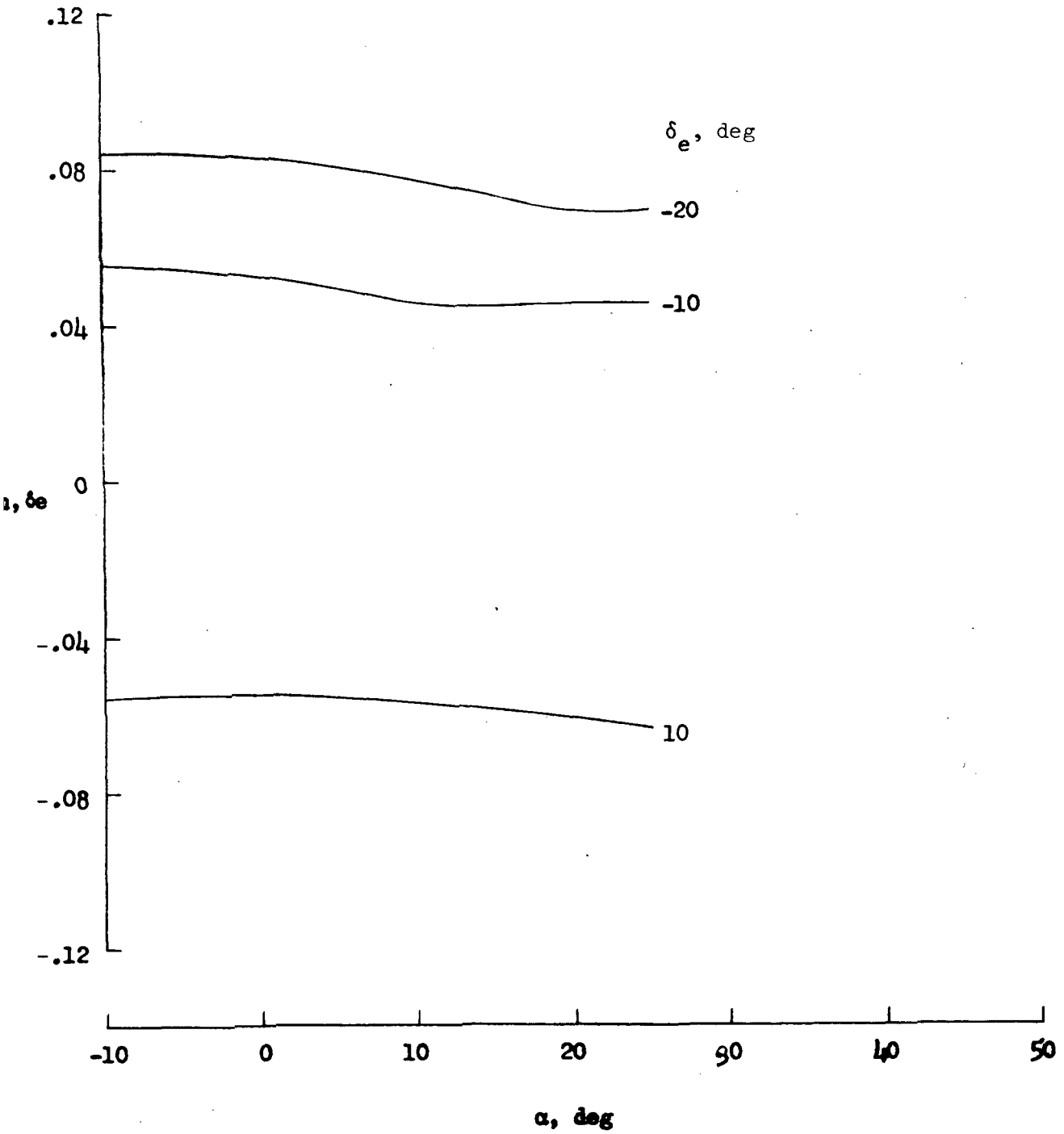

(a) M = 1.5.

Figure 6.- Elevon effectiveness.

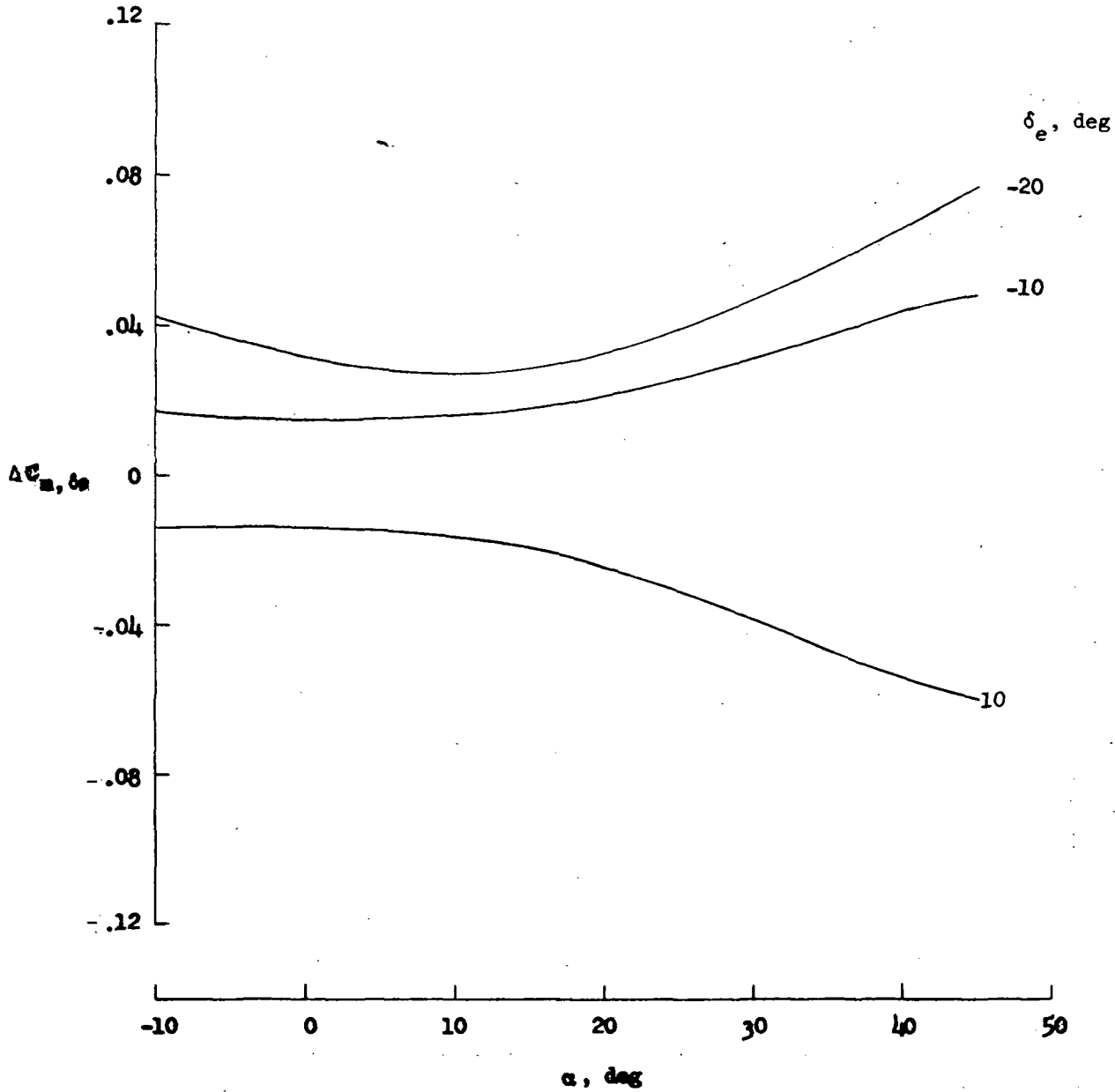

(b) M = 3.0

Figure 6.- Continued.

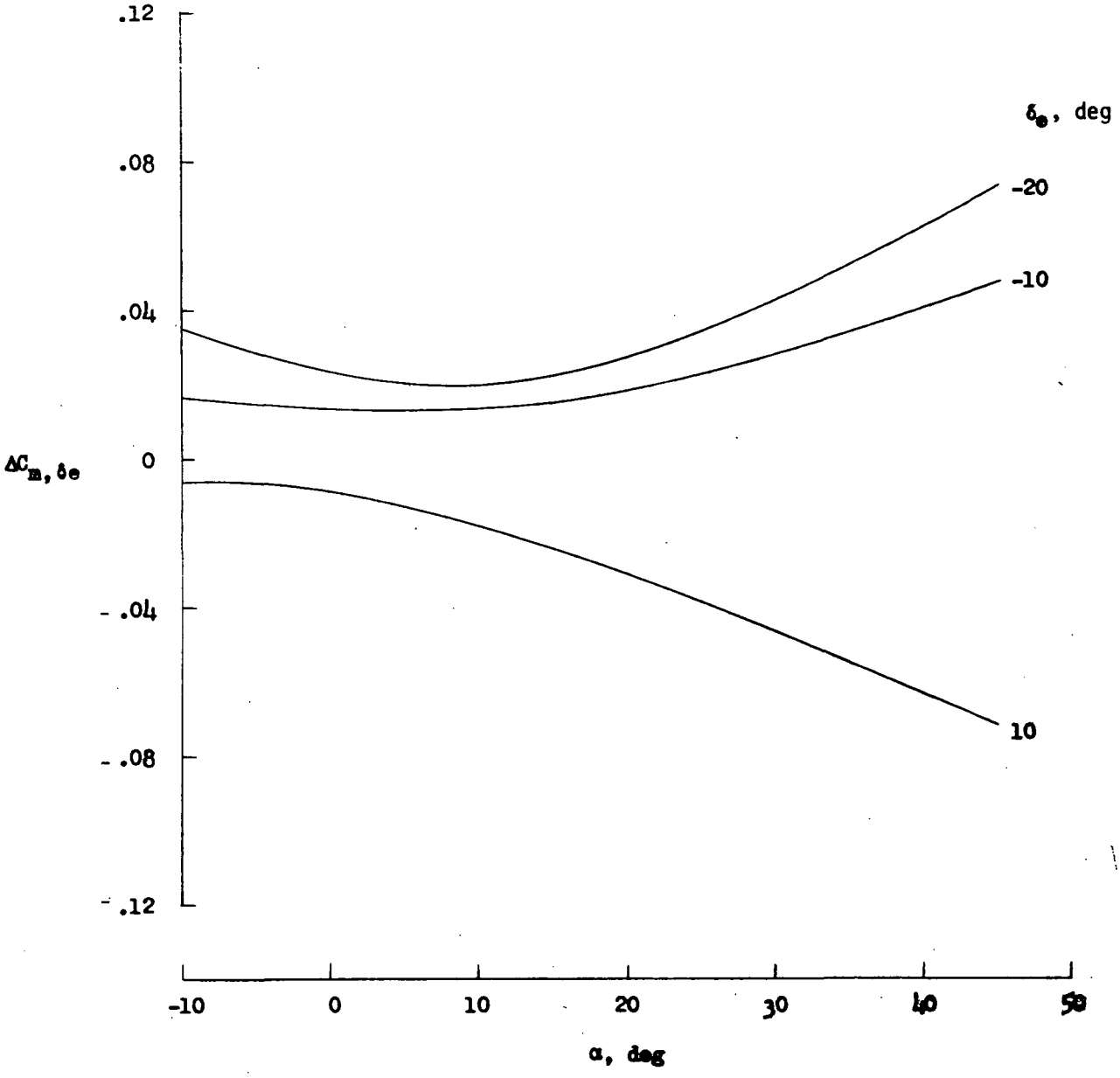

(c) M = 4.0.

Figure 6.- Continued.

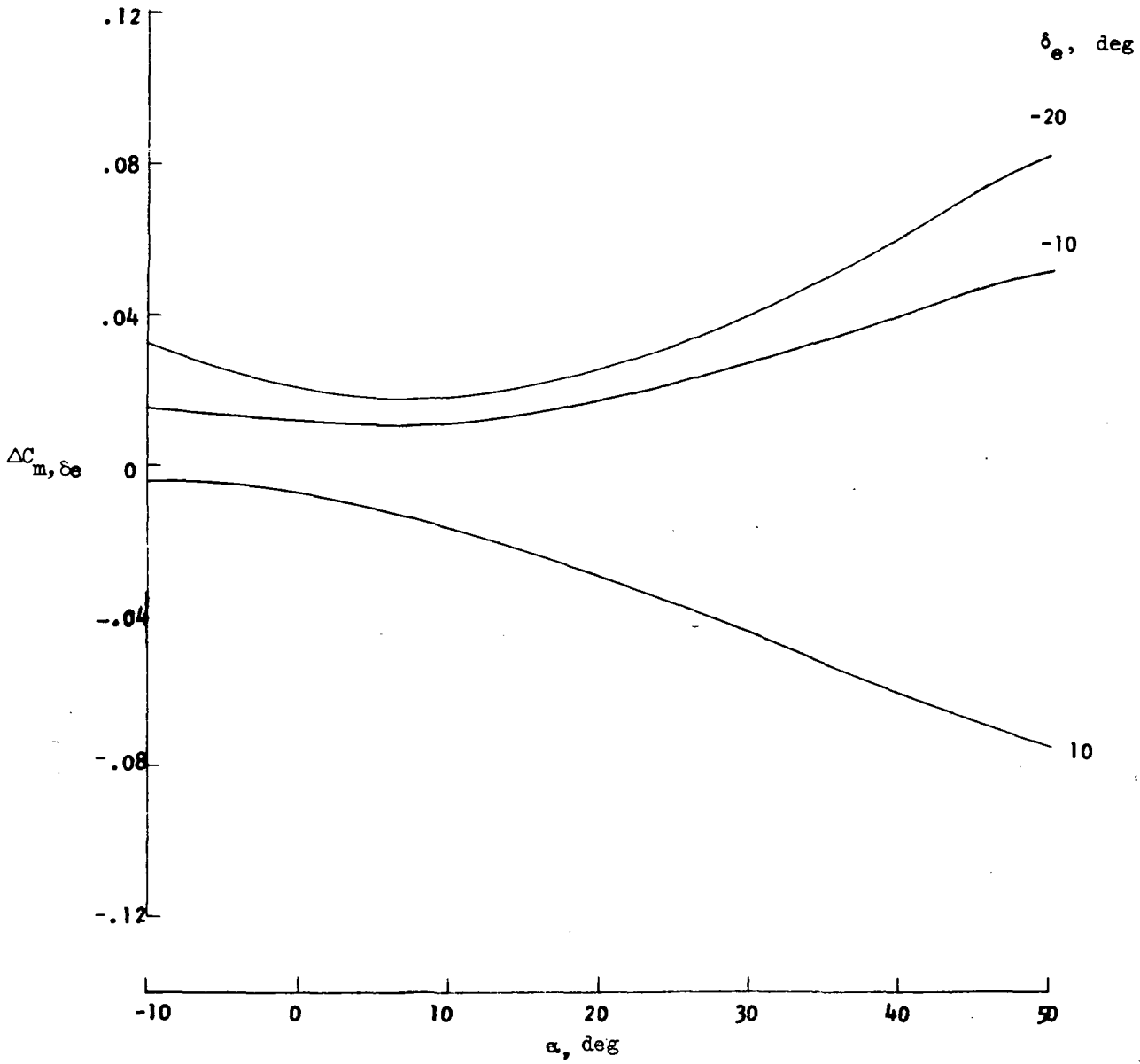

(d) M = 5.0.

Figure 6.- Concluded.

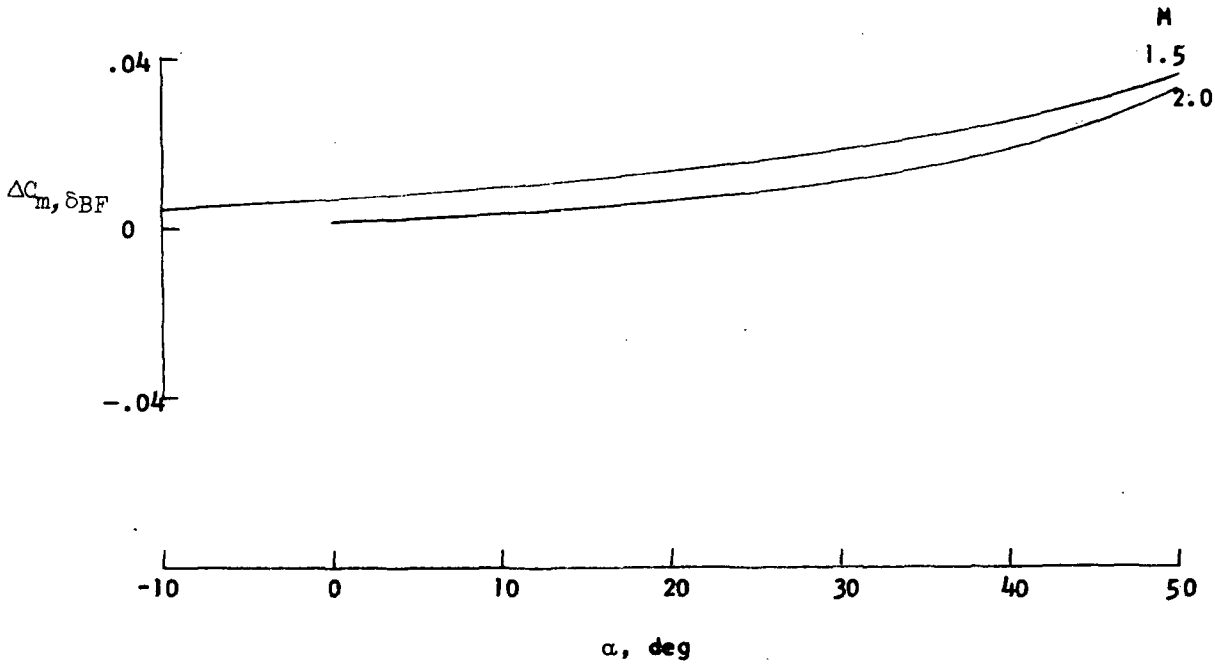

Figure 7.- Body flap effectiveness. $\delta_{BF} = -11.7^{\circ}$.

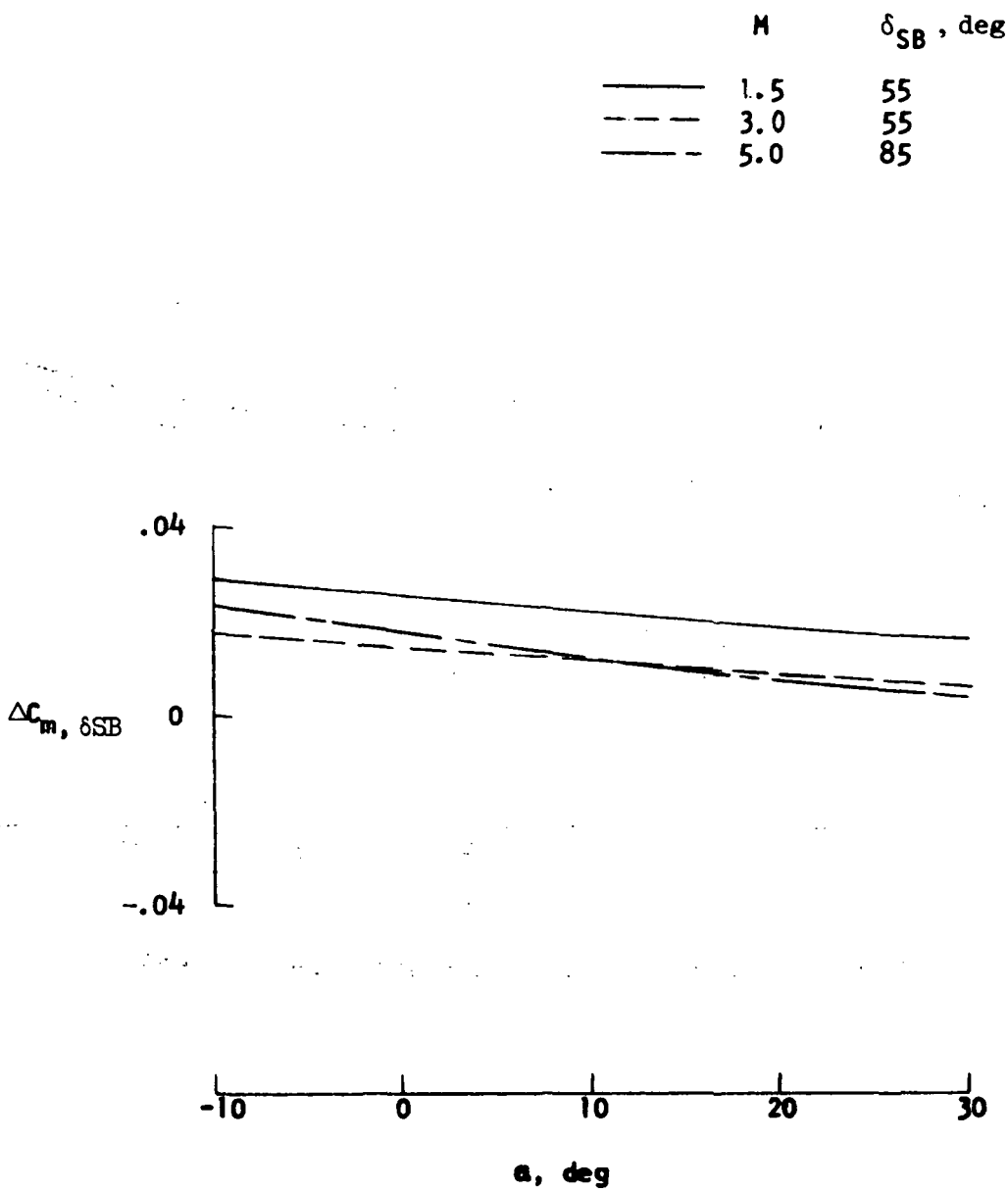

Figure 8.- Speed brake effectiveness.

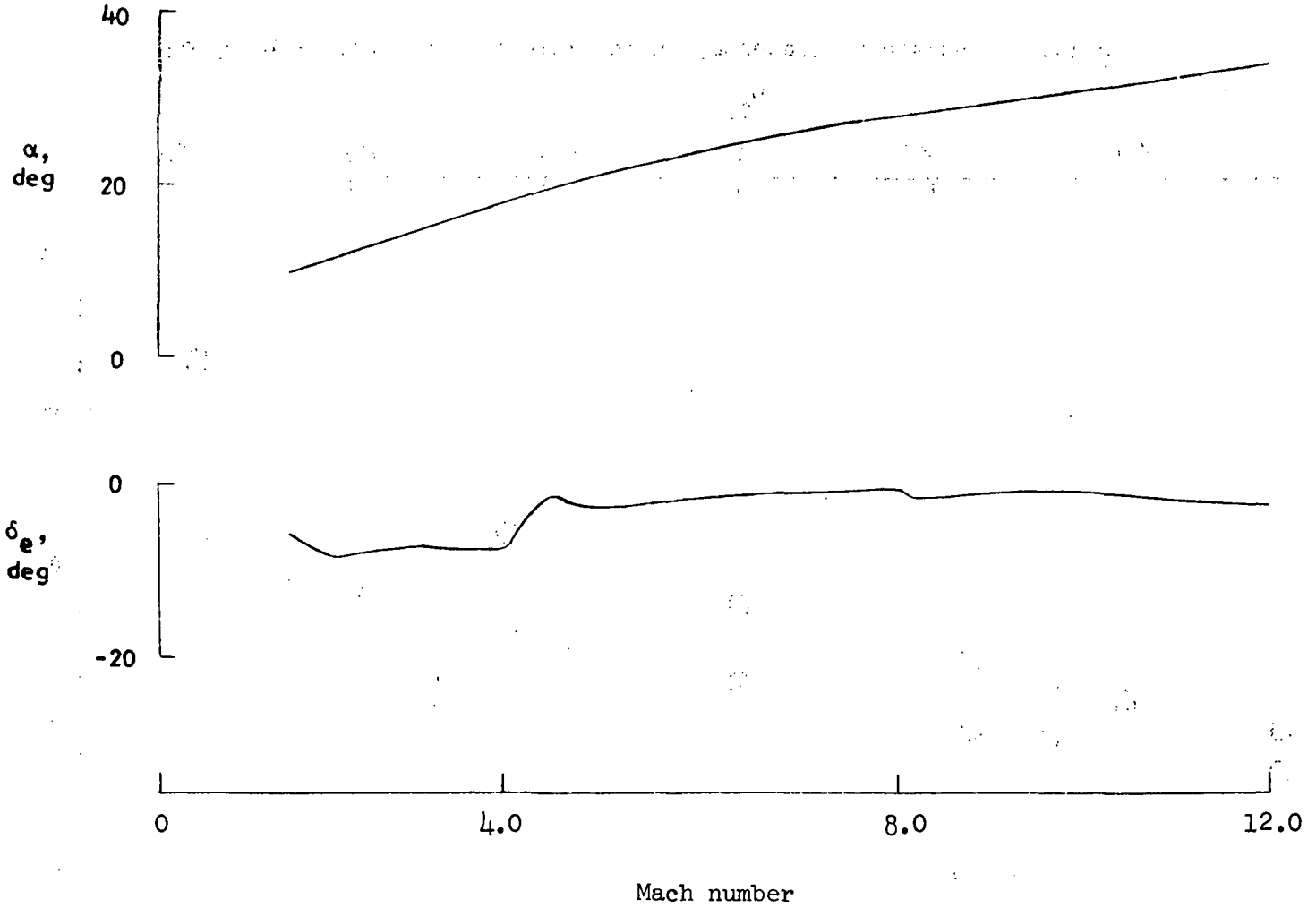

Figure 9.- Nominal elevon and angle-of-attack trends.

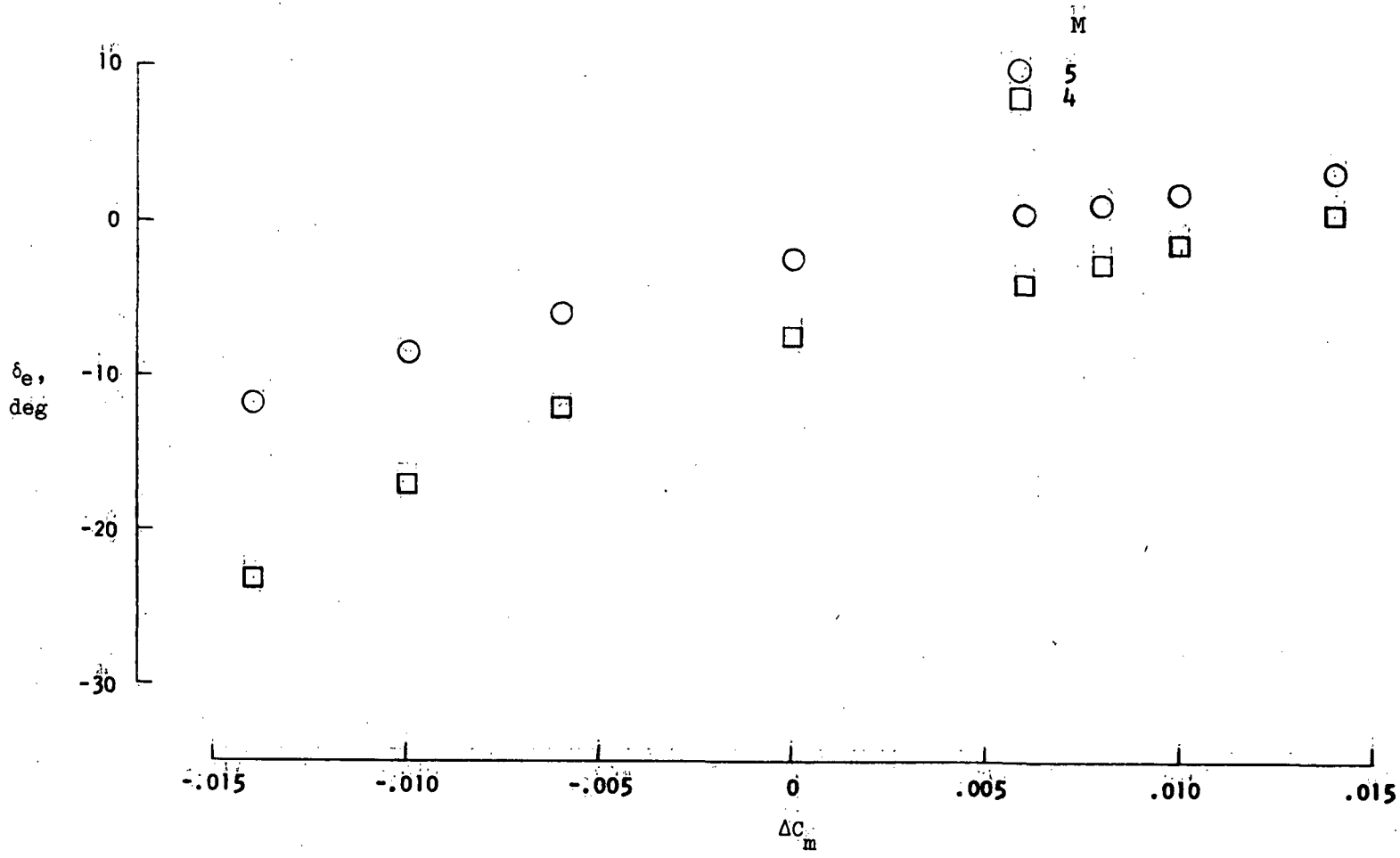

Figure 10.- Effect of pitching-moment increment on elevon deflection.

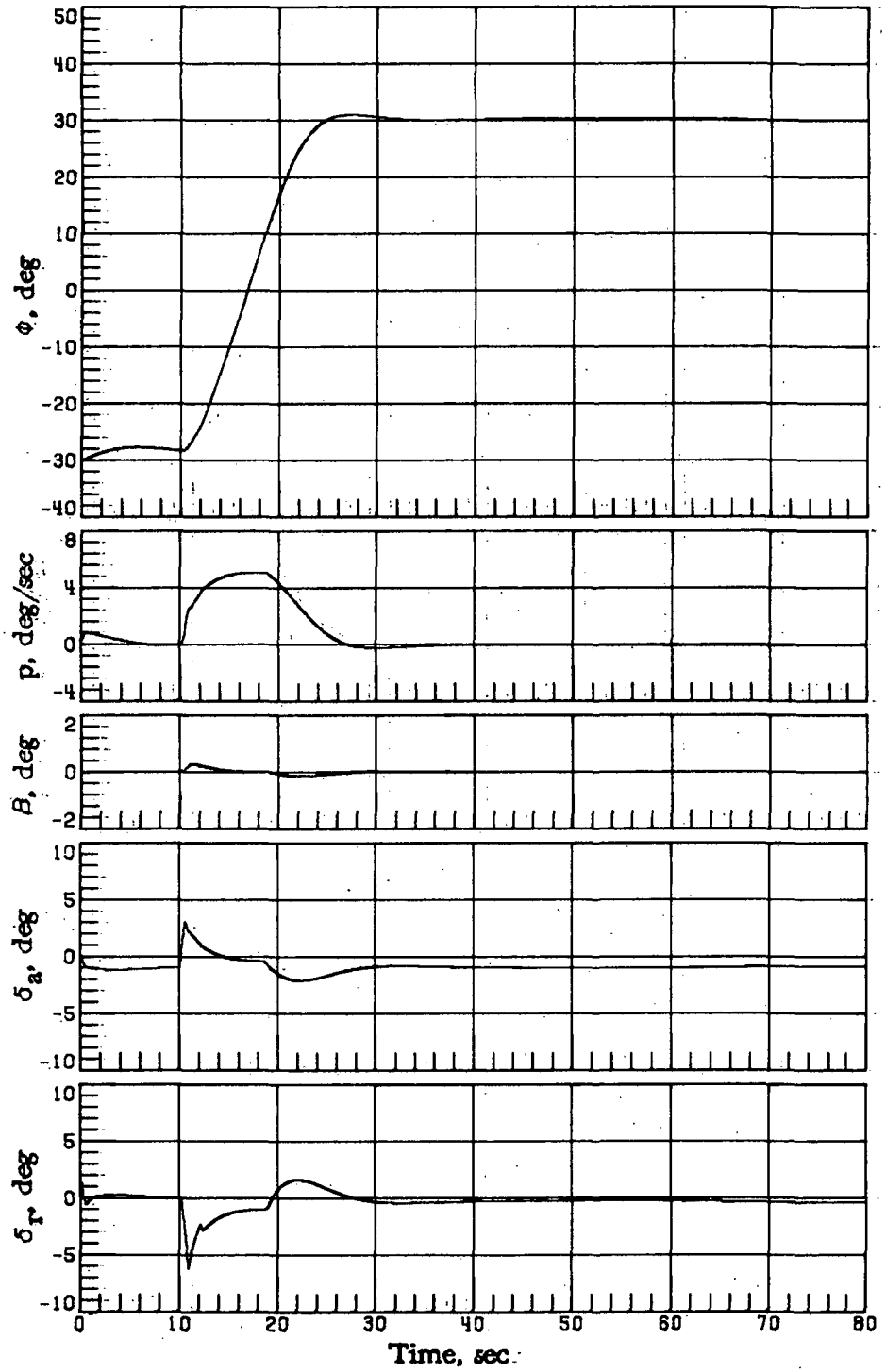

(a) $\Delta C_m = 0$ (nominal).

Figure 11.- Vehicle response simulations at $M_i = 4$ with various levels of ΔC_m ($\alpha_c = 17.6^o$, $\phi_c = -30^o$ for time <10 sec and $\phi = 30^o$ for time ≥ 10 sec).

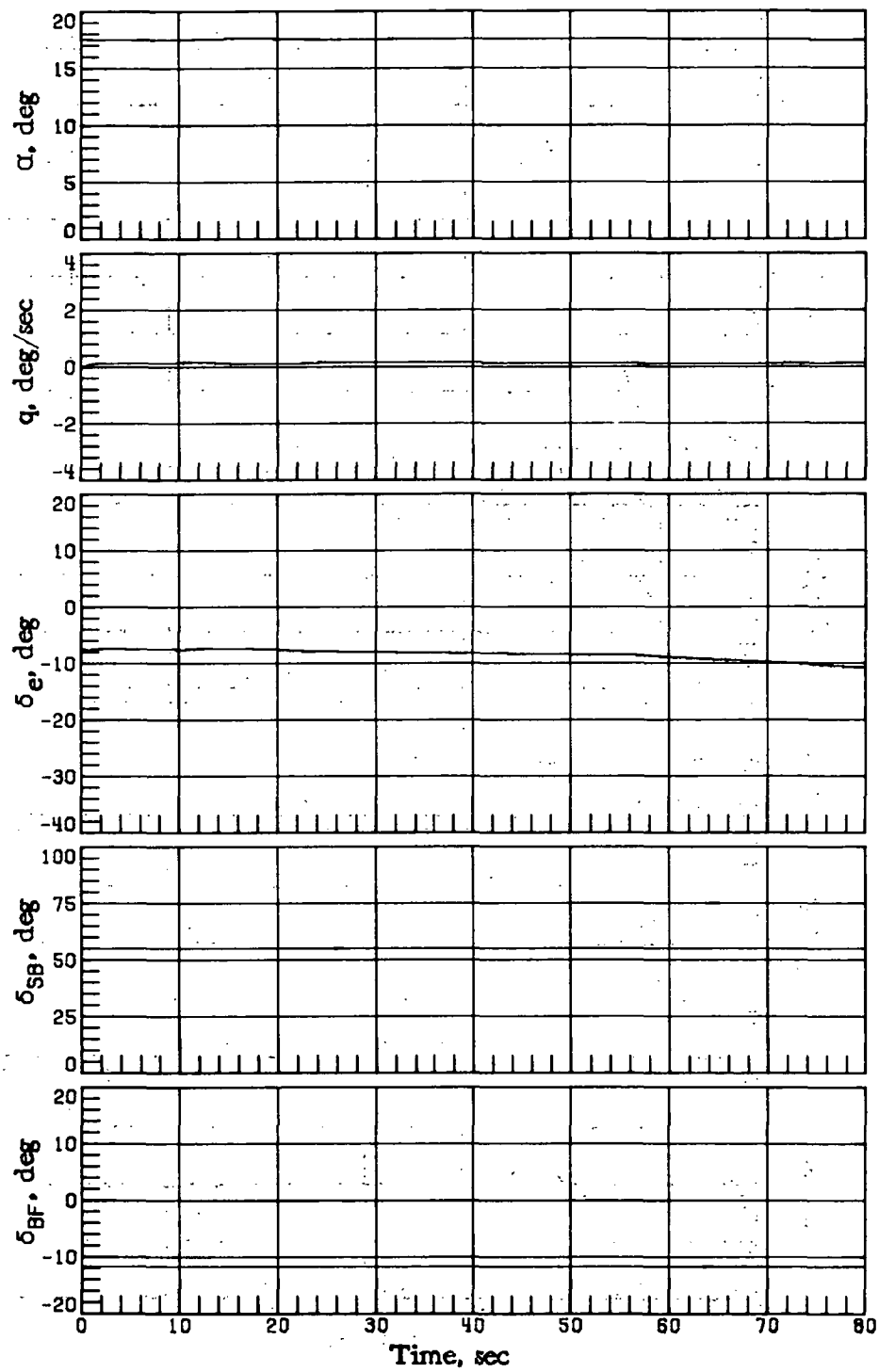

(a) Concluded.

Figure 11.- Continued.

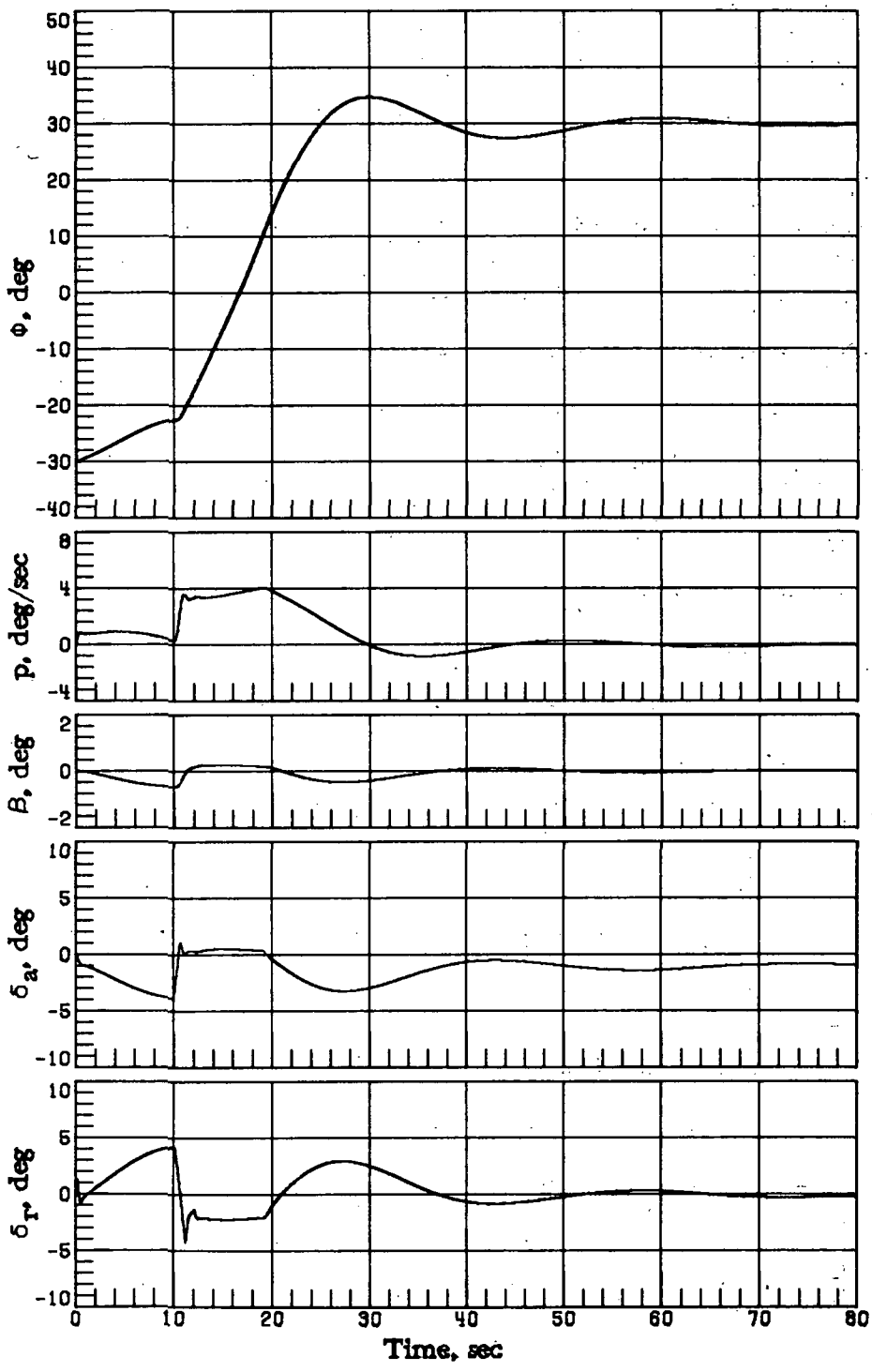

(b) $\Delta C_m = 0.014$.

Figure 11.- Continued.

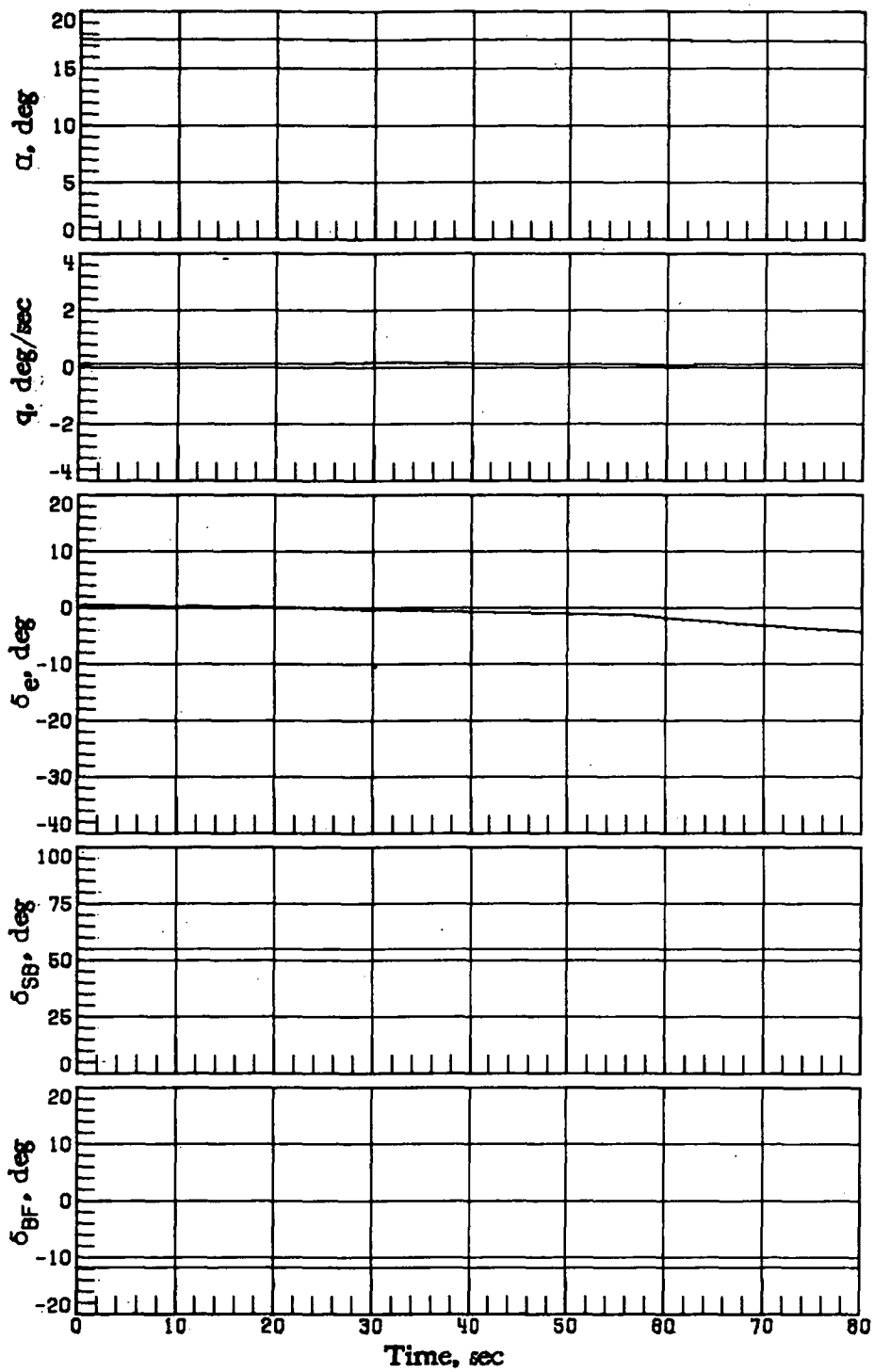

(b) Concluded.

Figure 11.- Concluded.

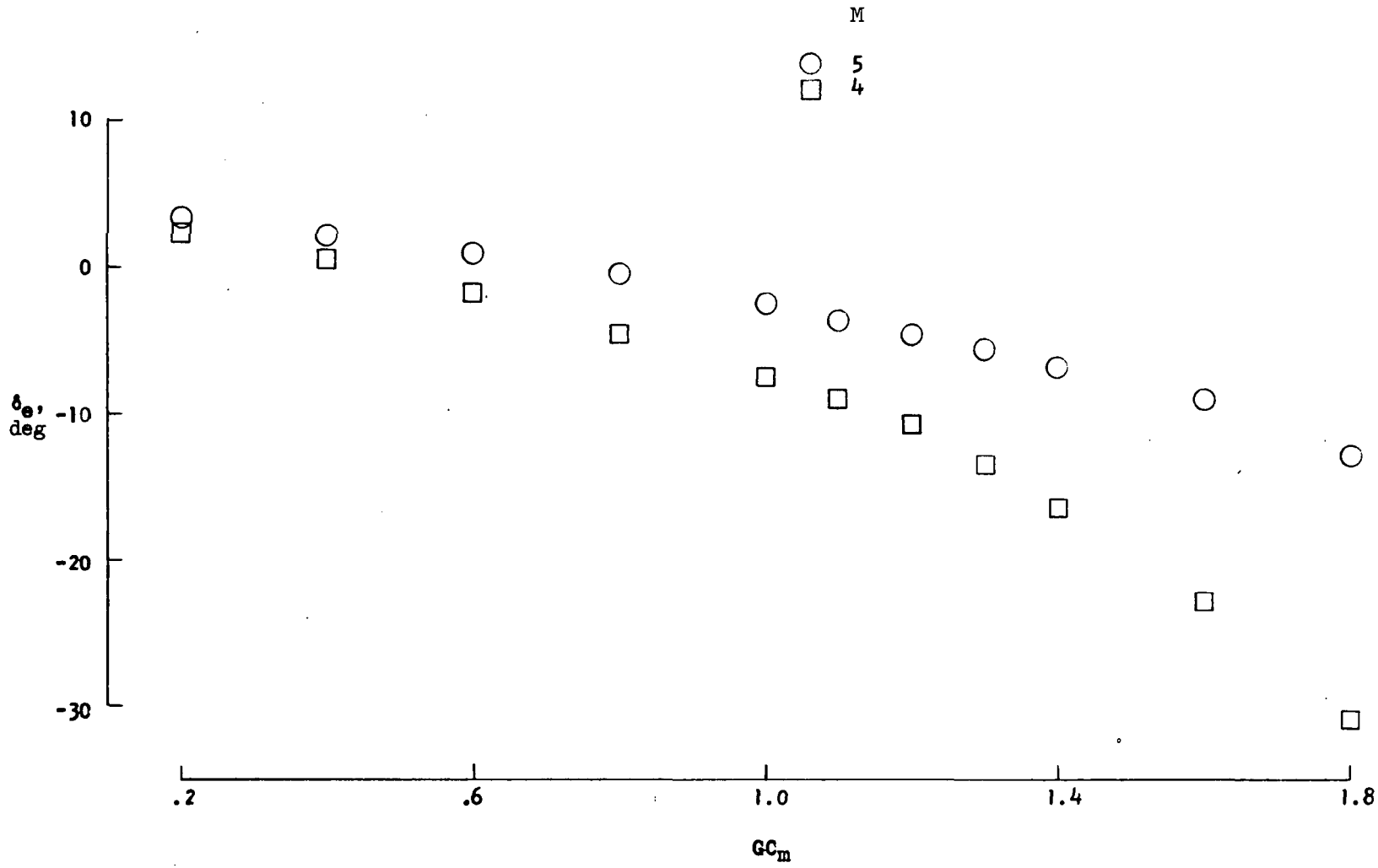

Figure 12.- Effect of pitch stability variation on elevon deflection.

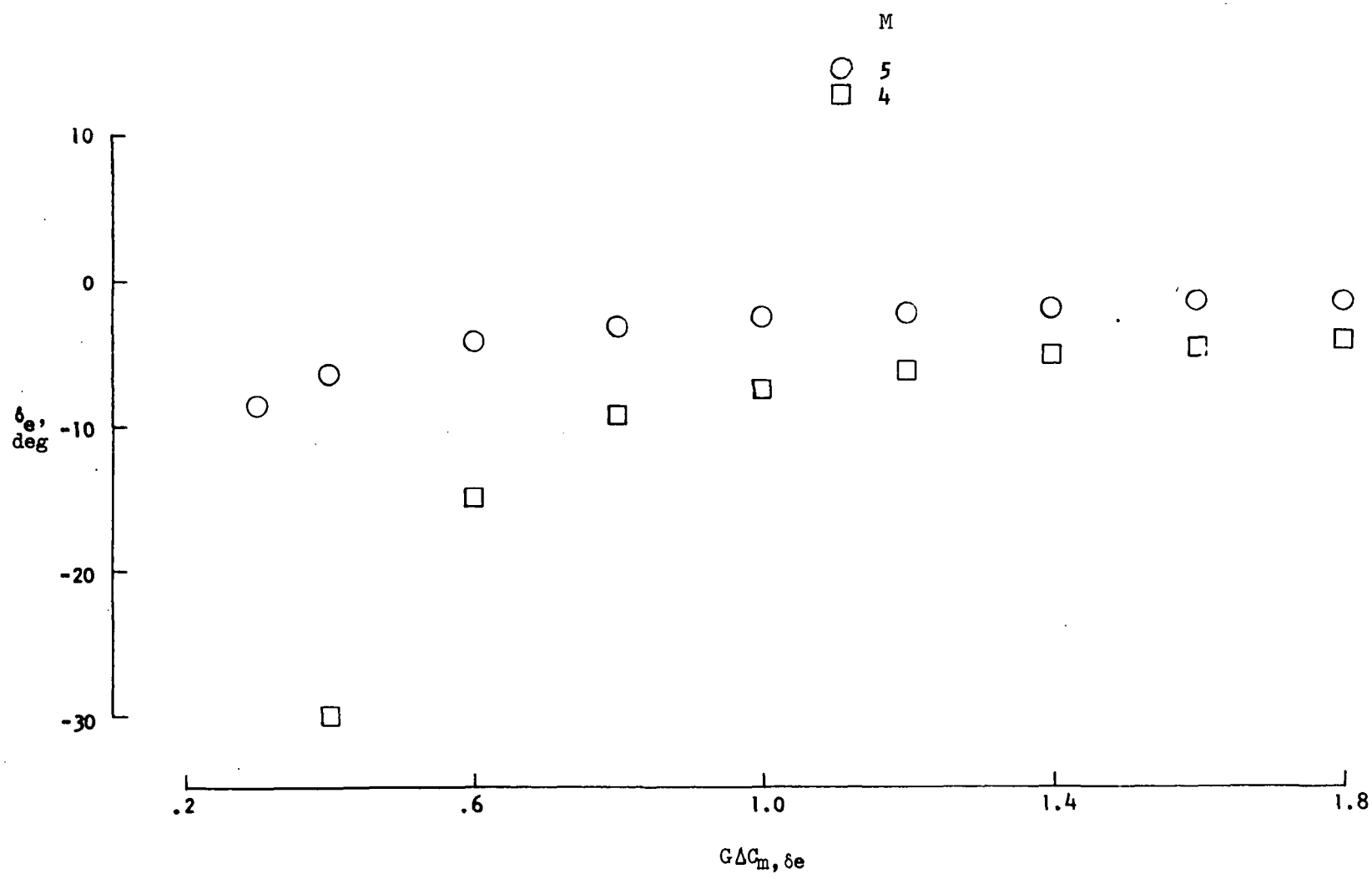

Figure 13.- Effect of elevon effectiveness variation on elevon deflection.

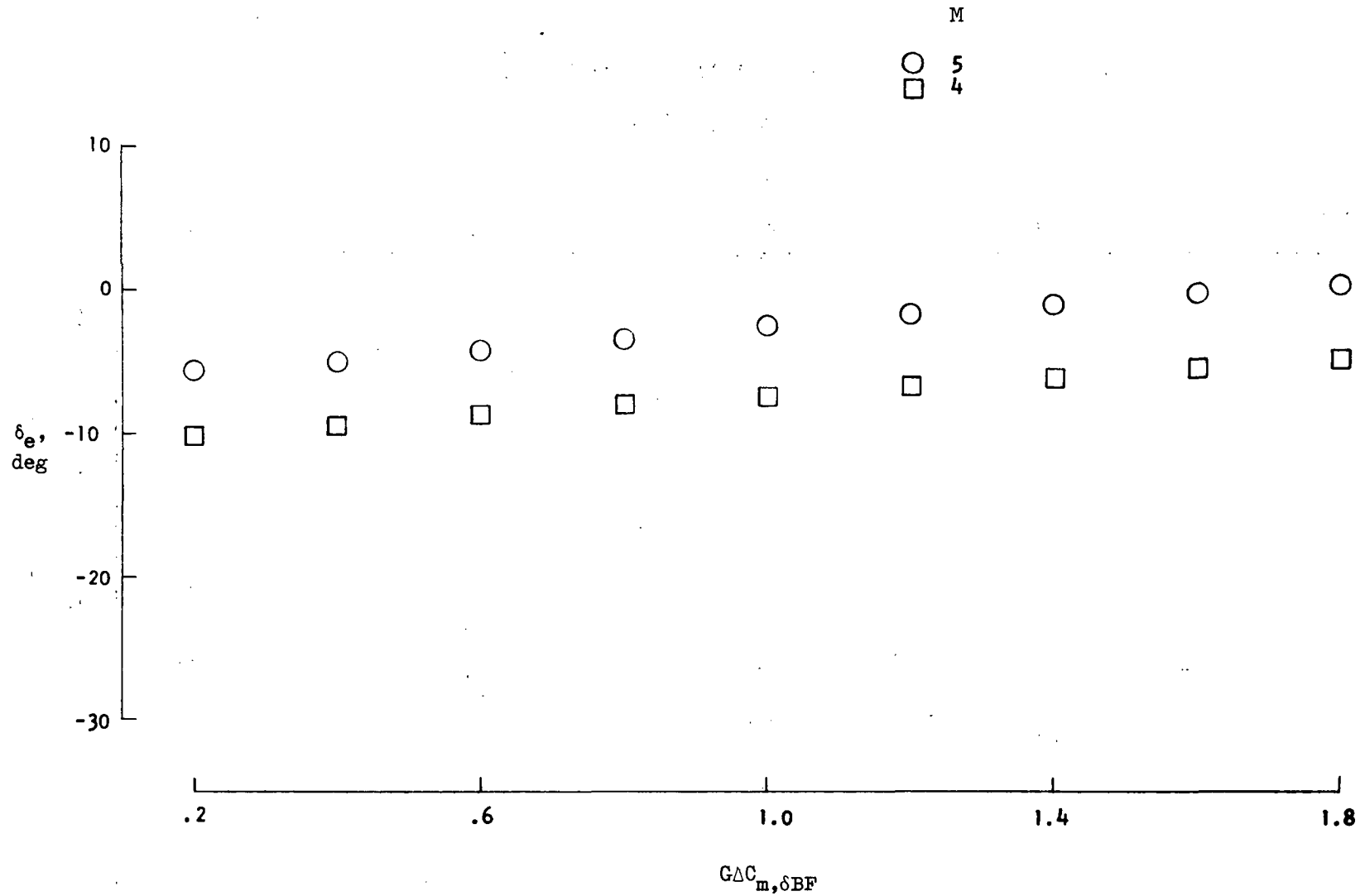

(a) Body flap.

Figure 14.- Effect of body-flap and speed-brake effectiveness variation on elevon deflection.

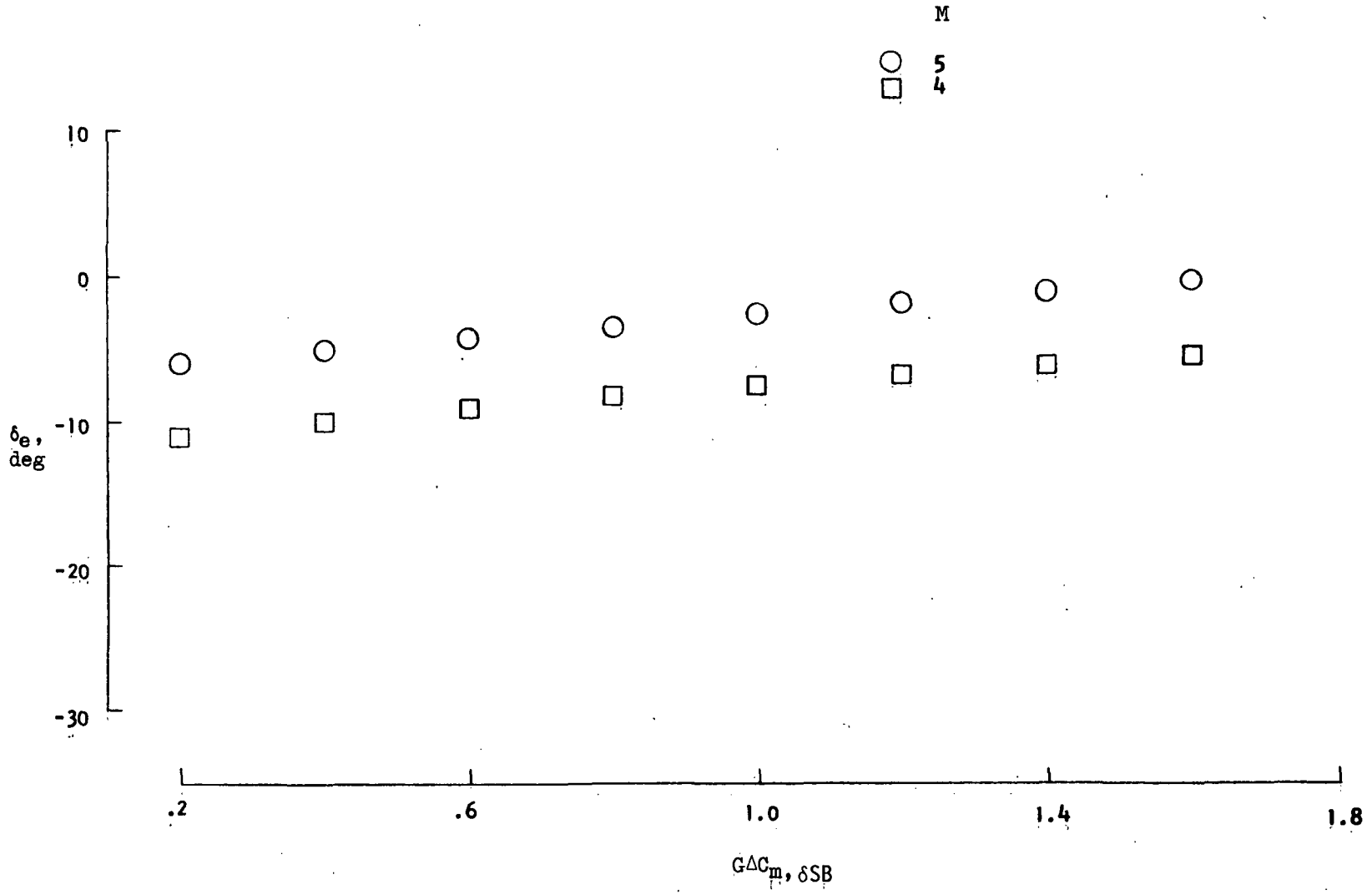

(b) Speed brake.

Figure 14.- Concluded.

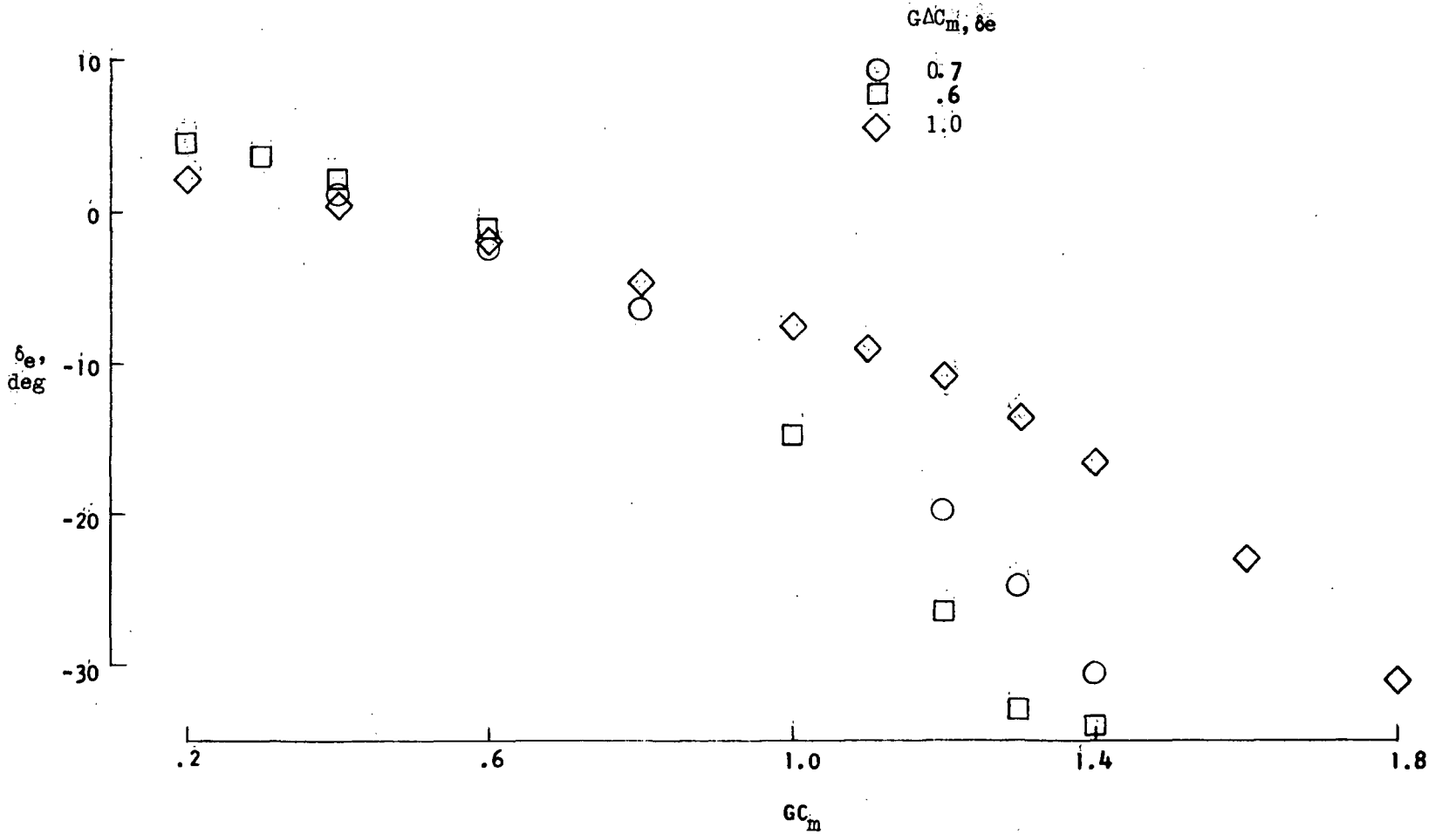

Figure 15.- Effects of pitch stability variation on elevon deflection with degraded elevon effectiveness. M = 4.

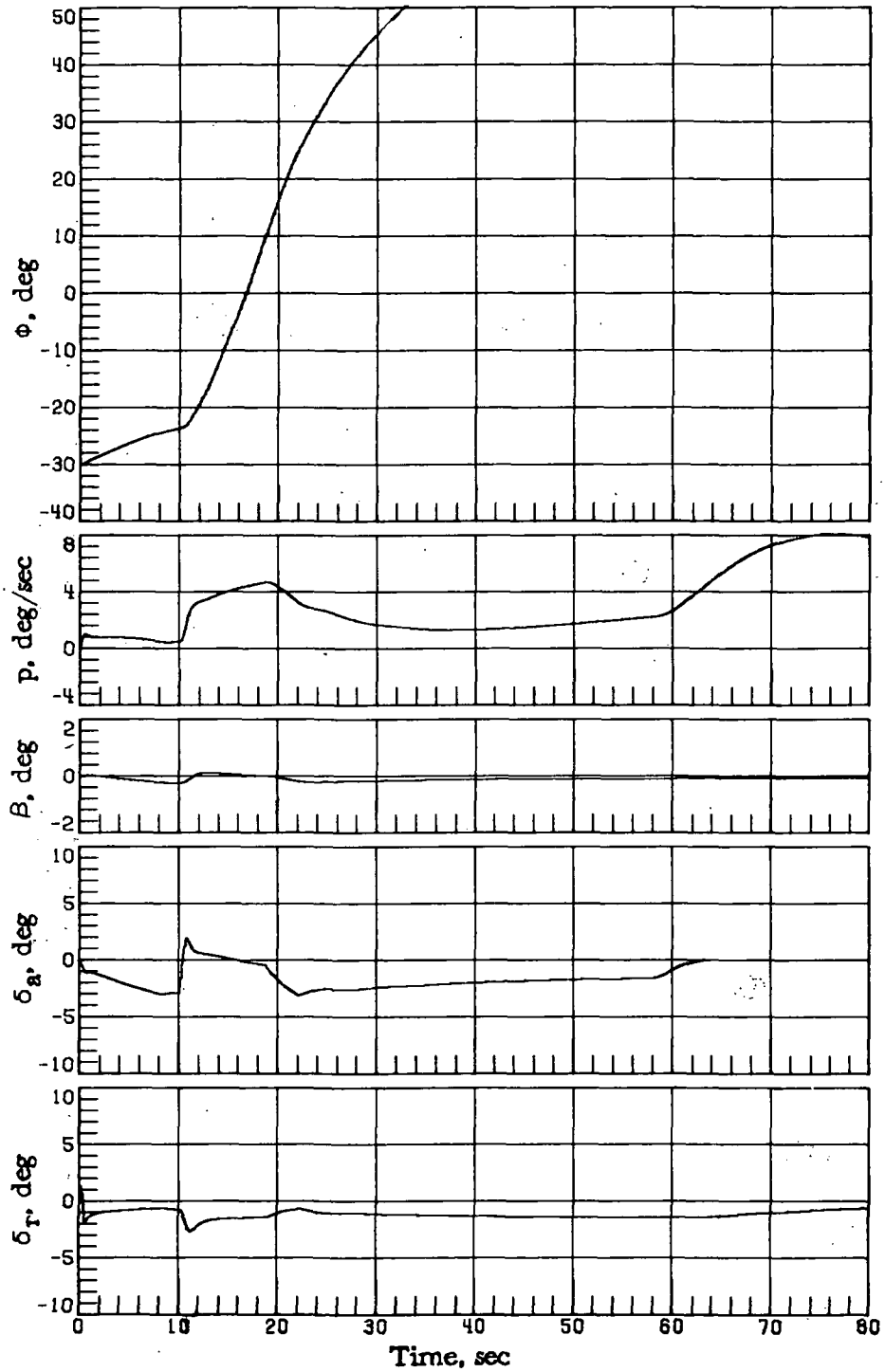

Figure 16.- Vehicle response simulations at $M_i = 4$ for $GC_m = 1.4$ and $G\Delta C_{m,\delta e} = 0.7$ ($\alpha_c = 17.6^o$, $\phi_c = -30^o$ for time <10 sec and $\phi_c = 30^o$ for time $\geq$10 sec).

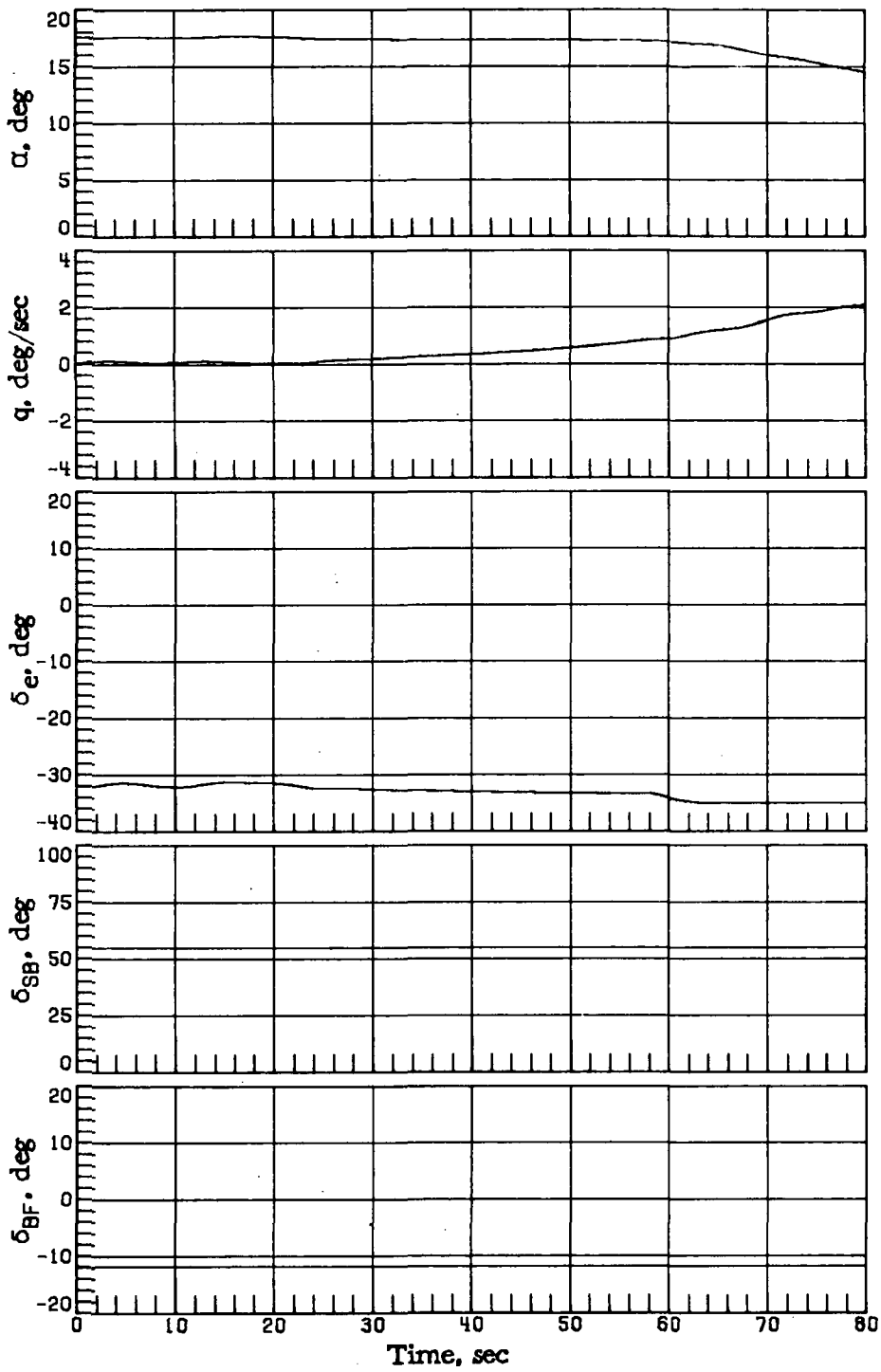

Figure 16.- Concluded.

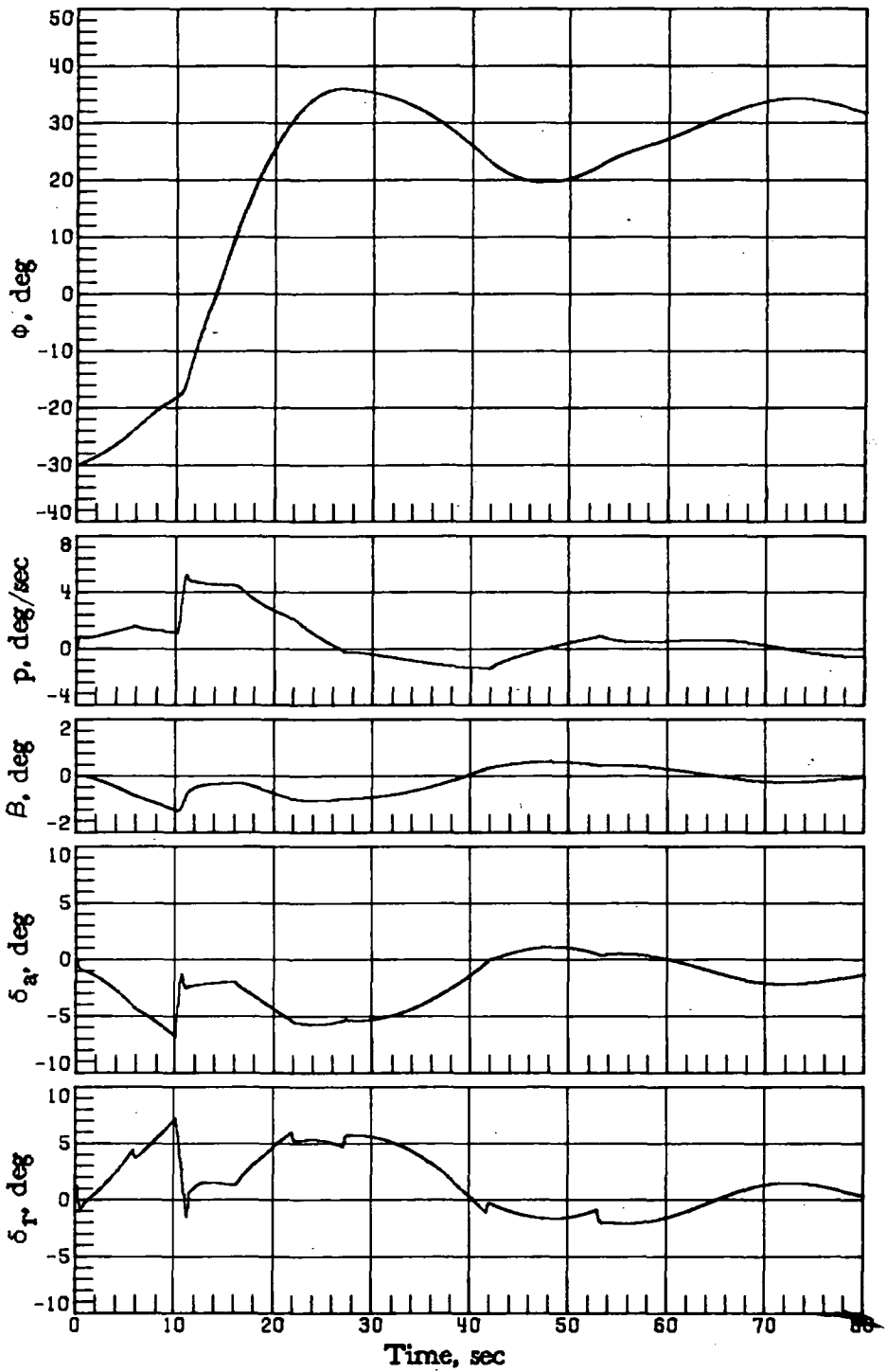

(a) $GC_m = 0.3$.

Figure 17.- Vehicle response simulations at $M_i = 4$ with $G\Delta C_{m,\delta e} = 0.6$ with varying GC_m ($\alpha_c = 17.6^o$, $\phi_c = -30^o$ for time <10 sec and $\phi_c = 30^o$ for time ≧10 sec).

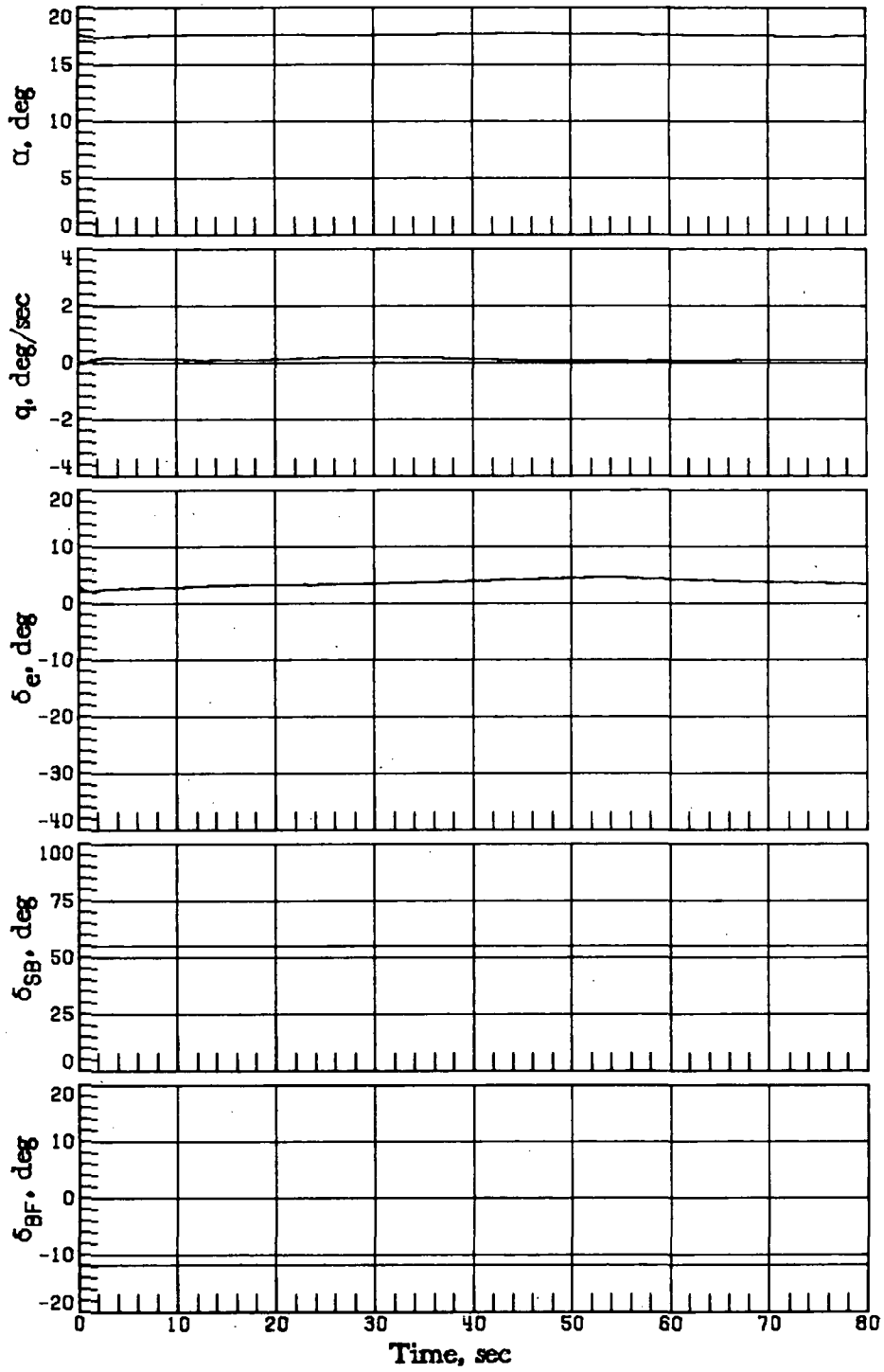

(a) Concluded.

Figure 17.- Continued.

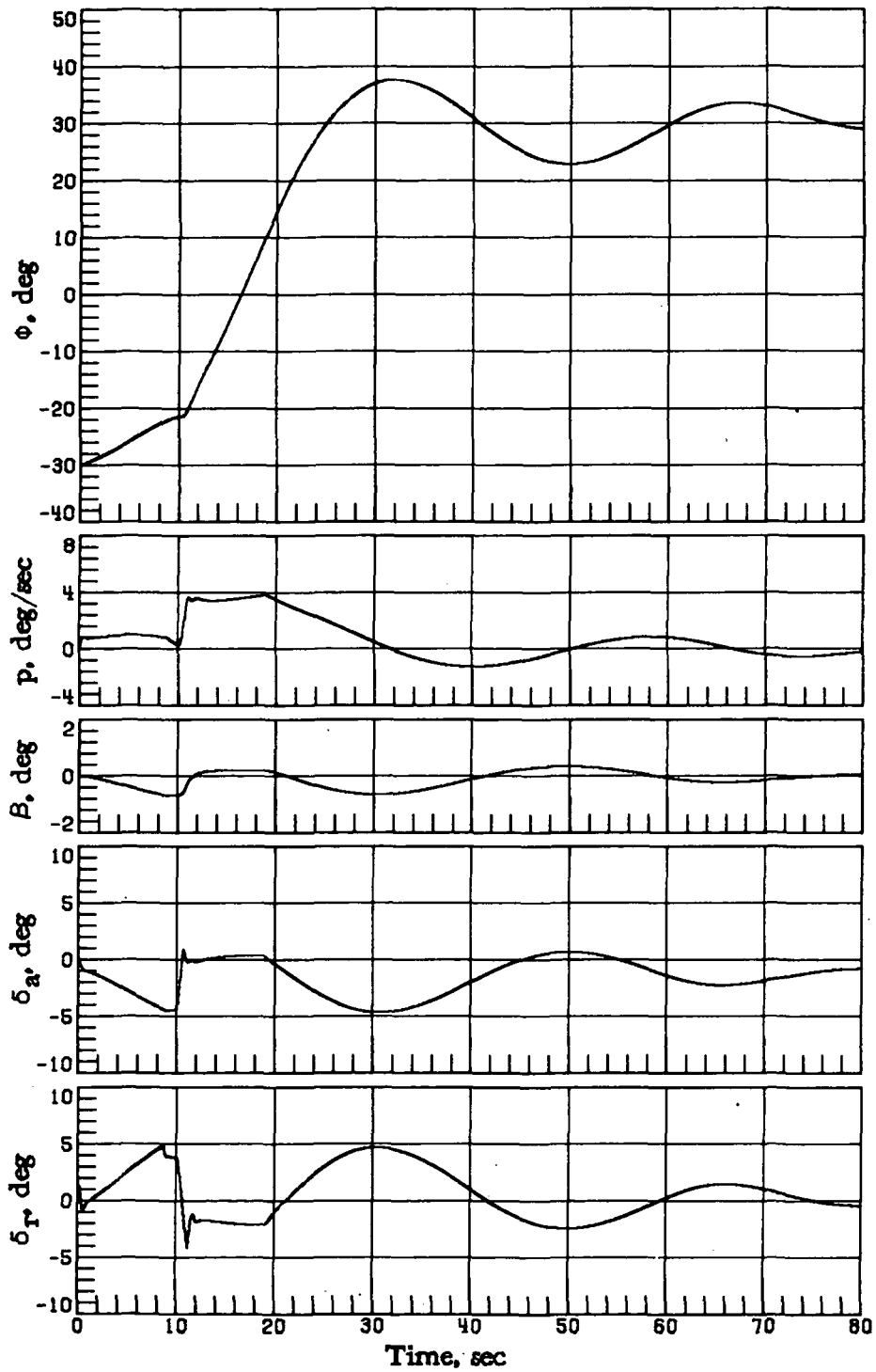

(b) $GC_m = 0.4$.

Figure 17.- Continued.

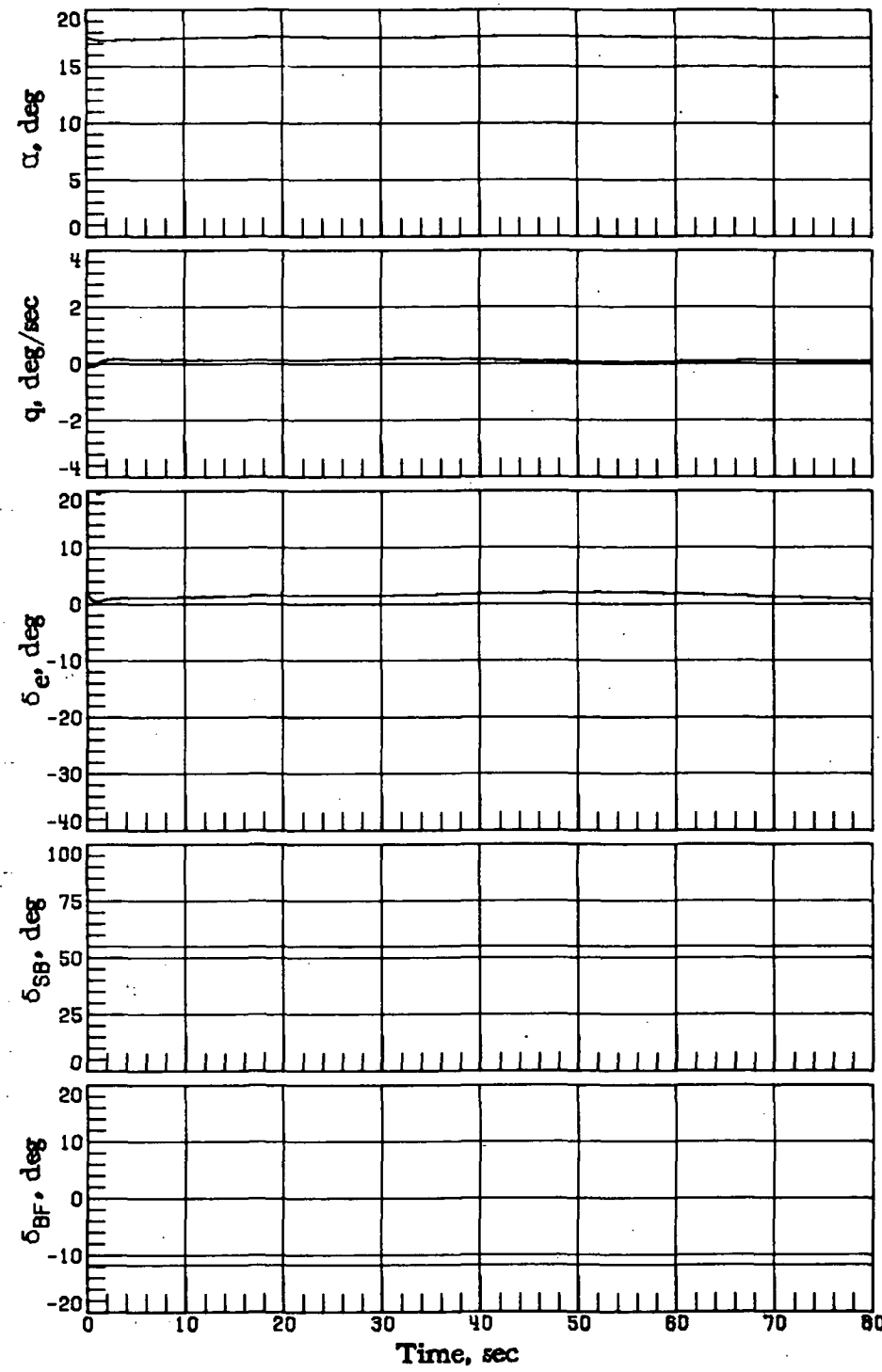

(b) Concluded.

Figure 17.- Concluded.

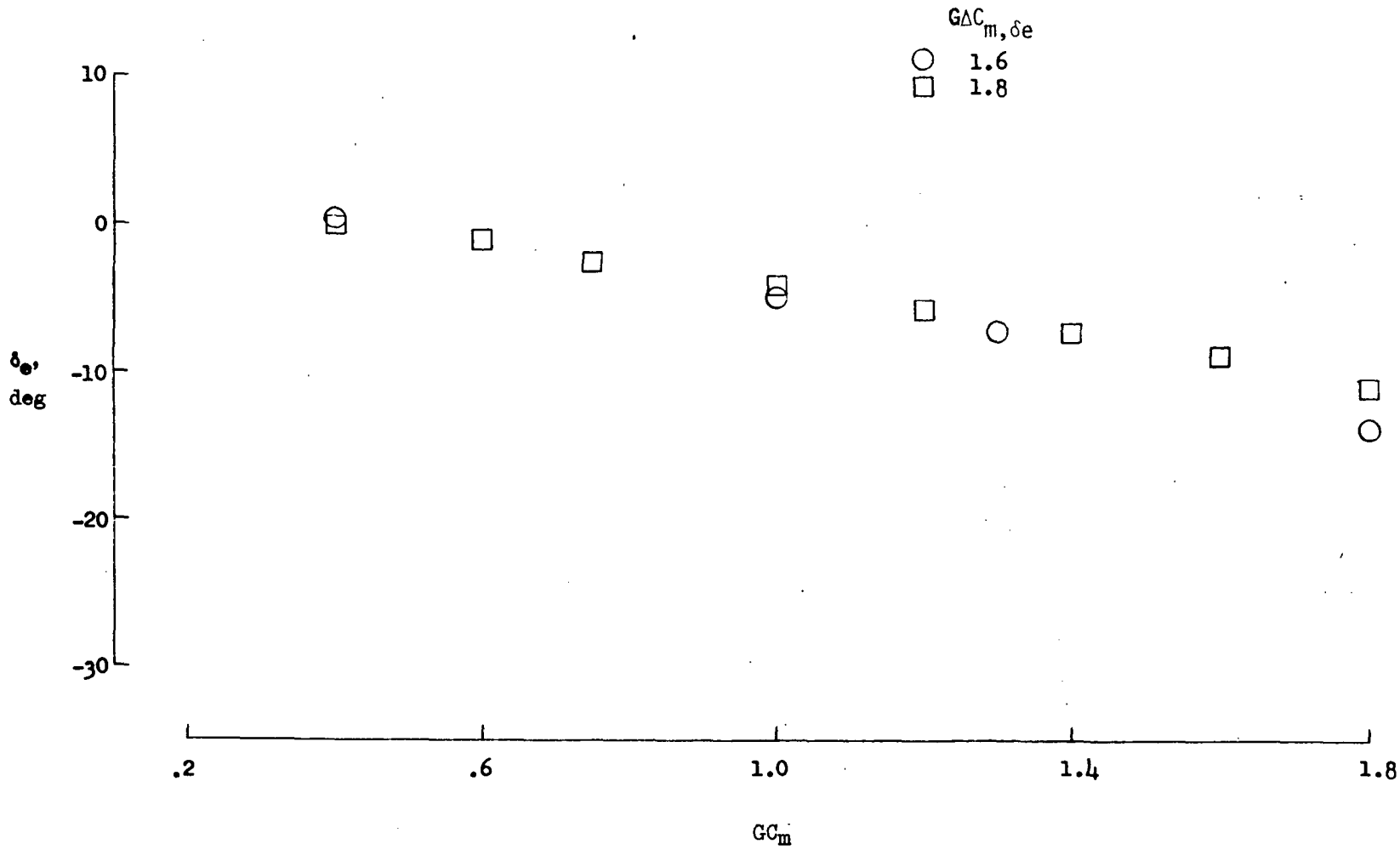

Figure 18.- Effects of pitch stability variations on elevon deflection with increased elevon effectiveness. M = 4.

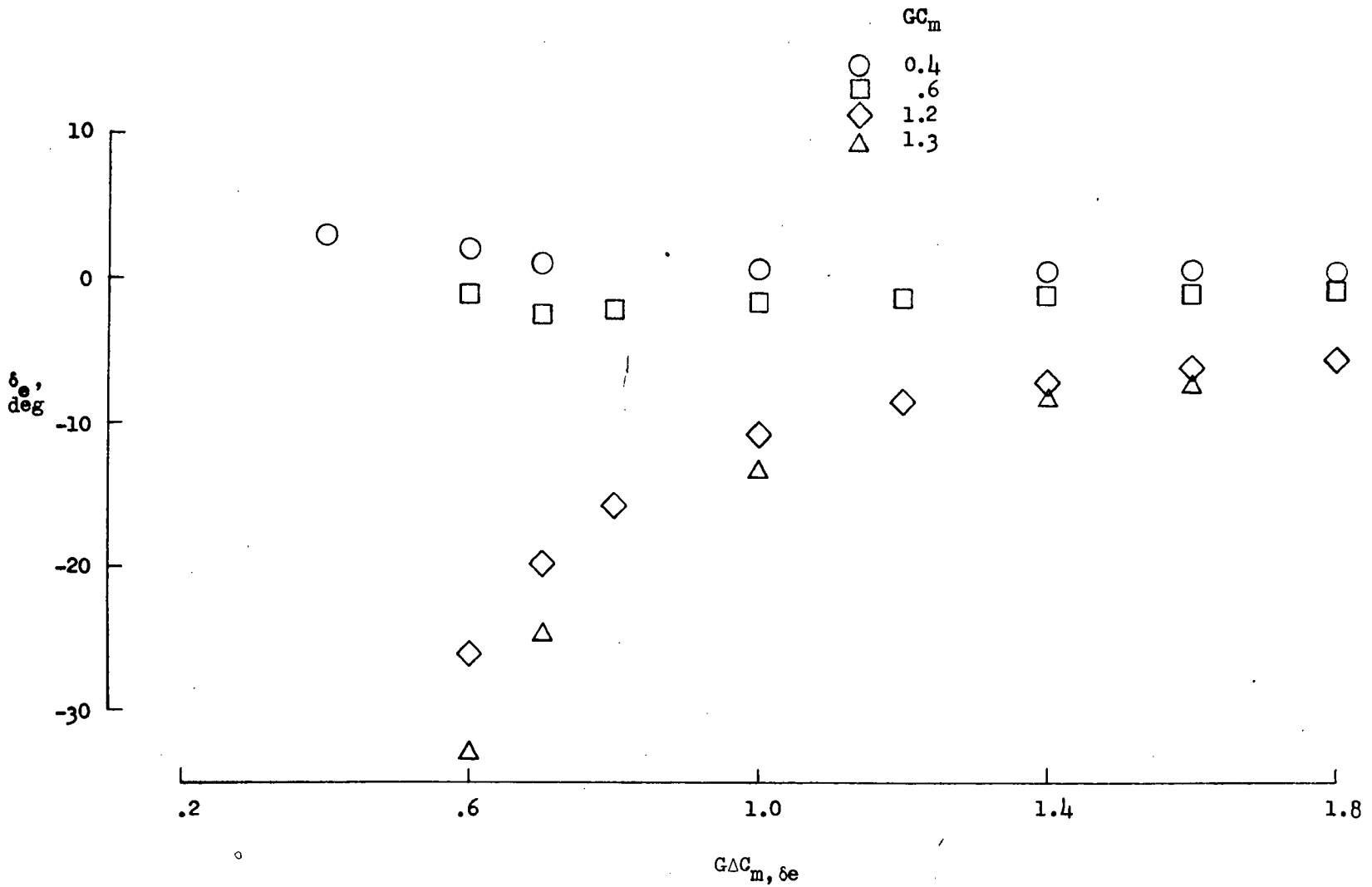

Figure 19.- Effects of elevon effectiveness variation on elevon deflection with increased and decreased pitch stability. M = 4.

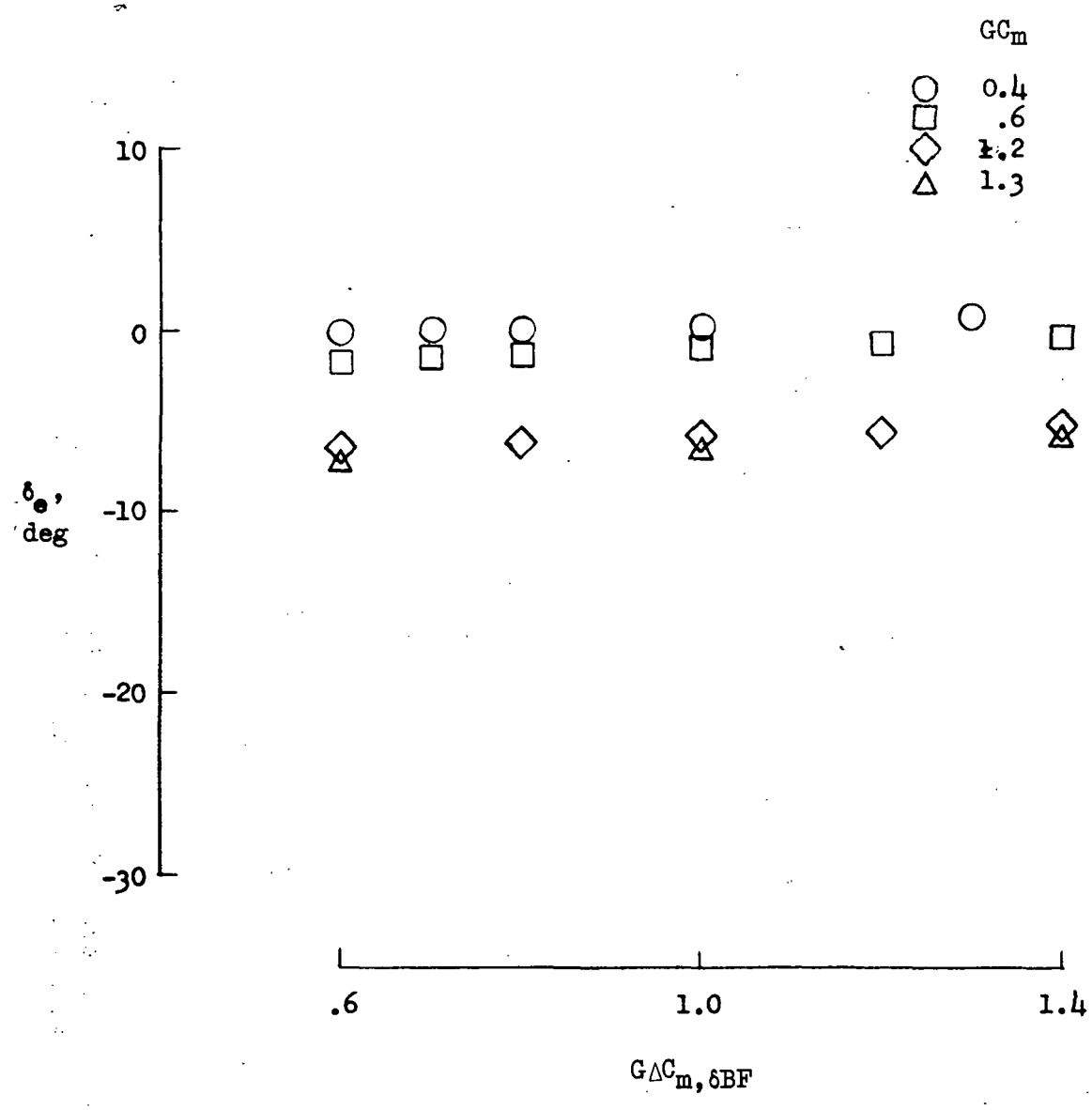

(a) $G\Delta C_{m,\delta e} = 1.8$.

Figure 20.- Effects of body-flap effectiveness variation on elevon deflection with increased and decreased pitch stability and elevon effectiveness. M = 4.

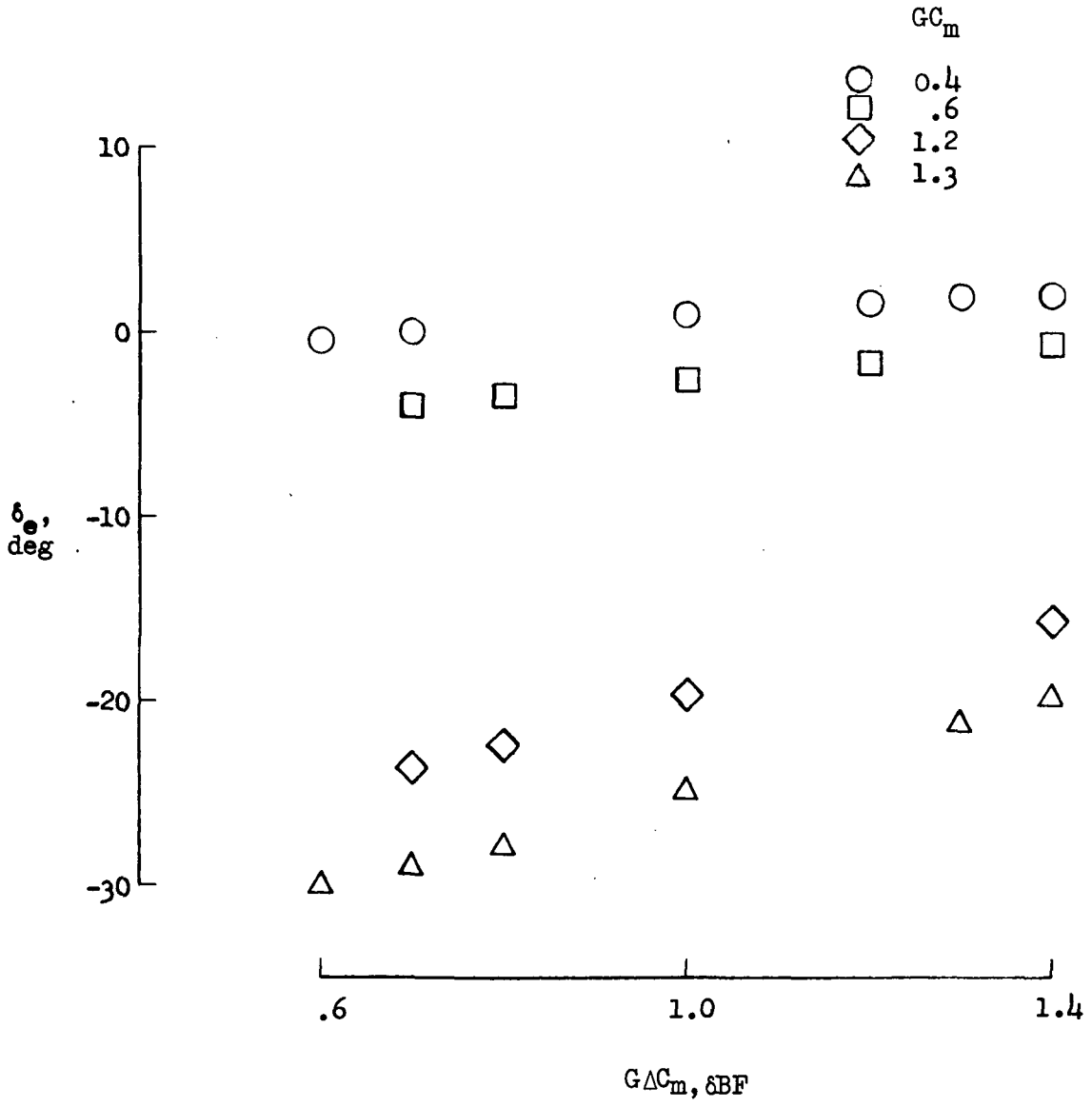

(b) $G\Delta C_{m,\delta e} = 0.7$.

Figure 20.- Concluded.

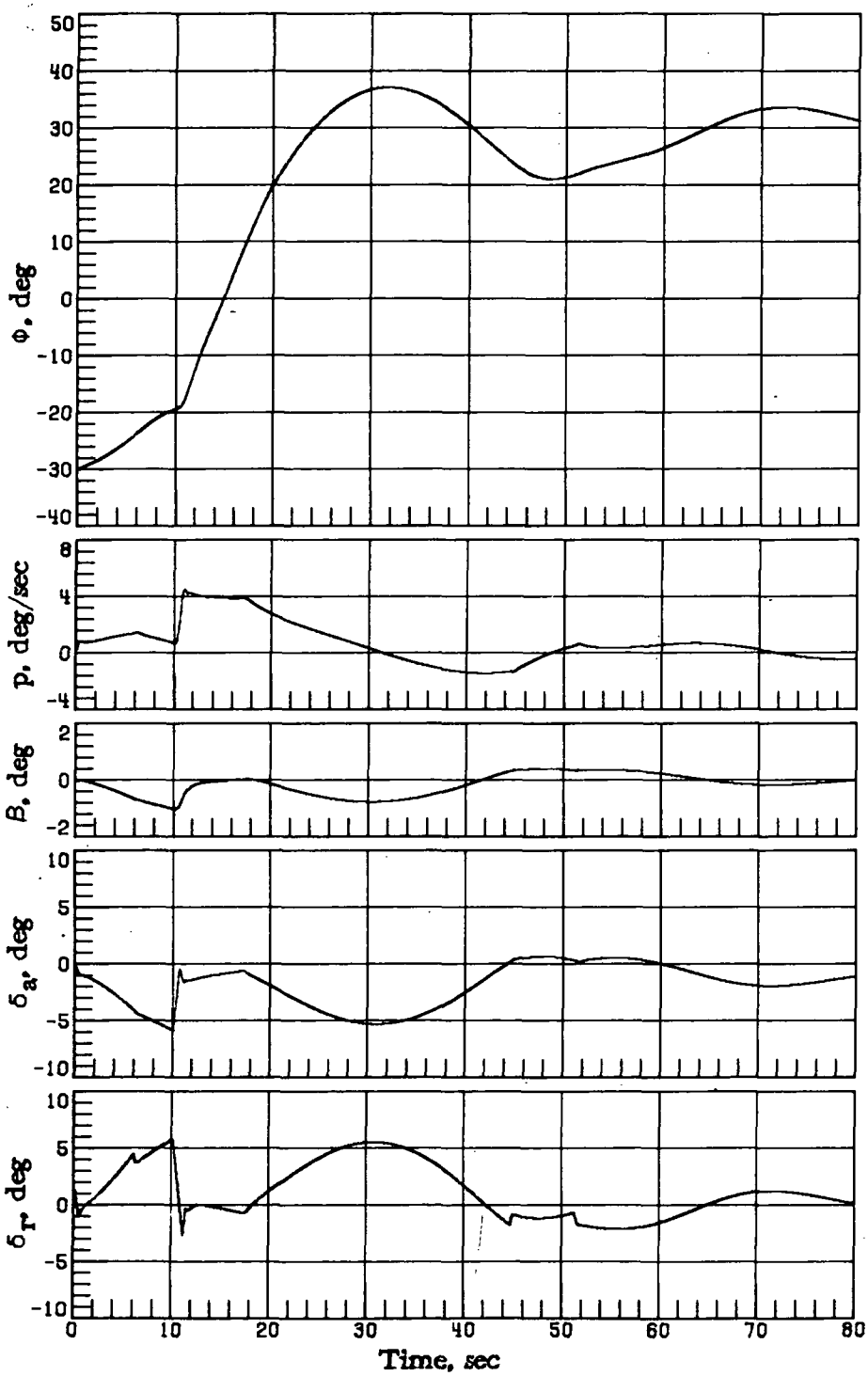

(a) $GC_m = 0.4$.

Figure 21.- Vehicle response simulations at $M_i = 4$ with $G\Delta C_{m,\delta e} = 0.7$ and $G\Delta C_{m,\delta BF} = 1.4$ with varying GC_m ($\alpha_c = 17.6^o$, $\phi_c = -30^o$ for time <10 sec and $\phi_c = 30^o$ for time $\geq$10 sec).

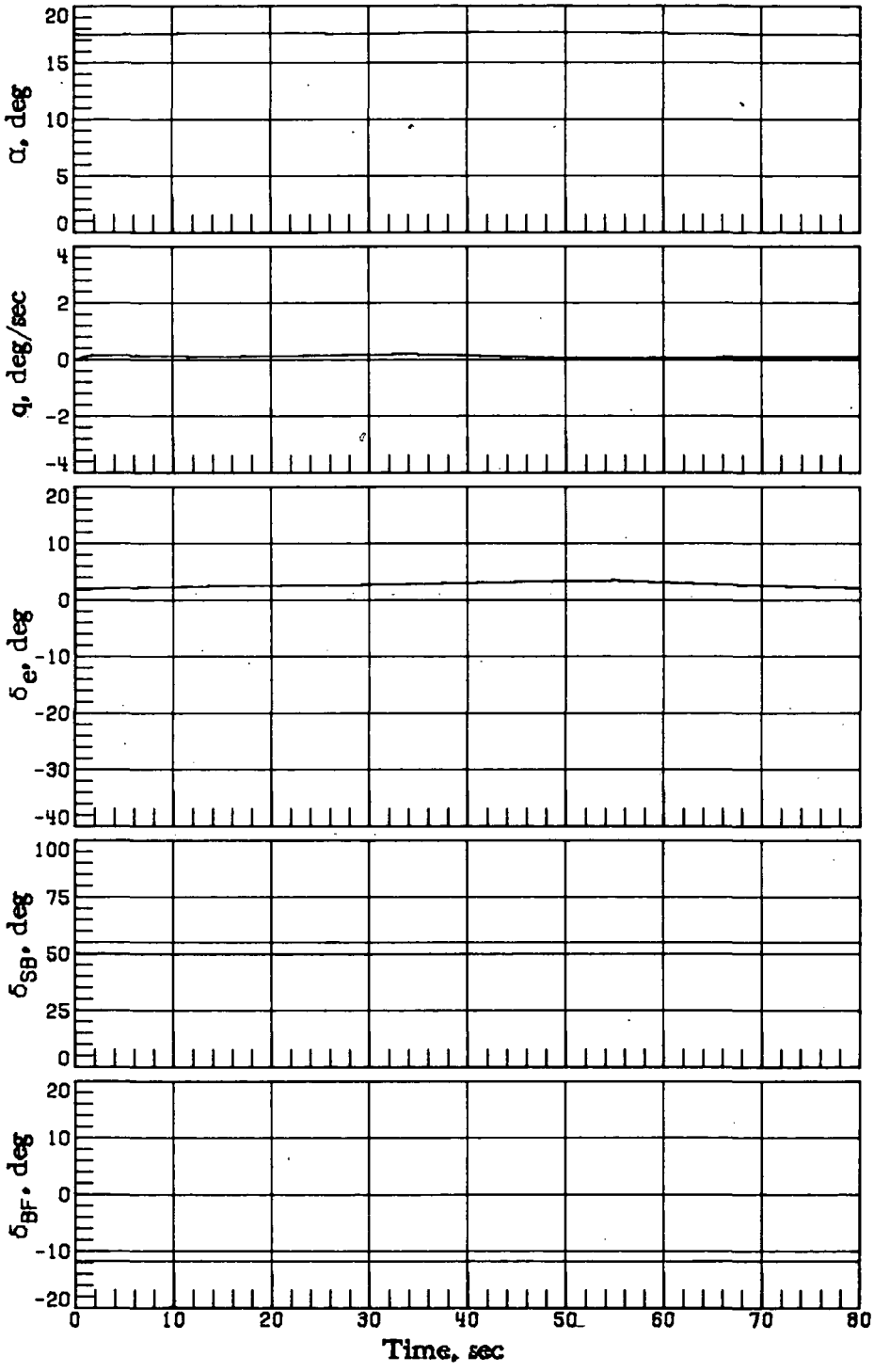

(a) Concluded.

Figure 21.- Continued.

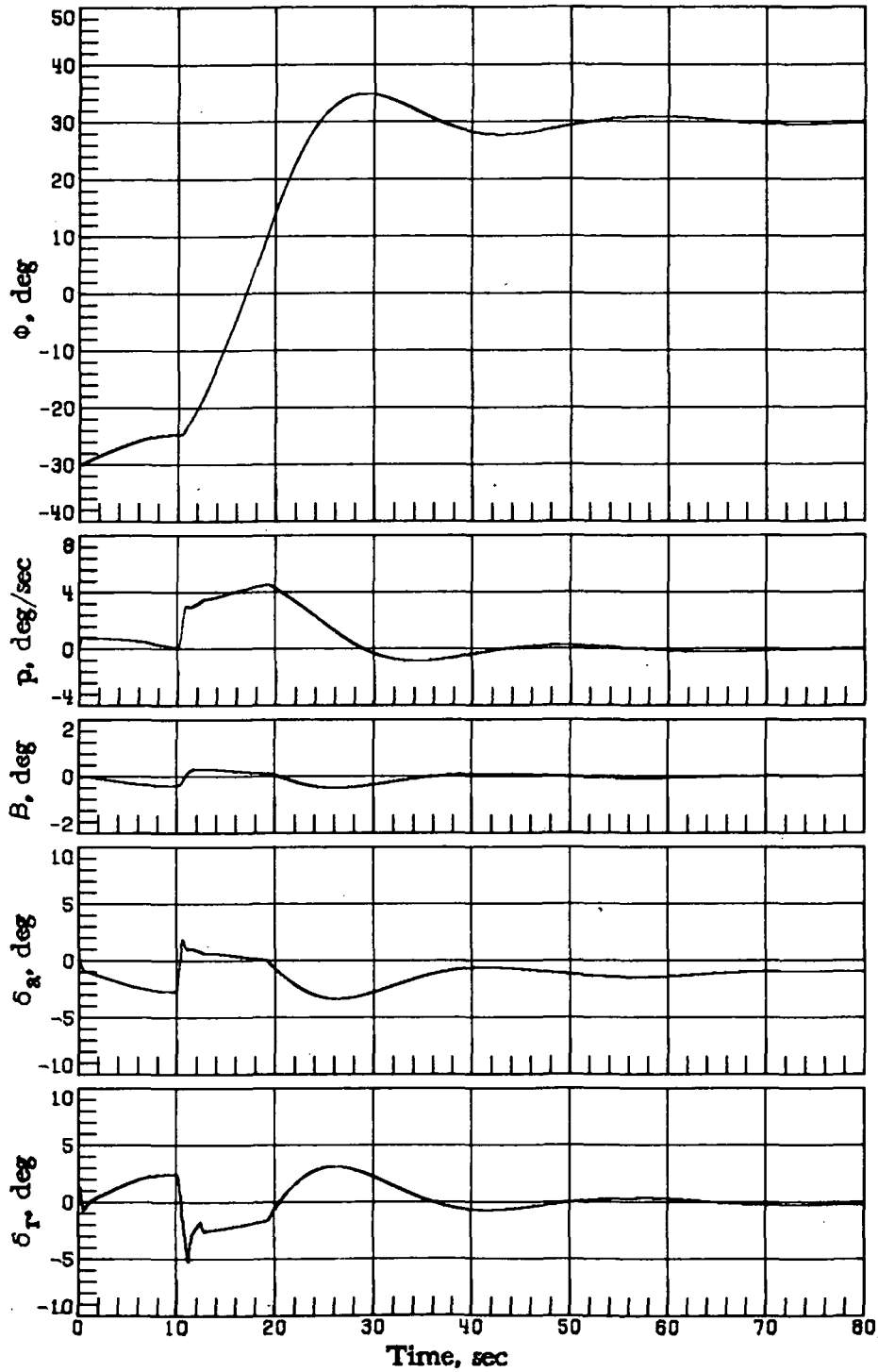

(b) $GC_m = 0.6$.

Figure 21.- Continued.

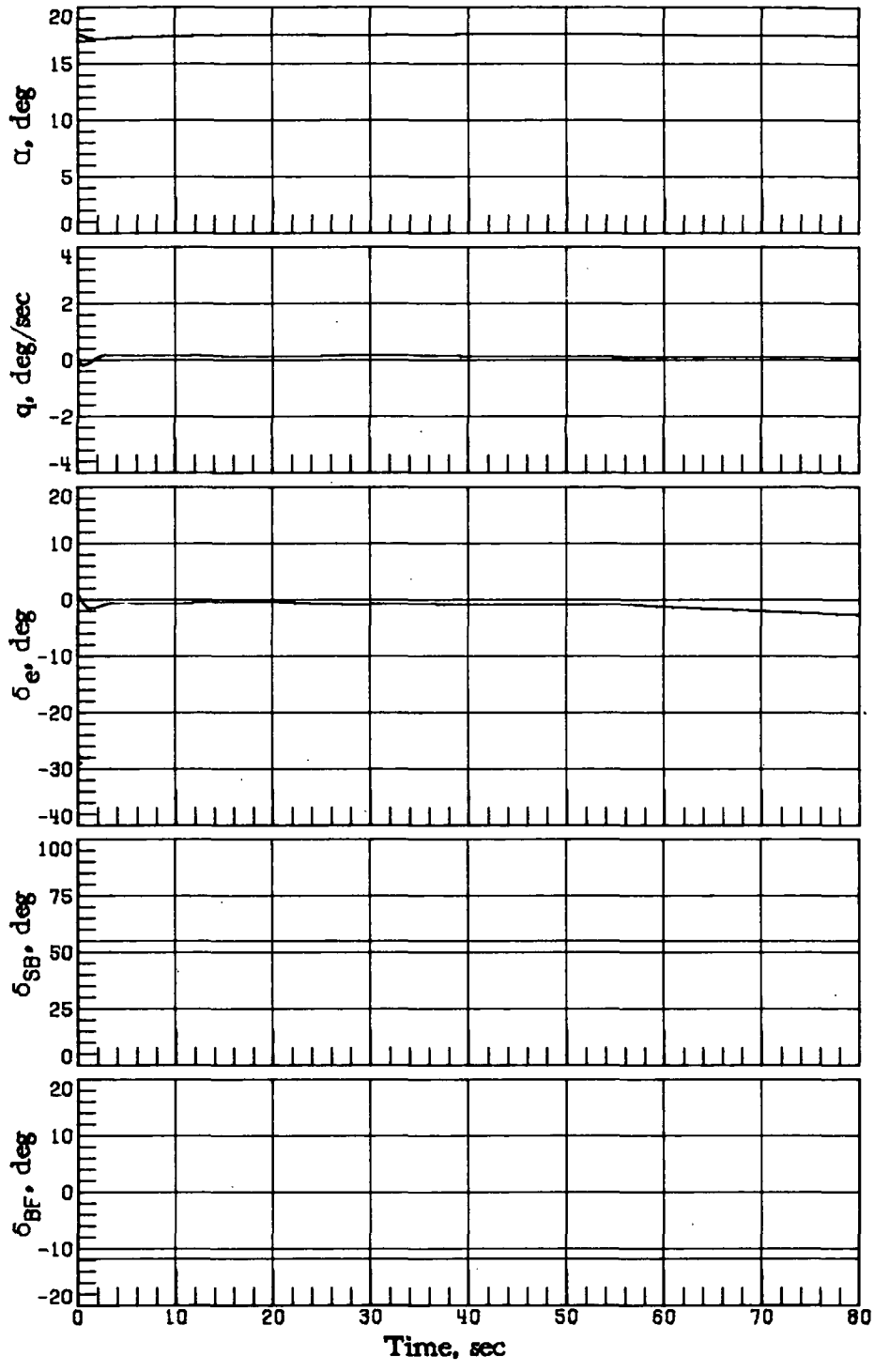

(b) Concluded.

Figure 21.- Concluded.

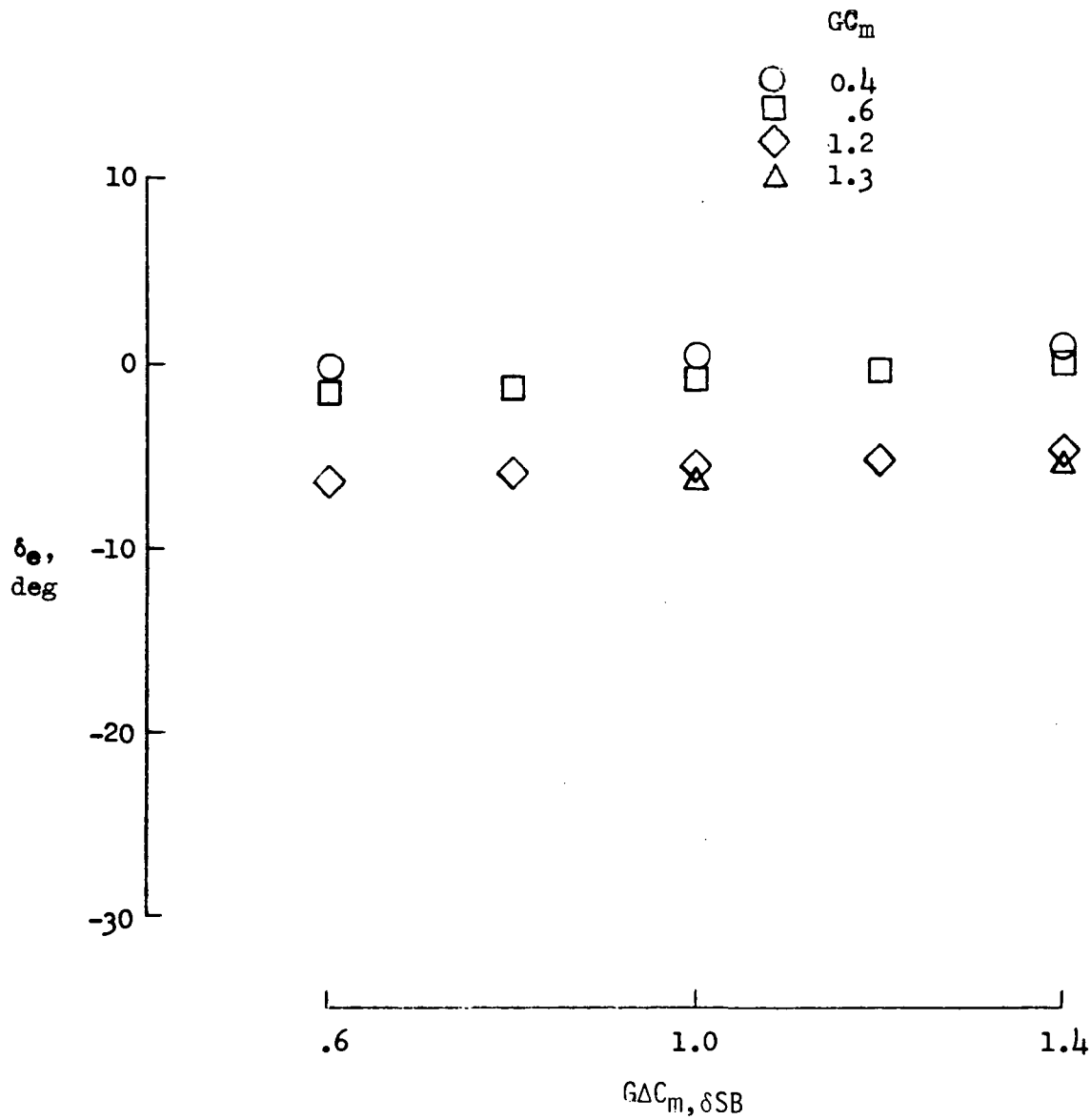

(a) $G\Delta C_{m,\delta e} = 1.8$.

Figure 22.- Effects of speed-brake effectiveness variation on elevon deflection with increased and decreased pitch and elevon effectiveness. M = 4.

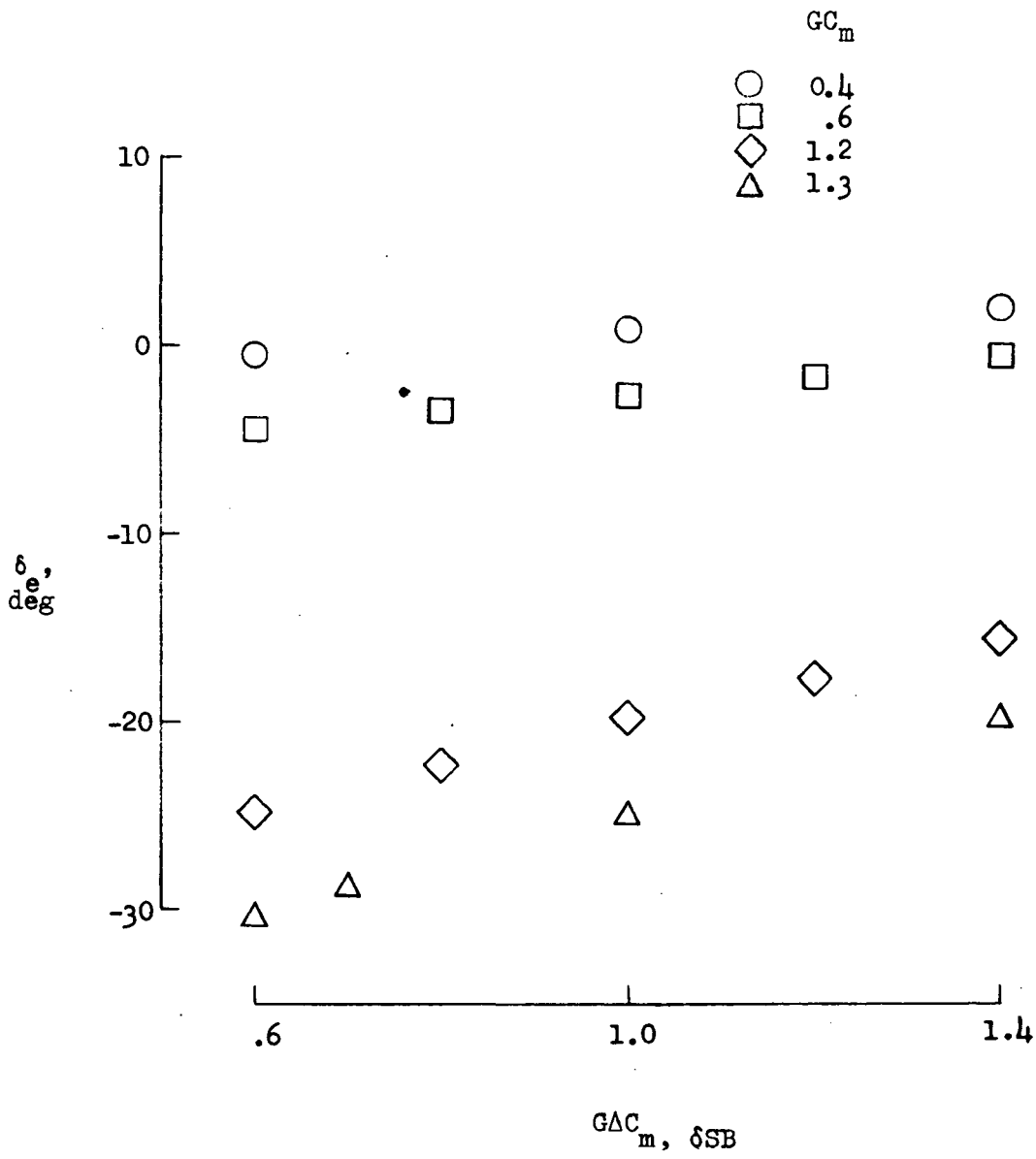

(b) $G\Delta C_{m,\delta e} = 0.7$.

Figure 22.- Concluded.

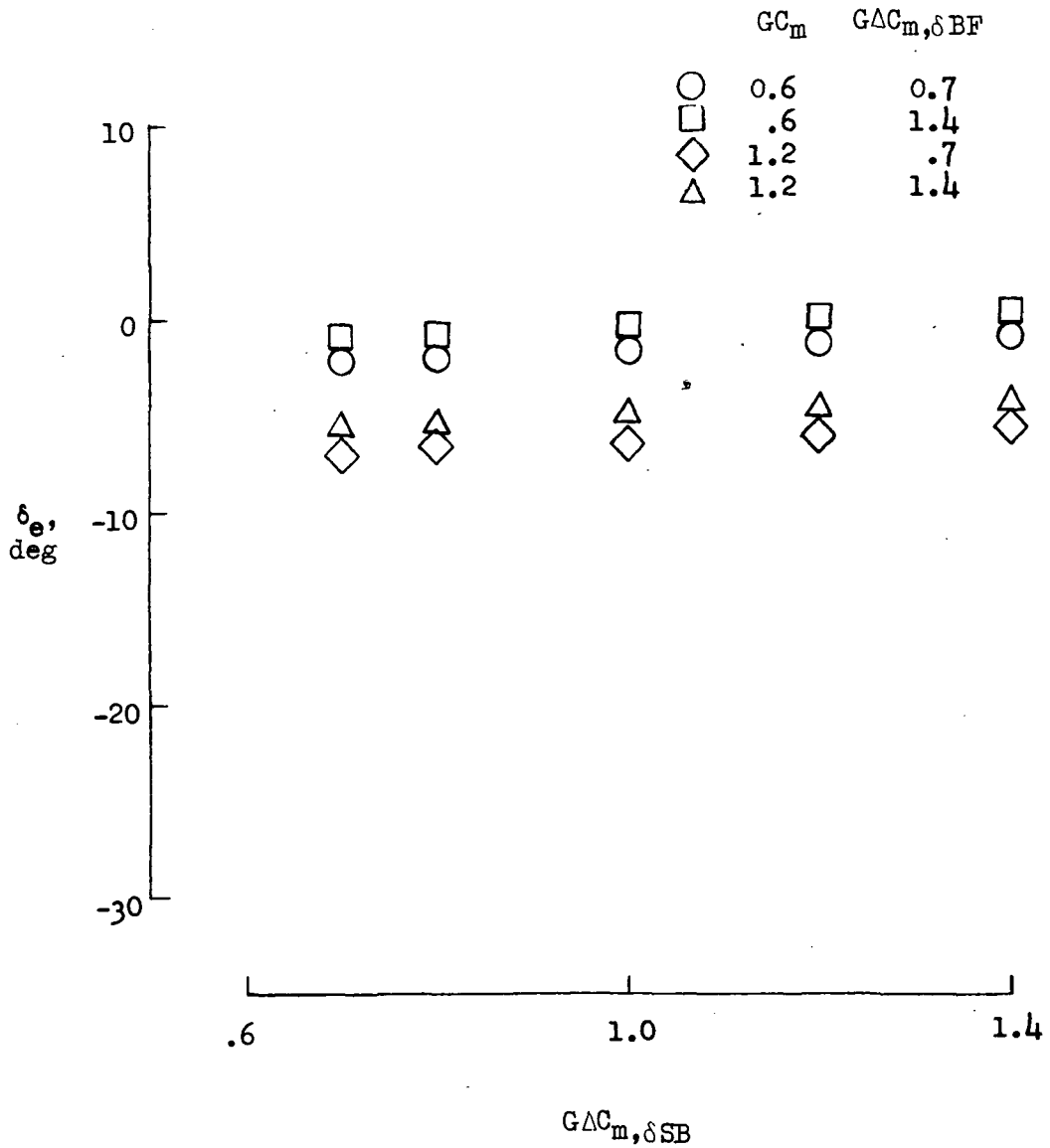

Figure 23.- Effects of speed-brake effectiveness variation on elevon deflection with increased and decreased pitch stability and body flap effectiveness and increased elevon effectiveness. $G\Delta C_{m,\delta e}$ = 1.8; M = 4.

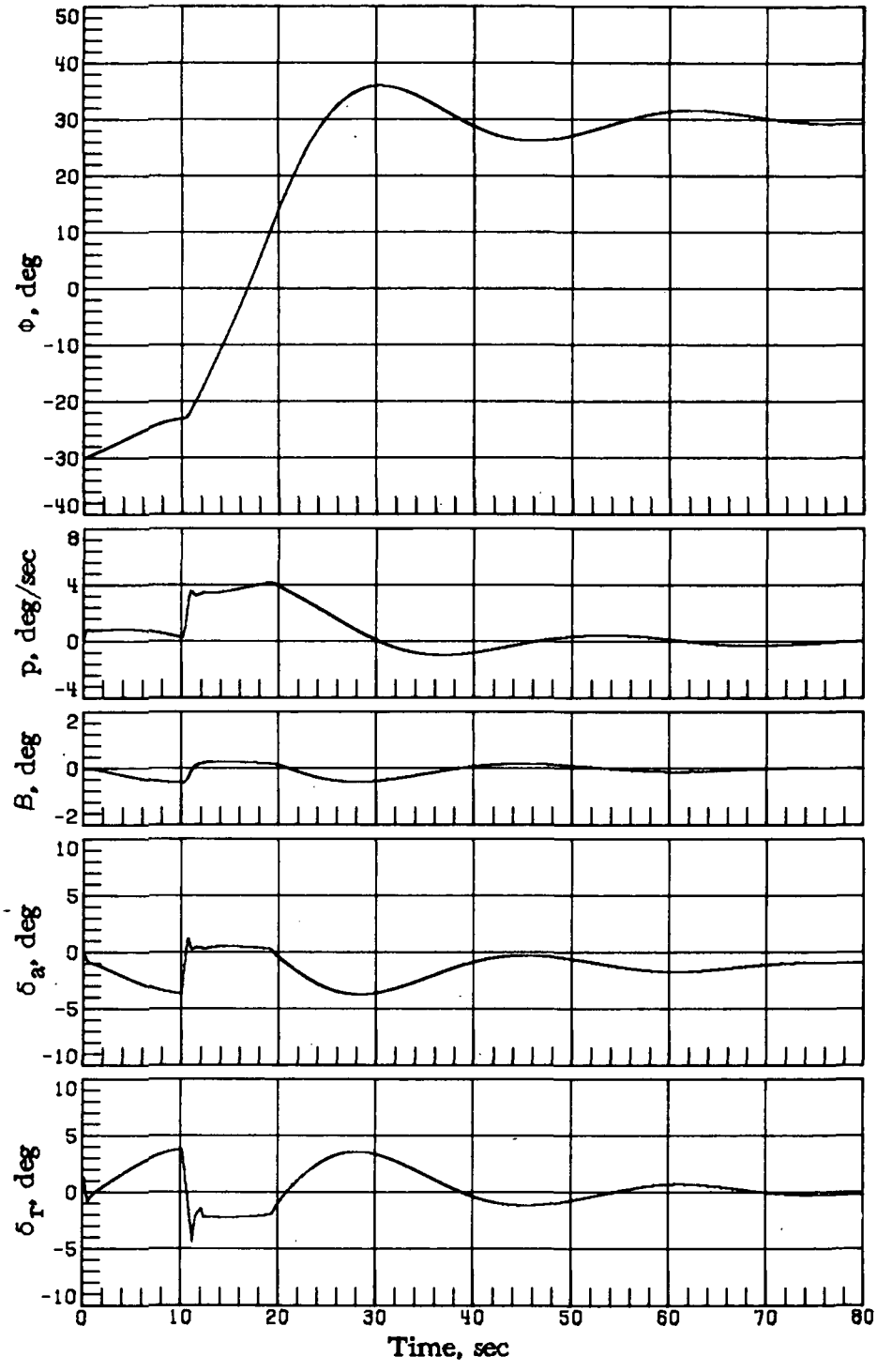

Figure 24.- Vehicle response simulations at $M_i = 4$ with $GC_m = 0.6$, $G\Delta C_{m,\delta e} = 1.8$, $G\Delta C_{m,\delta BF} = 1.4$, and $G\Delta C_{m,\delta SB} = 1.4$ ($\alpha_c = 17.6^\circ$, $\phi_c = -30^\circ$ for time <10 sec and $\phi_c = 30^\circ$ for time ≥ 10 sec).

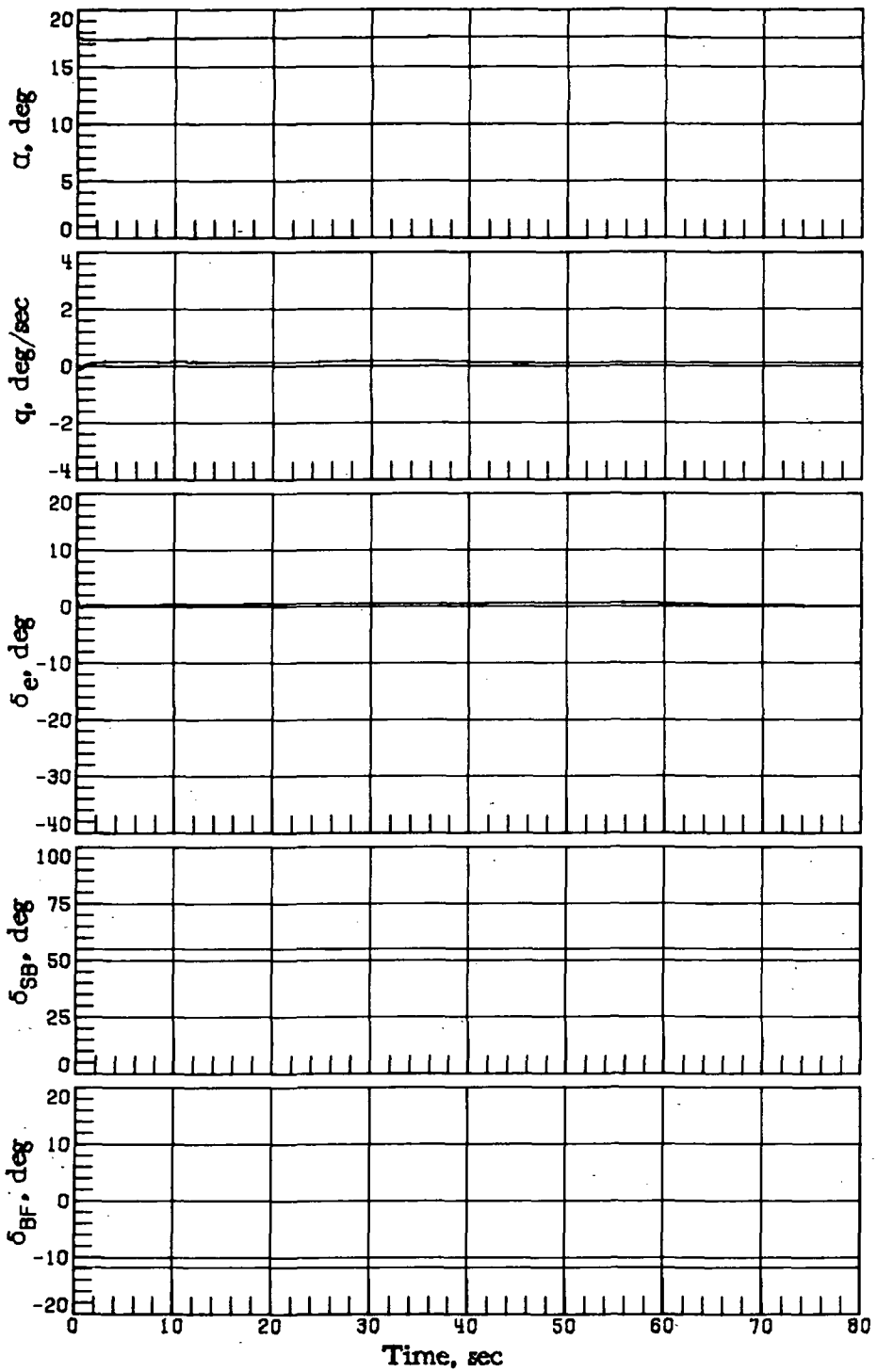

Figure 24.- Concluded.

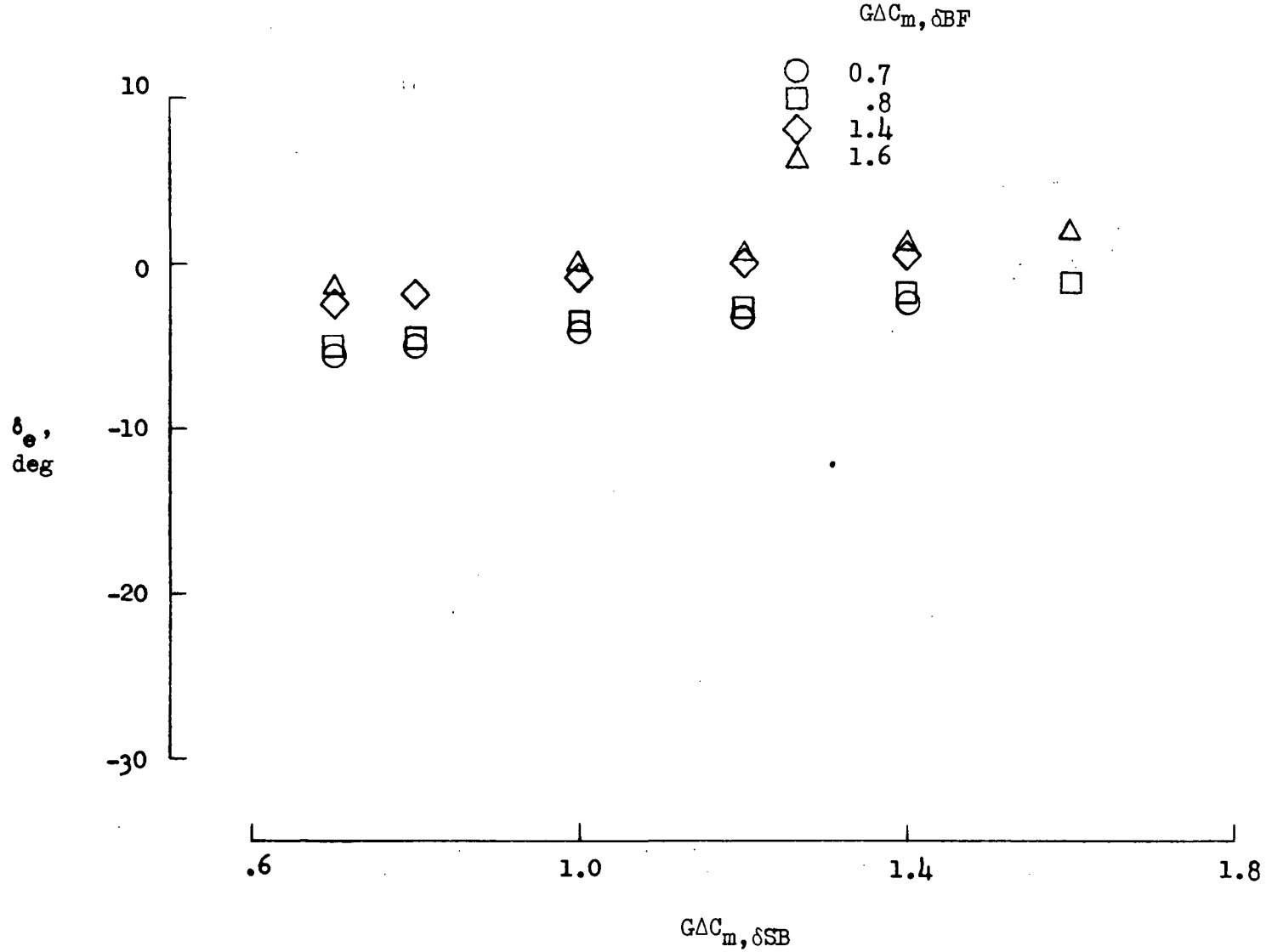

(a) $GC_m = 0.6$.

Figure 25.- Effects of speed-brake effectiveness variation on elevon deflection with increased and decreased body flap effectiveness and pitch stability and decreased elevon effectiveness. $G\Delta C_{m,\delta e} = 0.7$; $M = 4$.

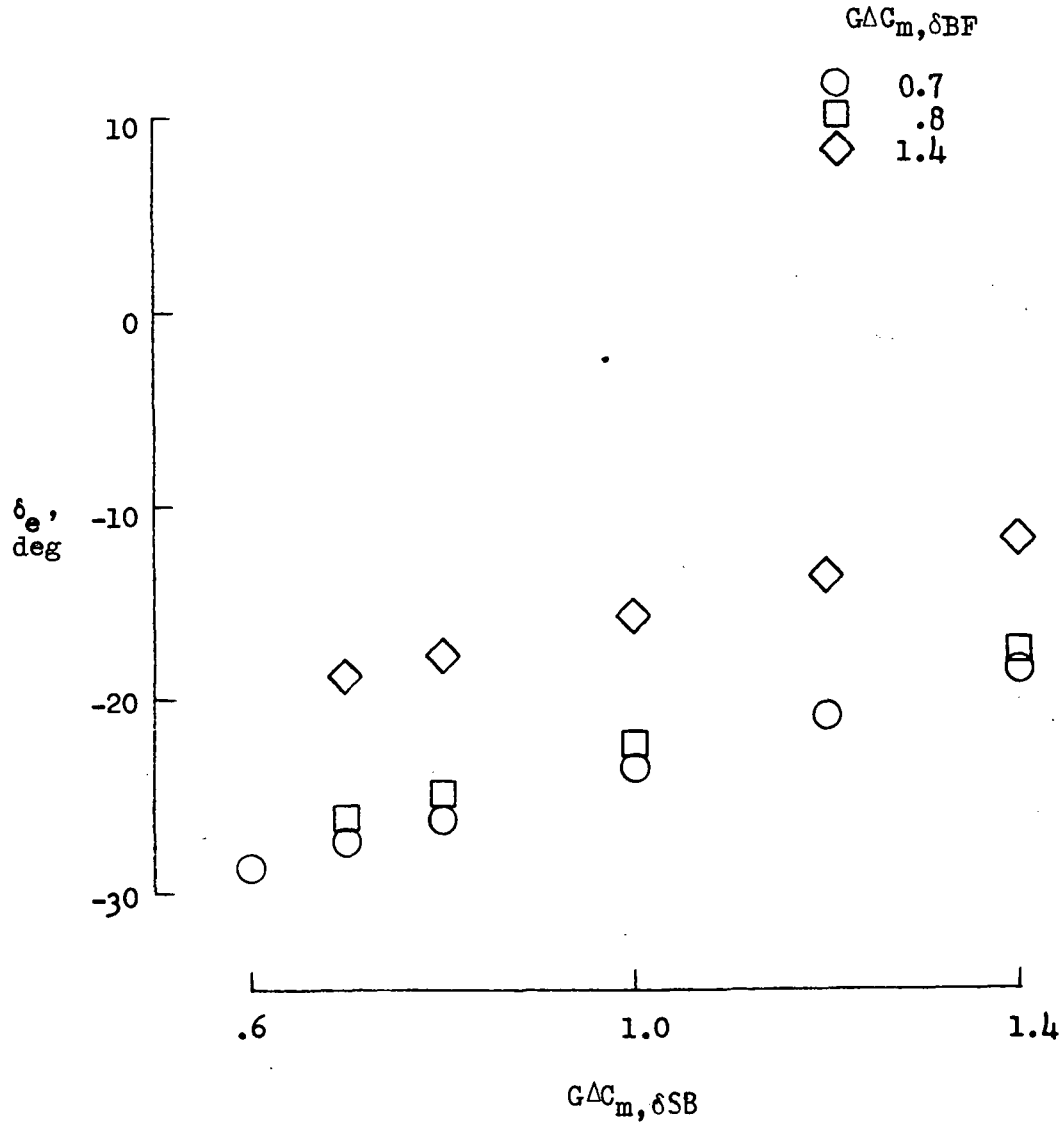

(b) $GC_m = 1.2$.

Figure 25.- Concluded.

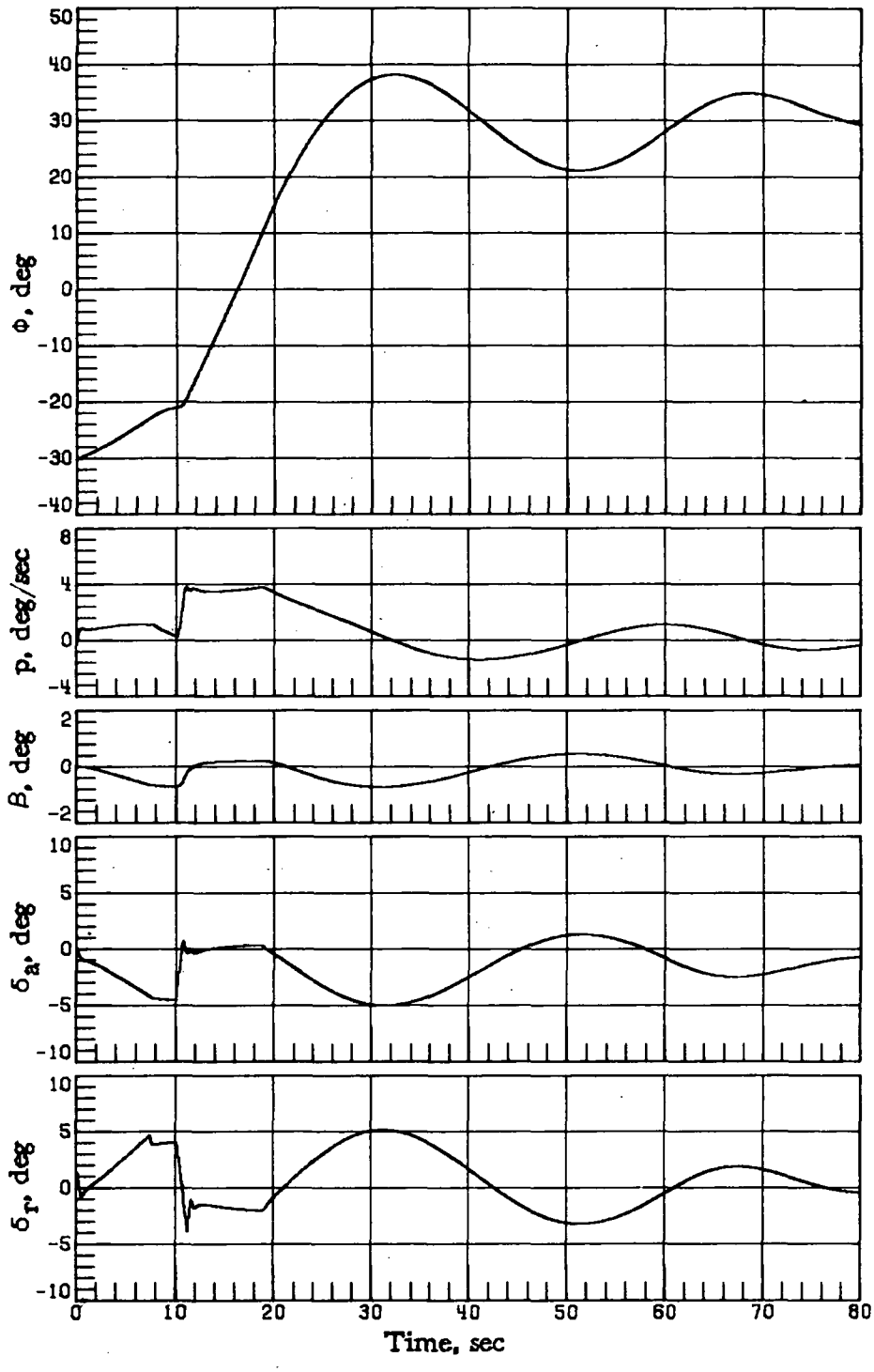

Figure 26.- Vehicle response simulations at $M_i = 4$ with $GC_m = 0.6$, $G\Delta C_{m,\delta e} = 0.7$, $G\Delta C_{m,\delta BF} = 1.6$, and $G\Delta C_{m,\delta SB} = 1.4$ ($\alpha_c = 17.6^\circ$, $\phi_c = -30^\circ$ for time <10 sec and $\phi_c = 30^\circ$ for time ≥ 10 sec).

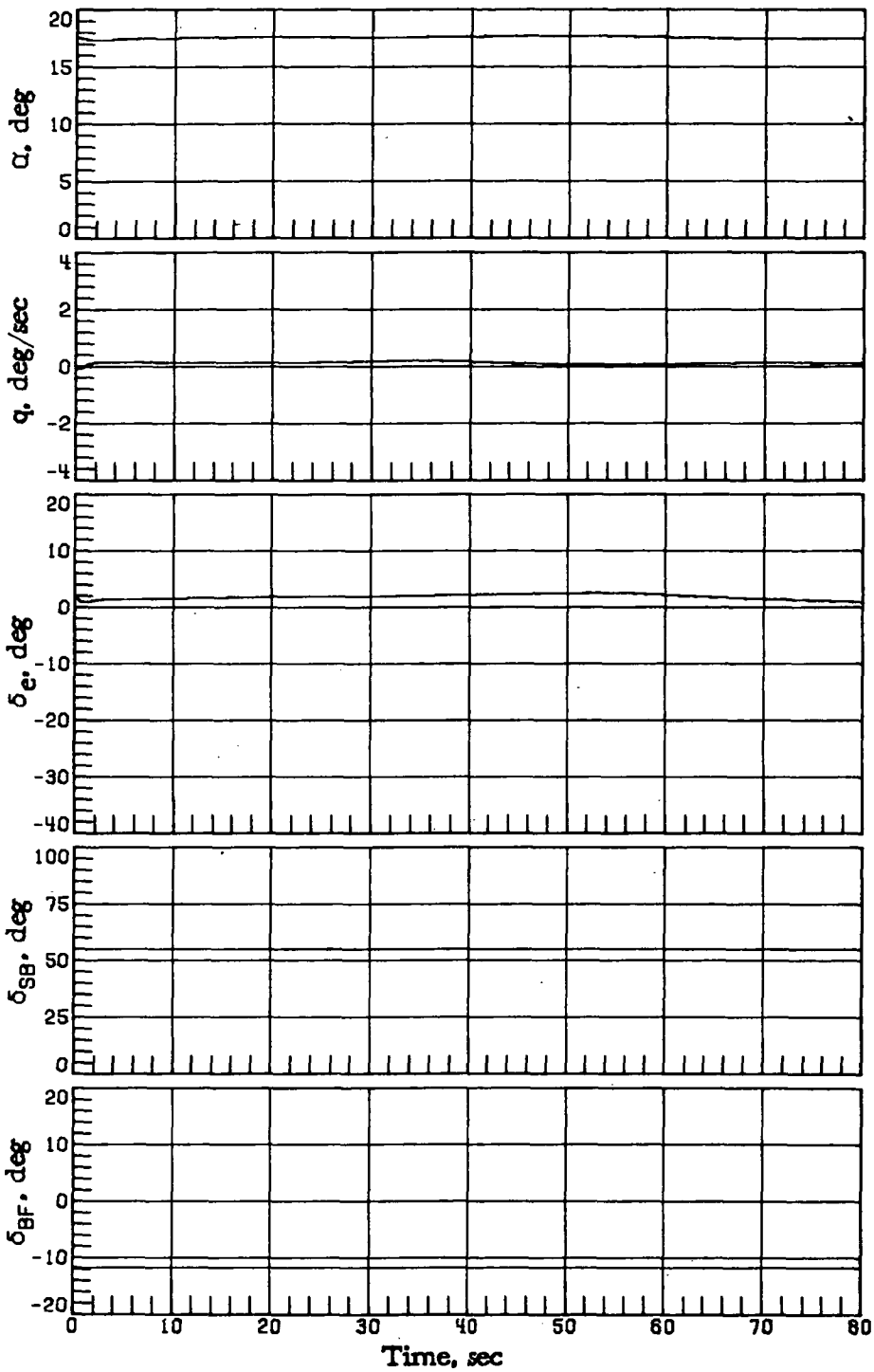

Figure 26.- Concluded.

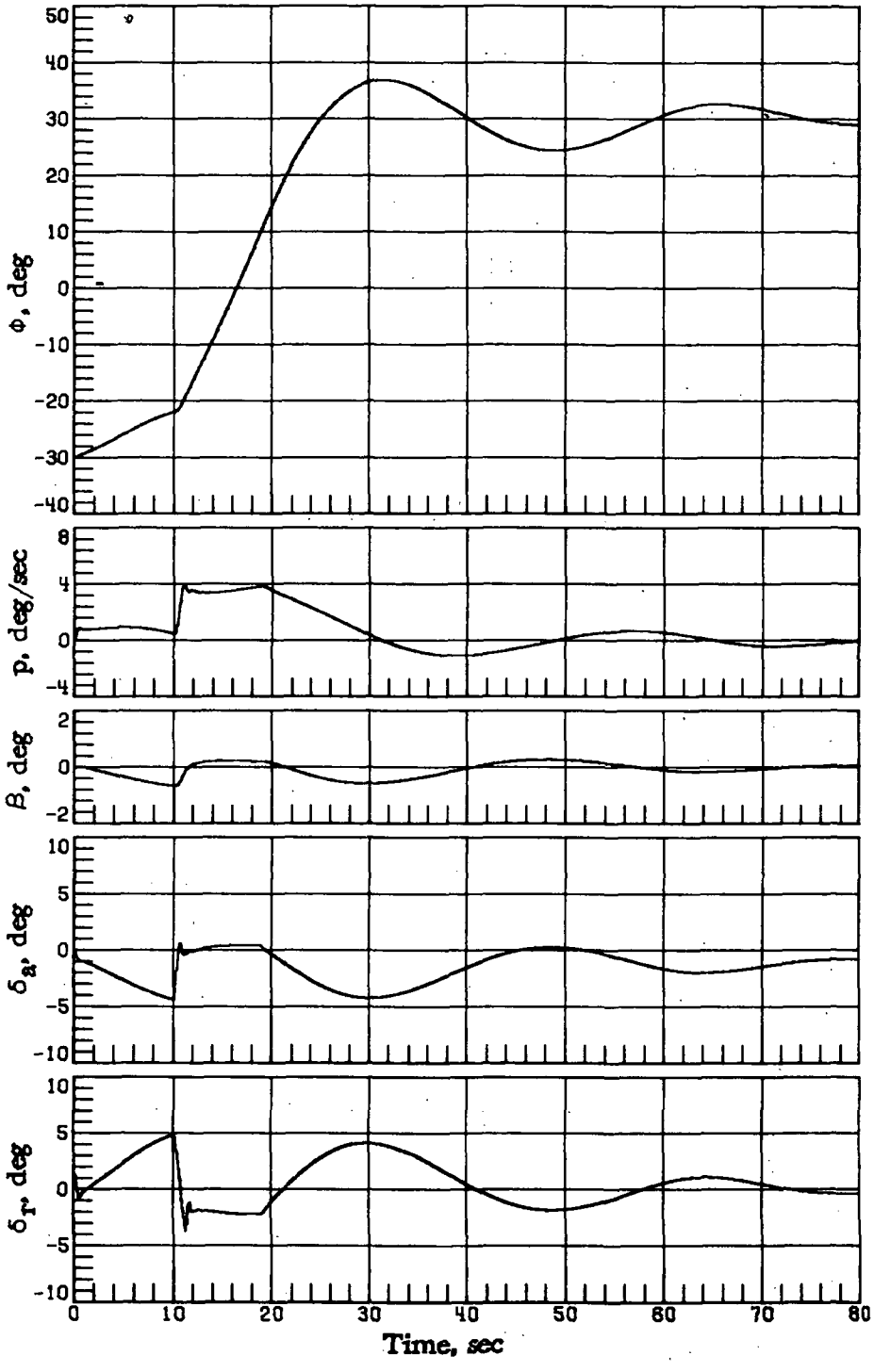

(a) Without increased rudder augmentation.

Figure 27.- Vehicle response simulations at $M_i = 4$ with $GC_m = 0.6$, $G\Delta C_{m,\delta e} = 0.7$, $G\Delta C_{m,\delta BF}$ and $G\Delta C_{m,\delta SB} = 1.4$ without and with increased rudder augmentation ($\alpha_c = 17.6^o$, $\phi_c = -30^o$ for time <10 sec and $\phi_c = 30^o$ for time $\geq$10 sec).

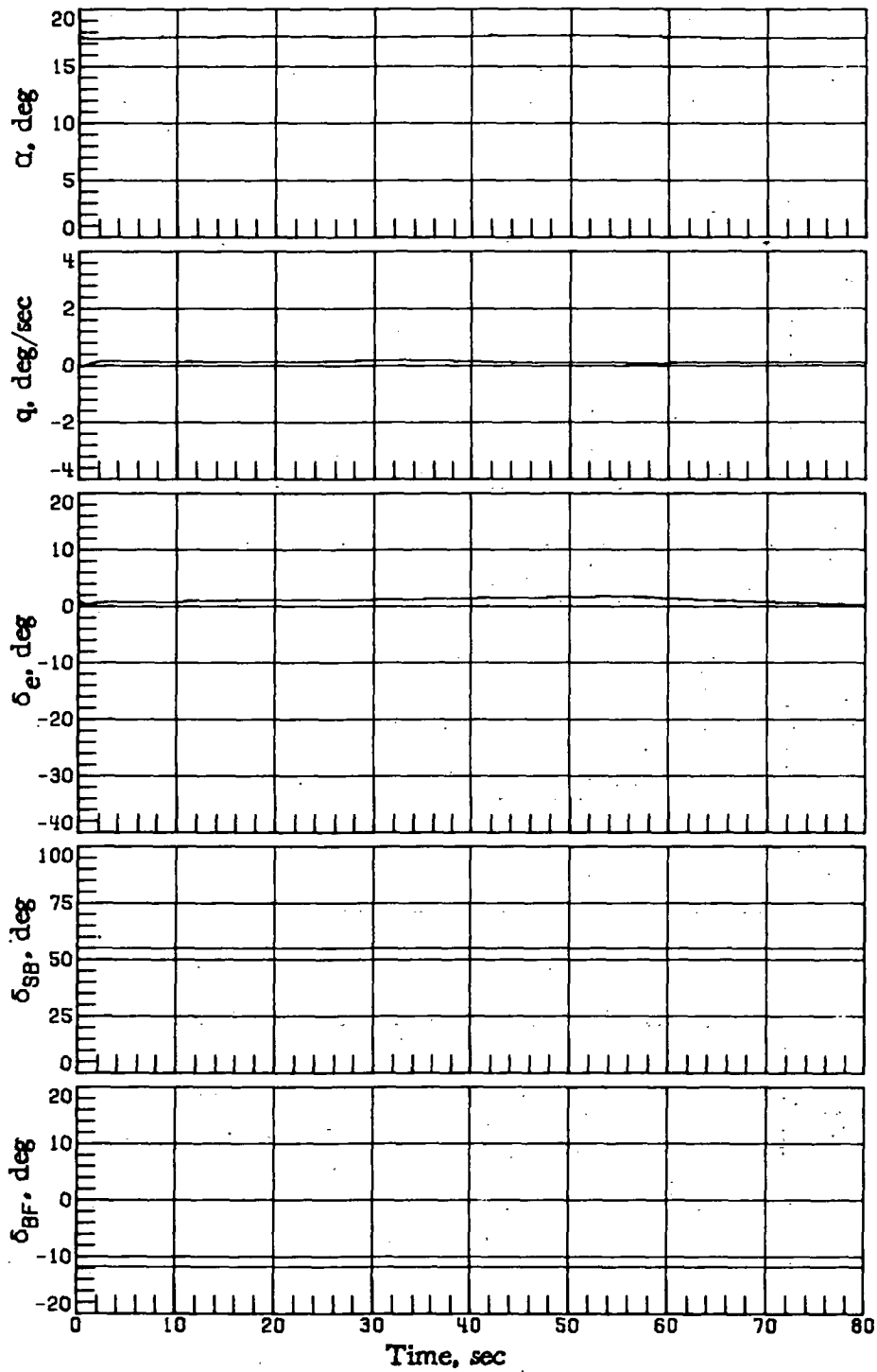

(a) Concluded.

Figure 27.- Continued.

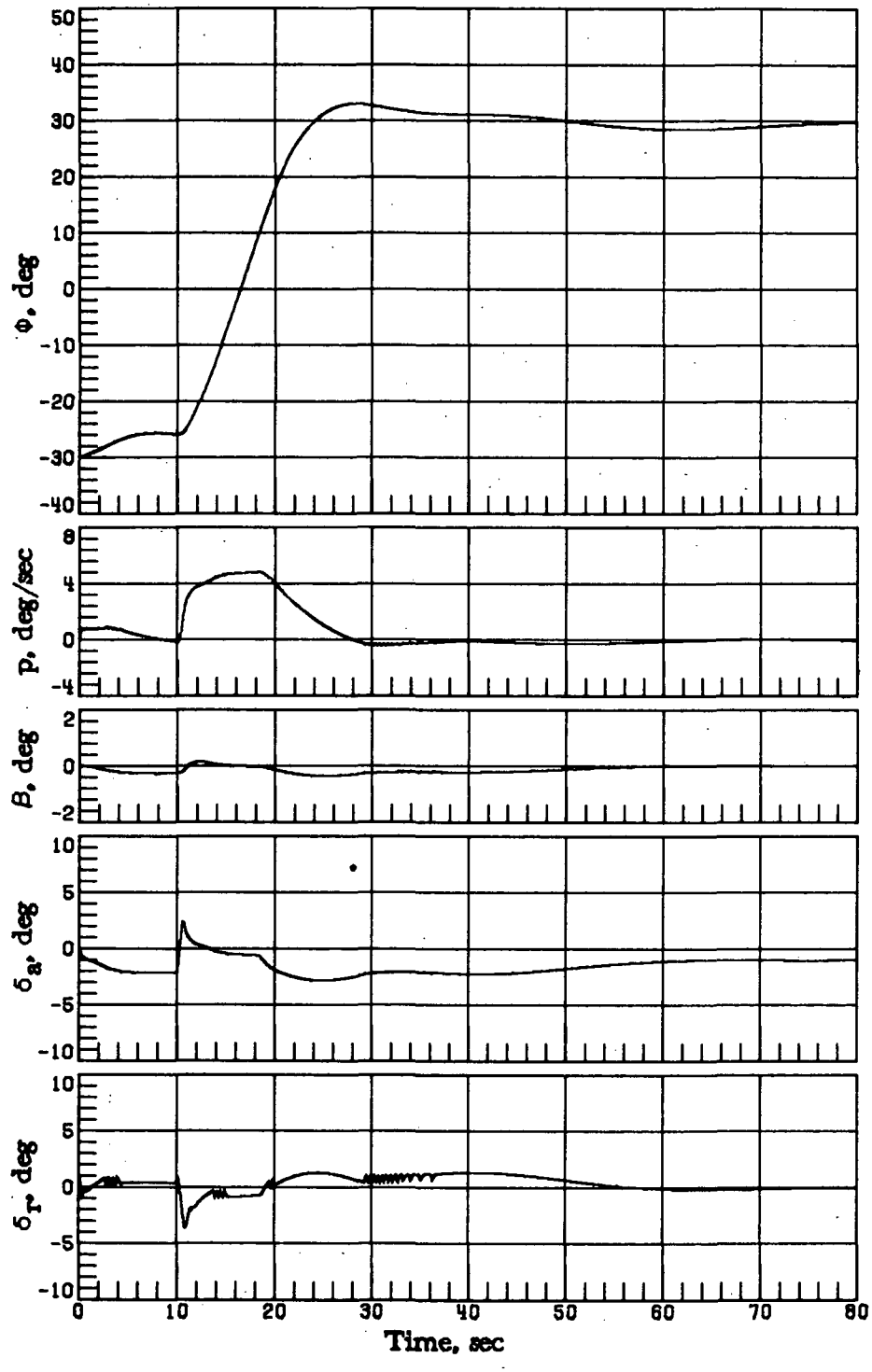

(b) With increased rudder augmentation.

Figure 27.- Continued.

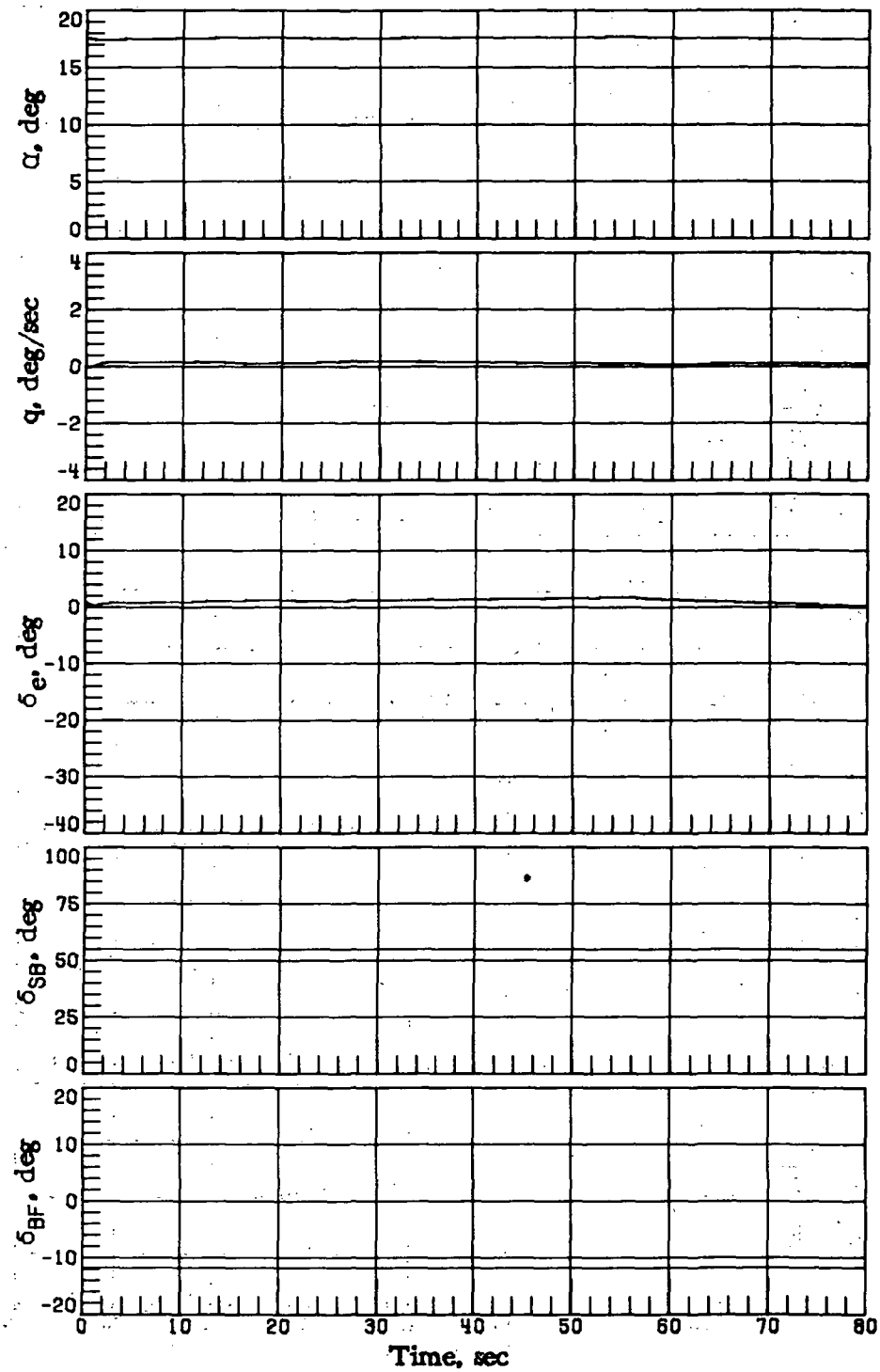

(b) Concluded.

Figure 27.- Concluded.

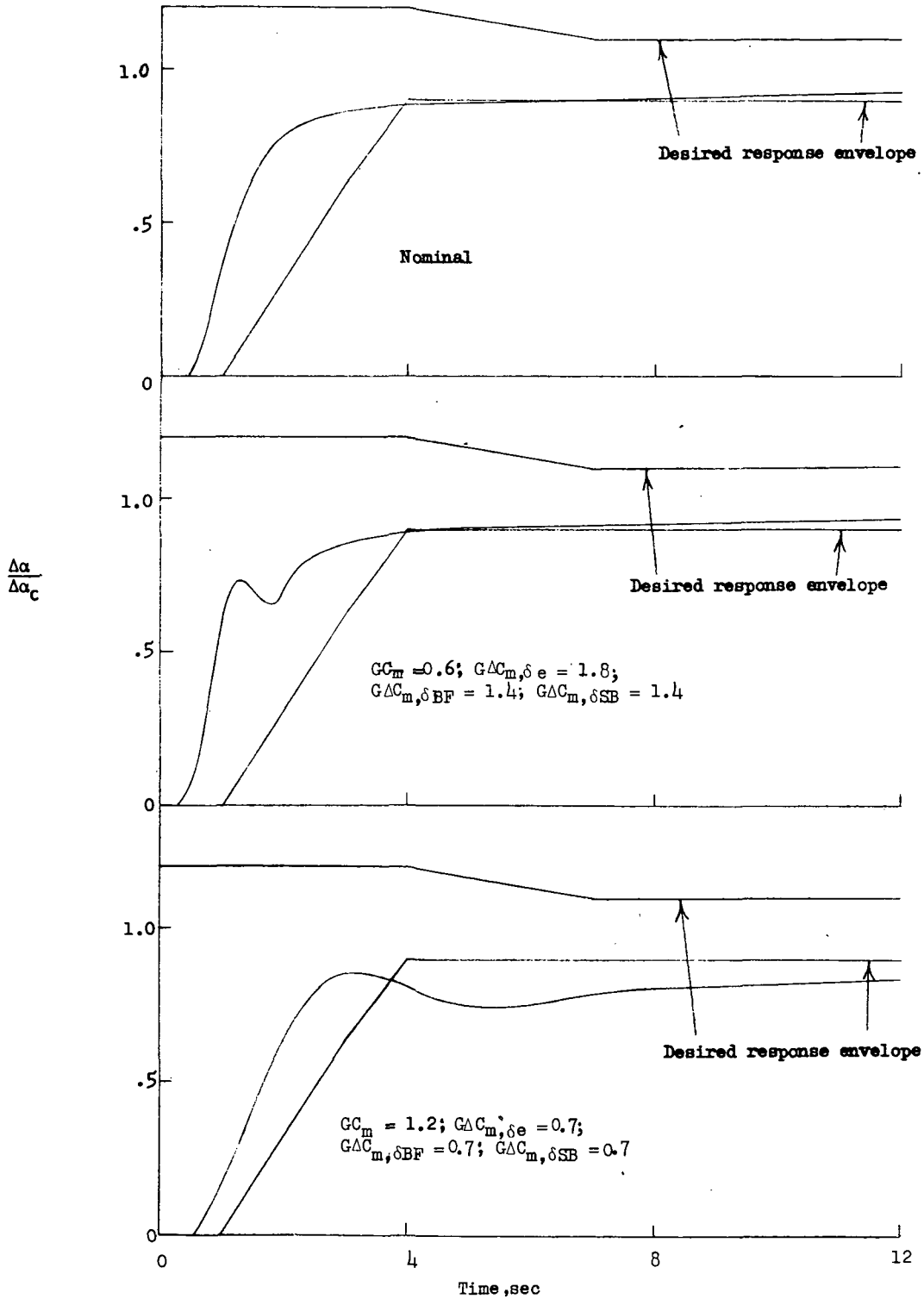

Figure 28.- Pitch response as a function of stability and control effectiveness. V_R = 0.61 km/sec (2000 ft/sec).

1. Report No.	2. Government Accession No.	3. Recipient's Catalog No.
NASA TP-1084		

4. Title and Subtitle	5. Report Date
ENTRY DYNAMICS OF SPACE SHUTTLE ORBITER WITH LONGITUDINAL STABILITY AND CONTROL UNCERTAINTIES AT SUPERSONIC AND HYPERSONIC SPEEDS	October 1977
	6. Performing Organization Code

7. Author(s)	8. Performing Organization Report No.
Howard W. Stone and Richard W. Powell	L-11288
	10. Work Unit No. 506-26-30-04
9. Performing Organization Name and Address NASA Langley Research Center Hampton, VA 23665	11. Contract or Grant No.
	13. Type of Report and Period Covered Technical Paper
12. Sponsoring Agency Name and Address National Aeronautics and Space Administration Washington, DC 20546	14. Sponsoring Agency Code

15. Supplementary Notes

16. Abstract

A six-degree-of-freedom simulation analysis was conducted to examine the effects of longitudinal static aerodynamic stability and control uncertainties on the performance of the space shuttle orbiter automatic (no manual inputs) entry guidance and control systems. To establish the acceptable boundaries, the static aerodynamic characteristics were varied either by applying a multiplier to the aerodynamic parameter or by adding an increment. With either of two previously identified control system modifications included, the acceptable longitudinal aerodynamic boundaries were determined.

17. Key Words (Suggested by Author(s))	18. Distribution Statement
Space shuttle orbiter Control system Aerodynamic uncertainties	Unclassified - Unlimited Subject Category 18

19. Security Classif. (of this report)	20. Security Classif. (of this page)	21. No. of Pages	22. Price*
Unclassified	Unclassified	65	$4.50

* For sale by the National Technical Information Service, Springfield, Virginia 22161

NASA-Langley, 1977

National Aeronautics and Space Administration

Washington, D.C.
20546

Official Business
Penalty for Private Use, $300

THIRD-CLASS BULK RATE

Postage and Fees Paid
National Aeronautics and Space Administration
NASA-451

NASA

POSTMASTER: If Undeliverable (Section 158 Postal Manual) Do Not Return